Anion and Ion-Pair Directed Self-Assembly of Urea Functionalized Molecules

A Dissertation

Submitted in partial fulfillment for the degree of

Doctor of Philosophy

Romen Chutia

(Roll No. 10612210)

Thesis Supervisor: Prof. Gopal Das

Department of Chemistry

Indian Institute of Technology Guwahati

Assam -781039, India

Anion and Ion-Pair Directed Self-Assembly of Urea Functionalized Molecules

A Dissertation

Submitted in partial fulfillment for the degree of

Doctor of Philosophy

Romen Chutia

(Roll No. 10612210)

Thesis Supervisor: Prof. Gopal Das

Department of Chemistry

Indian Institute of Technology Guwahati

Assam-781039, India

Dedicated to my

Parents

INDIAN INSTITUTE OF TECHNOLOGY GUWAHATI

Department of Chemistry

STATEMENT

I do hereby declare that the matter embodied in this thesis is the result of investigations carried out by me in the Department of Chemistry, Indian Institute of Technology Guwahati, India, under the guidance of Dr. Gopal Das, Professor, Department of Chemistry, Indian Institute of Technology Guwahati, India. In keeping with the general practice of reporting scientific observations, due acknowledgements have been made wherever this work is based on the findings of other investigators.

17th September, 2015 Romen Chutia

IIT Guwahati

INDIAN INSTITUTE OF TECHNOLOGY GUWAHATI

Department of Chemistry

CERTIFICATE

This is to certify that **Mr. Romen Chutia** (Roll No. 10612210) has been working under my supervision since July, 2010 as a regular registered Ph. D. student. His thesis entitled **"Anion and Ion-Pair Directed Self-Assembly of Urea Functionalized Molecules"** is an authentic record of the results obtained from the research work carried out under my supervision in the Department of Chemistry, Indian Institute of Technology Guwahati, Assam, India. I am forwarding his thesis to submit for the award of degree of Doctor of Philosophy, from this institute. I hereby certify that he has fulfilled all the requirements, according to the rules of this institute regarding the investigations embodied in his thesis and this work has not been submitted elsewhere for a degree.

Dr. Gopal Das
(Thesis Supervisor)
Professor
Department of Chemistry
IIT Guwahati
Assam - 781039, India

Acknowledgement

This opportunity to extend my gratitude should commence with my parents and family, whose love and inspiration has always been strength for me. Their eternal blessing and constant support has guided me this far and positively, this will take me far forward in future to achieve the success they dreamt of. Besides, no words would suffice to express my feelings for beloved Aparajita, whose love and care have so luxuriously continued to enrich my life. She has always been there to support and encourage me even in frustrating and difficult times of my life, for which I wish to submit my hearty thanks to her.

I wish to express my sincere gratitude towards my PhD supervisor Prof. Gopal Das and doctoral committee members, Dr. Sandip Paul, Dr. Debasis Manna and Dr. Lal Mohan Kundu for their advice and suggestions. I would also like to thank ex-Head Prof. A. Chattopadhyay, present-Head Prof. B. K. Patel, scientific officer Dr. Babulal Das and other technical and non-technical staff members of the Department of Chemistry, IIT Guwahati for providing me with the necessary facilities whenever required.

I take this opportunity to thank my Lab members and friends, Sandeep Da, Arghya Da, Bimlesh Da, , Jiban Da, Beda Da, Chirantan Da, Sadda Hoque (Najbul), Abhijit, Barun, Soham, Nilotpal, Utsab and Rupinder for their co-operation in my research work, without which it would not been easy to complete the PhD thesis. It was great to work and spend times with these interesting human beings and I will always cherish the memories of their jokes, laughter and humor throughout my life. Most of these people have a positive approach towards life and I wish them success in every aspects of their life.

Finally, I would like to pay my sincere thanks of appreciation to my teacher cum friend Bulu Sir, who has been an idol of motivation and inspiration for my academic career. Some friends without whom the list would be incomplete are my childhood friend Tridip, Anupal, Arabinda, Palash Amlan, Paramartha and Jharna and whose friendship had enrich my life and we often spend some good time whenever together.

Still many names are missing whose contribution and help is worth mentioning.

Romen

Synopsis

The objective of the thesis entitled **"Anion and Ion-Pair Directed Self-Assembly of Urea Functionalized Molecules"** is to explore the molecular self-assembly and anion and ion-pair recognition chemistry of some urea functionalized acyclic receptors bearing halo-aryl and nitro-aryl function functions. The contents of this thesis have been divided into five chapters based on the results of experimental work performed during the research period.

Chapter 1: Introduction

This chapter provides a brief introduction on 'supramolecular host-guest chemistry' of ionic and neutral species with special reference to recognition of anions and ion-pairs. Cationic and anionic charged species are ubiquitous in nature and they play key role in chemical, biological, medical, environmental, and industrial processes.

Supramolecular chemistry examines the weaker and reversible noncovalent interactions between molecules such as hydrogen bonding, halogen bonding (XB), hydrophobic forces, Van-der Waals forces, π···π interactions and electrostatic effects. Important concepts that have been demonstrated by Supramolecular Chemistry include molecular self-assembly, host-guest chemistry which includes anion and molecular recognition, self-sorting, mechanically-interlocked molecular architectures, and dynamic covalent chemistry. Inspired by the recognition tools exploited by nature, anion coordination chemistry has emerged into a prominent and active field of research within the realm of ''Supramolecular Chemistry'' with new synthetic hosts that employ hydrogen and halogen bonds.

The binding chemistry of acyclic receptors remain more elusive than the preorganized macrocyclic systems. When two or more identical subunits are geometrically and functionally complementary with one another, they may self-assemble to form a super molecule. Structural features of the cavity or crystal void such as, shape, size or electronic properties, determine the worth of the super-structure. Based on this possession, acyclic multi-armed podand receptors have been shown to coordinate with targeted anionic species via formation of monomeric and dimeric capsular or pseudo-capsular assemblies and in dimeric capsular assembly with two podand molecules has the beautiful possibility to satisfy the higher coordination numbers required for the stable binding of multi-charged oxyanions and hydrated anions.

Chapter 2: Materials and Experimental Methods

In this chapter, a detailed discussion of the various reagents used in the synthesis of anion receptors(**L_1-L_5**), their synthetic procedures, crystallization techniques and specifications of instruments employed in the characterization of synthesized receptors and anion binding studies are presented.

Chapter 3: Concert Act of Hydrogen and Halogen Bonding in Aerial CO_2 Uptake by a Simple Urea Receptor

While HB is a full-blown tool in molecular recognition as well as in anion recognition, halogen bonding (XB), the parallel non-covalent world to hydrogen bonding (HB), is still adolescent from this point of view. However halogen-bonding is continuing to expand its horizon in a rapid way because of its widespread applicability in the assembly of functional materials. Even with its delicacy, halogen bonding has been sensibly approached in recently developed anion recognition. Yet, supramolecular anion host systems utilizing both (HB & XB) with defined functions is a challenging prospect.

This chapter describes the evidence of fluoride induced uptake of atmospheric CO_2 and its stabilization as HCO_3^- anion by a structurally simple acyclic 1,3-bis(4-iodophenyl)urea receptor, **L_1** (air-stable crystals) (Fig. 1). The *in situ* formed HCO_3^- complex (**1a**) is stabilized by a concert act of hydrogen and halogen bonding donated by the receptors. To the best of our knowledge, 1,3-bis(4-iodophenyl)urea is the simplest of anion receptors that displays a concert act of hydrogen and halogen bonding to stabilize aerial CO_2 as HCO_3^-. Further evidence of the

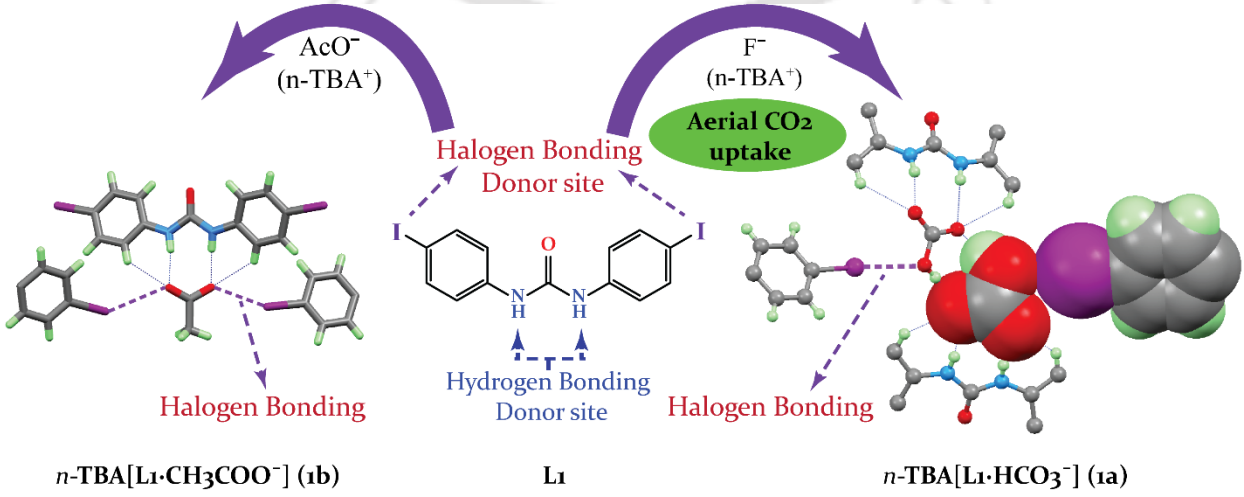

Figure 1 A comprehensive representation of the research work included in the Chapter 3.

potentiality of **L_1** as a halogen bond donor is unanimous as confirmed by single crystal analysis of the acetate (CH_3COO^-) complex of **L_1** (**1b**) (Fig. 1). Following the trend in strength of halogen bond formation *viz.*, −I > −Br > −Cl, we have examined the structural aspects of anion binding with the 1,3-bis(4-bromophenyl)urea as a control receptor, **L_2**. The outcome of the **L_2**-fluoride solution has been a complex with octahedral SiF_6^{2-} anion where the coordination environment of the anion is merely governed by multiple N−H···F (anion) interactions.

The fluoride induced uptake of aerial CO_2 by **L_1** only is due to the unique ability of **L_1** to form both HB and XB with anionic guest simultaneously. The most decisive evidence, supporting the ability of **L_1** to form XB is obtained via crystallizing the acetate complex of **L_2**, where the receptor **L_2** has been found to be involved only in HB interactions with acetate anion. The solution-state anion binding properties of **L_1** and **L_2** have been investigated by qualitative and quantitative ^{1}H NMR titration experiments with halides and oxyanions in DMSO-d_6. Both the receptors showed strong solution state binding with F^-, HCO_3^- and CH_3COO^-, as observed in the solid-state, whereas both of them have been found to be less interactive with other anions such as Cl^-, Br^-, I^-, NO_3^-, HSO_4^-, and $H_2PO_4^-$.

Chapter 4: Anion and Ion-pair Binding and Encapsulation by the Positional Isomers of a Nitrophenyl Tris(urea) Receptor

This Chapter has been divided into two parts. Part 1 involves recognition of anionic guests and Part 2 involves recognition of an ion-pair based on a dual host system.

Part 1. First part of this chapter deals with a set of three nitrophenyl functionalized tripodal urea scaffolds, **L_3**, **L_4** and **L_5** and demonstrate the effect of positional isomerism in anion coordination (Fig. 2).

Structural studies revealed oxyanion induced self-assembly of the *para*-isomer (**L_3**) into dimeric (pseudo)molecular capsules as observed in carbonate and terephthalate complexes (**3a** and **3b**). On the other hand, the meta-isomer (**L_4**) self-assembles into dimeric capsules only in the presence of inorganic oxyanions, as observed in the hydrogenphosphate complex (**4a**), and assembles into a 2D sheet-like structure in the presence of terephthalate dianion (**4b**). In contrast to **L_3** and **L_4**, structural authentication of the *ortho*-isomer (**L_5**) in the presence of different oxyanions was not fruitful presumably due to the steric effect provided by the $-NO_2$ group at the *ortho*-position, which hinders the facile inclusion and coordination of an anion due to electrostatic factor, as confirmed by 2D-NOESY NMR analysis of the free receptor. Qualitative

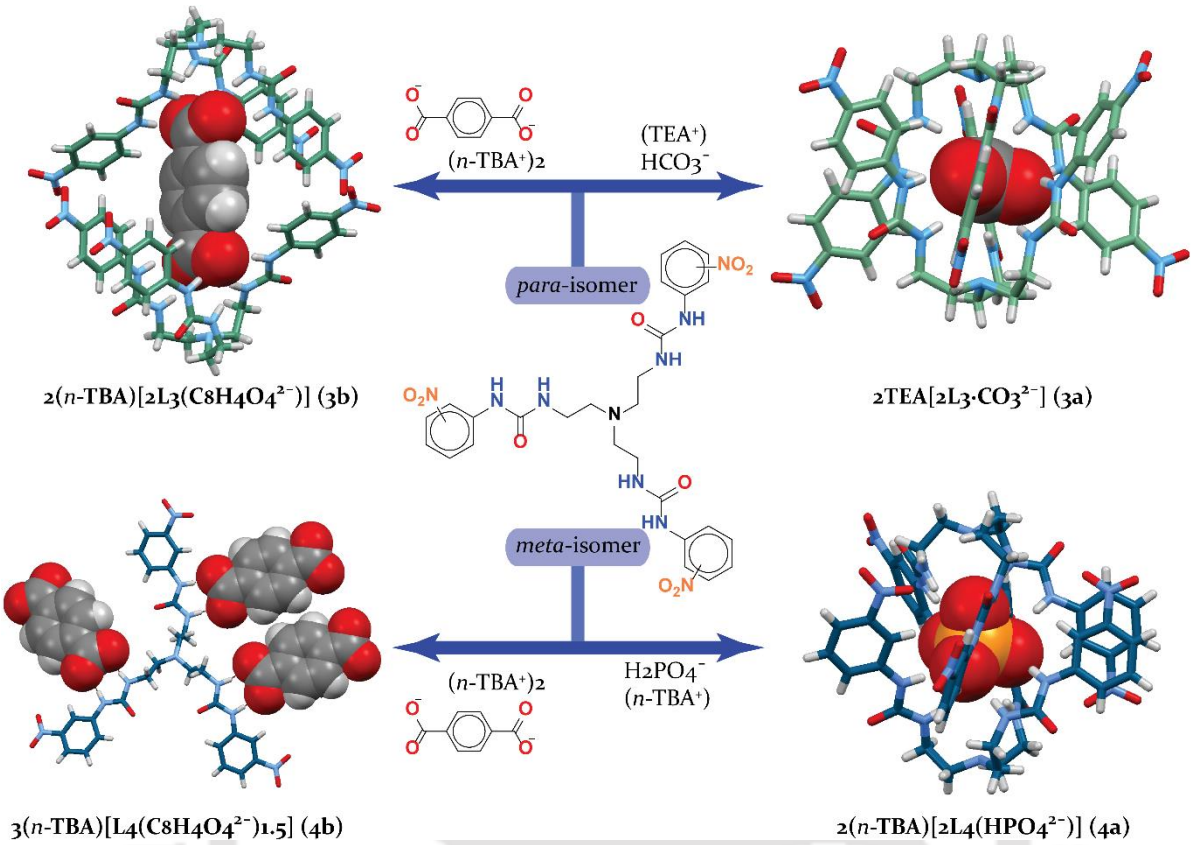

Figure 2 A comprehensive representation of the research work included in Part 1 of Chapter 4.

and quantitative ^{1}H NMR experimental results showed that the *ortho*-isomer binds with oxyanions rather feebly as reflected from the apparent binding constant values of HCO_3^- and $H_2PO_4^{2-}$. This is in contrast to the results obtained for *meta*- and *para*-isomers which can coordinate to these anions very strongly via encapsulation, as confirmed by 2D-NOESY NMR analysis. However, F^- is bound almost equally by all the three isomeric receptors.

Part 2. Ion-pair receptors have potential applications in various fields, such as salt solubilization, salt extraction and transmembrane ion transport. In spite of their prospective applications, the number of well characterized ion-pair receptors, which might permit a greater level of control over these processes, remains limited. This reflects a combination of synthetic challenges and experimental complexities associated with tracking multiple ionic species as well as the high inherent lability of many ion-pairs. From this perspective, a dual-host (using separate anion and cation hosts) approach has been proven to be fruitful in directions like the extraction of different alkali metal salts.

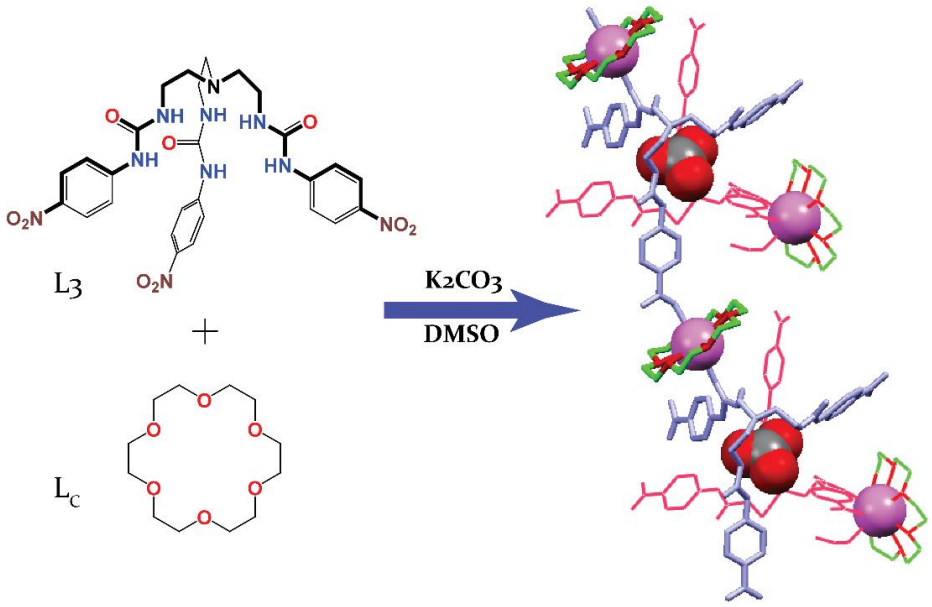

Figure 3 A comprehensive representation of the research work included in Part 2 of Chapter 4.

Part 2 of the Chapter 4 deals with the *para*-isomer (**L_3**), which in association with 18-crown-6-ether (**L_C**) self-assembles into an integrated 1D coordination polymer in the presence of potassium carbonate (K_2CO_3) (complex **3d**). This association is because of the complementarity in functional groups and their orientation in the anion (CO_3^{2-}) induced dimeric capsular assembly. This dimeric capsular assembly is structurally supposed to be playing the role of an organic linker in the 1D coordination polymer coordinating through its outward directed urea-carbonyl O-atom and nitro O-atom to crown-ether bound potassium ions (Fig. 3).

Chapter 5: Tetrameric mixed phosphate cluster encapsulation/recognition by a tris(urea) receptor

This Chapter is about the recognition of tetrameric mixed phosphate clusters by *para*-nitrophenyl functionalized tris(urea) receptor **L_3** in its neutral and charged state (Fig. 4). In this particular unusual example, receptor **L_3** self-assembles, in the presence of excess *n*-TBA(H_2PO_4), into a tetrahedral molecular cage by encapsulation of a tetrameric tetrahedral mixed phosphate cluster $(H_2PO_4^-{\cdot}HPO_4^{2-})_2$ via 24 –NH hydrogen bonds [complex (*n*-TBA)$_3${2**L_3**$(H_2PO_4^-{\cdot}HPO_4^{2-})$}] (**3e**). Further, in the presence of orthophosphoric acid, the receptor **L_3** has been observed to be self-assembled with side-cleft bonded tetrameric anion-acid cluster $(H_2PO_4^-{\cdot}H_3PO_4)_2$ [complex $\{(\mathbf{L_3}H)^+(H_2PO_4^-{\cdot}H_3PO_4)DMSO{\cdot}H_2O\}$] (**3f**).

In a proof of concept experiment, transformation of complex **3f** with cationic host into a phosphate encapsulated complex with neutral host has been demonstrated in solution-state by

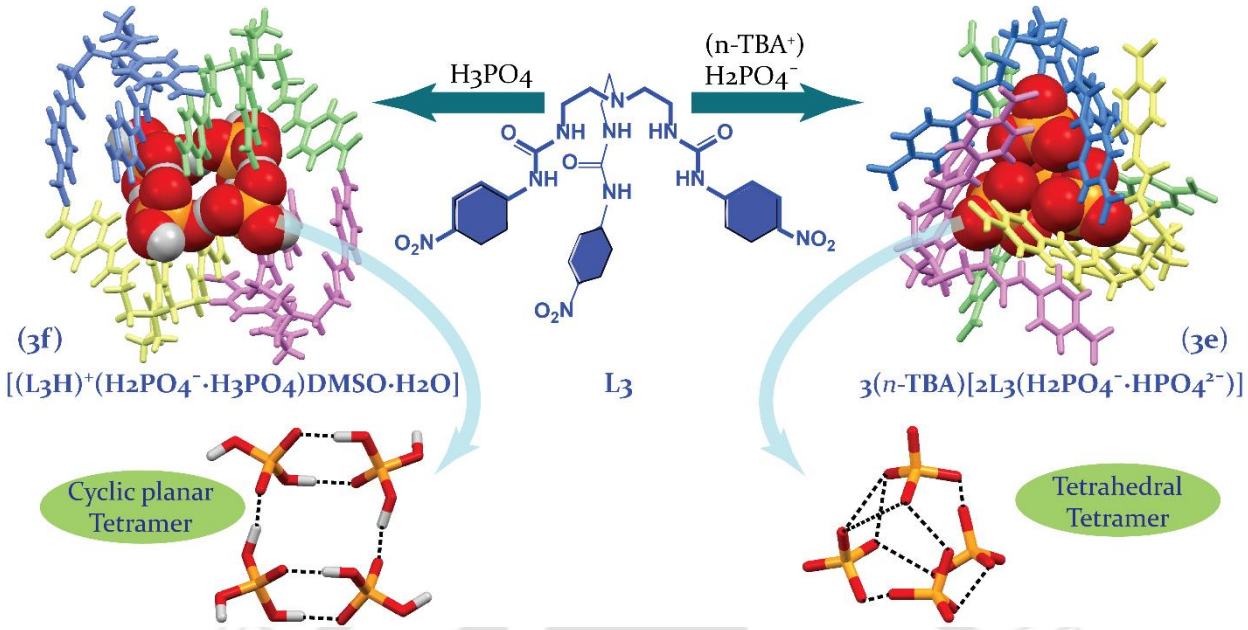

Figure 4 A comprehensive representation of the research work included in Chapter 5.

quantitative ^{1}H NMR titration with (*n*-TBA)OH in DMSO-d_6 (298 K). Also, extensive studies of receptor $\mathbf{L_3}$ with other halides have been carried out in the solid-state. Crystal structure elucidation revealed the formation of a pseudodimeric (2+2) capsular self-assembly with 1:1 ratio of the host and guest in the fluoride encapsulated complex, (TEA)[$\mathbf{L_3}$(F)] (**3g**). 2D-NOESY NMR (DMSO-d_6) experiments were carried out on the phosphate complexes (complexes **3e** and **3f**) to study the binding discrepancies of phosphate anion with the neutral and charged host.

Contents

Chapter 1- Introduction

Chapter 2- Experimental Methods and Characterization

Chapter 3- Aerial CO_2 Uptake by a Simple Urea Receptor: Concert Act of Hydrogen and Halogen Bonding

Chapter 4 - Anion Binding and Encapsulation by the Positional Isomers of a Nitrophenyl Tris(urea) Receptor

Chapter 1

Introduction

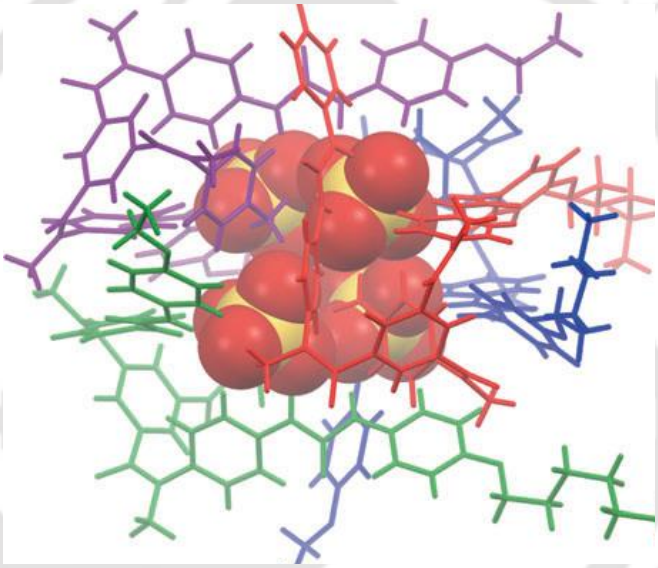

1.1 Supramolecular Chemistry: An Introduction

Supramolecular chemistry has been defined by one of its leading proponents, Jean-Marie Lehn, who won the Nobel Prize for his work in the area in 1987, as the 'chemistry of molecular assemblies and of the intermolecular interactions'. While traditional chemistry focuses on the covalent bond and coordinative bond formation, supramolecular chemistry examines the weaker and reversible noncovalent interactions between molecules such as hydrogen bonding, halogen bonding, ion-ion and ion-dipole interactions, cation–π and anion–π interactions, π–π interactions, Van der Waals forces, and hydrophobic effects.[1] Understanding these noncovalent interactions and exploiting them in new ways continues to define the essence of the field. Important disciplines that have been demonstrated by supramolecular chemistry include molecular self-assembly, host-guest chemistry such as molecular recognition and anion recognition, mechanically-interlocked molecular architectures, and dynamic covalent chemistry.

In principle, originally it was defined in terms of the non-covalent interaction between a 'host' and a 'guest' molecule, where the host is commonly referred to a large molecule or aggregate such as an enzyme or synthetic cyclic and acyclic compounds possessing a sizeable central hole or cavity[1] and the guest may be a monatomic cation, a simple inorganic anion, an ion pair or a more sophisticated molecule such as a hormone, pheromone or neurotransmitter possessing divergent binding sites (e.g. a spherical, Lewis acidic metal cation or hydrogen bond acceptor halide anion). The thermodynamic stability of a supramolecular host-guest complex may be enhanced by operation of a chelate effect or macrocyclic effect. The macrocyclic effect makes cyclic hosts such as corands (e.g. crown ethers) up to a factor of 10^4 times more stable than closely related acyclic podands with the same type of binding sites. Therefore, the binding of guests within pre-organized macrocyclic systems is relatively straight forward to understand but the binding processes of acyclic receptors remain more elusive. In order to bind, a host molecule must have binding sites that are of the correct electronic character (polarity, hydrogen bond donor/acceptor ability, hardness or softness etc.) to complement the guest. Host preorganization is a key concept because it represents a major enhancement in the overall free energy of guest complexation.[2]

1.2 Hydrogen bond (HB)

A hydrogen bond may be regarded as a particular kind of dipole-dipole interaction in which a hydrogen atom attached to an electronegative atom (or electron withdrawing group) is attracted to a neighboring dipole on an adjacent molecule or functional group. Hydrogen bonds are commonly written D–H···A and usually involve a hydrogen atom attached to an electronegative atom such as O or N as the donor (D) and a similarly electronegative atom, often bearing a lone

pair, as the acceptor (A). There are also significant hydrogen bonding interactions involving hydrogen atoms attached to carbon, rather than electronegative atoms such as N and O (electronegativities: C: 2.55, H: 2.20, N: 3.04, O: 3.44). Because of its relatively strong and highly directional nature, hydrogen bonding has been described as the 'masterkey interaction in supramolecular chemistry'.[1] Typical examples include, the formation of carboxylic acid dimer and base pairing in DNA by hydrogen bonding (Scheme 1.1). Hydrogen bonding is perhaps the most important discriminating cohesive force in directing the crystallization and self-assembly of organic molecules.[3]

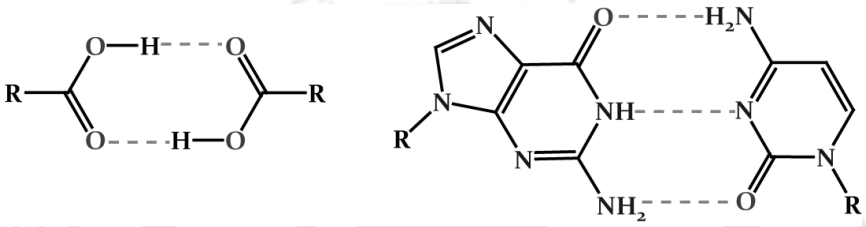

Scheme 1.1 A hydrogen bonded carboxylic acid dimer and base pairing in DNA (Guanine–Cytosine) by hydrogen bonding.

1.3 Halogen bond (XB)

Halogen bonding (XB) is the parallel non-covalent world to hydrogen bonding (HB). This relatively younger, highly directional, non-covalent interaction is the charge-transfer interaction between Lewis bases and polarizable halogen atoms.[4] XBs can be described in general as D···X–Y, where X is the electrophilic halogen atom (Lewis acid, XB donor), D is a donor of electron density (Lewis base, XB acceptor), and Y is a carbon, nitrogen, or halogen atom (Scheme 1.2).[5] Experimental data from the solid, liquid, and gas phases confirm the theoretical predictions that the strength of the halogen-bond donor increases in the order Cl<Br<I. The strength of the halogen bonds increase as the electron-withdrawing nature of the atom, or moiety, bonded to a given halogen increases [C(sp)-X>C(sp2)-X> C(sp3)-X].[6] The ability of halogen atoms to attractively interact with electron donors was recognized in dihalogens and halocarbons in the early 19th century.[7]

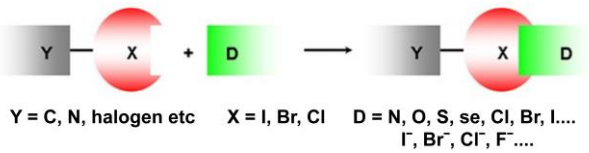

Scheme 1.2 Schematic representation for the formation of halogen bond. This scheme is reproduced from reference 5.

The first case of intermolecular donor–acceptor complexes was reported by Benesi and Hildebrand that were formed from iodine and aromatic hydrocarbons.[8] However, it was O. Hassel who introduced this promising non-covalent interaction, namely halogen bonding as

'interatomic charge transfer bonding' and its importance for directing molecular self-assembly phenomena to the people in 1970 in his Nobel lecture. [9]

Halogen-bonding is continuing to expand its horizon in a rapid way because of its widespread applicability in the assembly of functional materials (such as liquid crystals and molecular-imprinted polymers),[10] conducting and magnetic molecular materials,[11] tuning of second-order nonlinear optical responses,[12] supramolecular polymers and crystalline assemblies,[13] even in medicinal chemistry.[14]

The objective of the thesis is to explore the molecular self-assembly in the course of anion and ion-pair coordination chemistry of some newly synthesized and some less reported acyclic receptors bearing specific terminal aryl functions, which are playing key role in effective anion binding and recognition.

1.4 Anion receptor chemistry

Anions are ubiquitous in biology. They are present in roughly 70% of all enzymatic sites, play essential structural roles in many proteins, and are critical for manipulation and storage of genetic information (DNA and RNA are polyanions). Anions also take part in regulating osmotic pressure, activating signal transduction pathways, maintaining cell volume and in the production of electrical signal. Not surprisingly, the disruption of anion flux across the cell membranes is increasingly recognized as being the primary determinant of many diseases. In fact the transport of anions through cell phospholipid bilayers is known to be mediated by a variety of channels and anion transport proteins with at least 14 mitochondrial anion transport system have been identified so far. These include (among others) systems responsible for the trafficking of ADP, ATP, phosphate, citrate maleate, oxaloacetate, sulphate, glutamate, fumarate and halide anions. Nature exemplifies how proteins can selectively and efficiently bind anions by weak intermolecular forces. (Figure 1.1).[15, 16]

The halogen bonding (XB), though comparatively much younger, has been established as a potential tool for the rational design and construction of molecular materials with DNA and other biological macromolecules. Ho and co-workers have studied Holliday junctions (four-stranded DNA junctions, the key structural intermediates during the homologous recombination of DNA) and estimated that a halogen bond that can direct the conformation of a biological molecule, which is stronger than an analogous hydrogen bond in the same environment.[17]

The anion recognition chemistry is of growing attention in supramolecular chemistry[18] due to the essential roles that anions play in catalysis, and environmental science.[16] Binding affinities between anions and their hosts are mostly attributed to hydrogen-bonding and/or electrostatic interactions, with the former being the more influential in promoting selective binding through

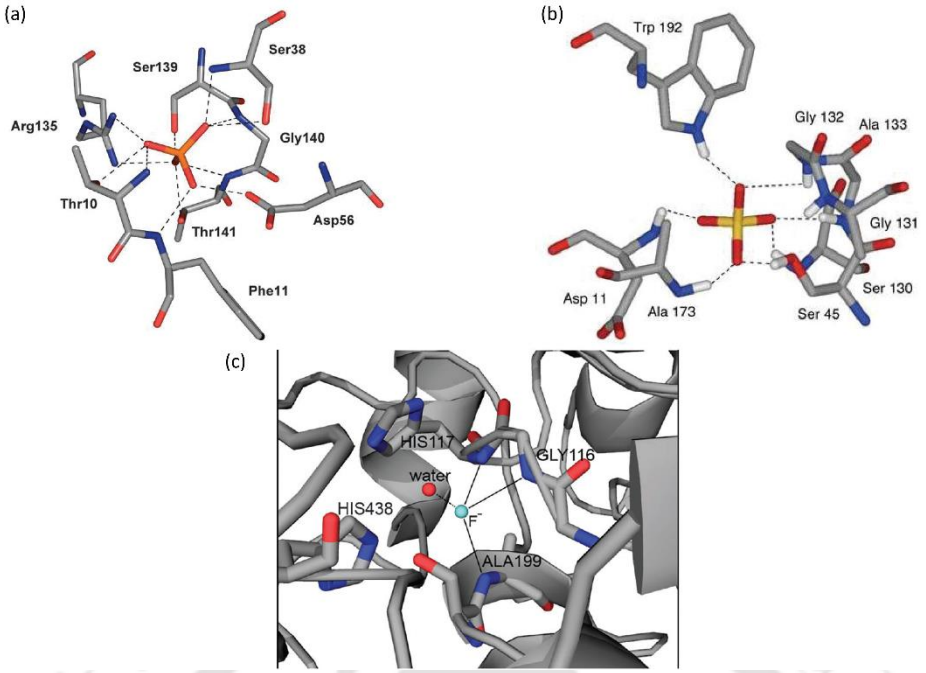

Figure 1.1 Anion binding in biology (a) Showing binding mode of phosphate anion in phosphate-binding protein;[15a] (b) X-ray crystal structure of sulfate-binding protein. The sulfate anion is bound by seven hydrogen bonds from NH and OH bond donor group;[15b] (c) Showing bound mono hydrated fluoride anion in human butyrylcholinesterase complex (PDB code = 2XMC).[15c]

topological complementarity. As Moyer and Bonnesen et al. has pointed out that the factors influencing anion recognition in the traditional analytical sense are of key concern, where simple physical properties such as size, charge, basicity and hydrophilicity tend to govern selective exchange of one anion over another.[19] They introduced the term *bias* for this type of phenomenon and deduce that truly selective anion receptors must involve some elements of strategic design, including appropriately positioned hydrogen bond coordination sites.[19] The introduction of multiple hydrogen bonding sites along with the resulting topological considerations in anion receptors leads to the concept of double valence for anions as well as for transition-metal ions. For anions, however, the primary valence is the negative charge on the anion and the secondary valence is provided by hydrogen bonds to the anion.[20] Bowman-James et al. has categorized the binding of anions based on their coordination numbers which is helpful

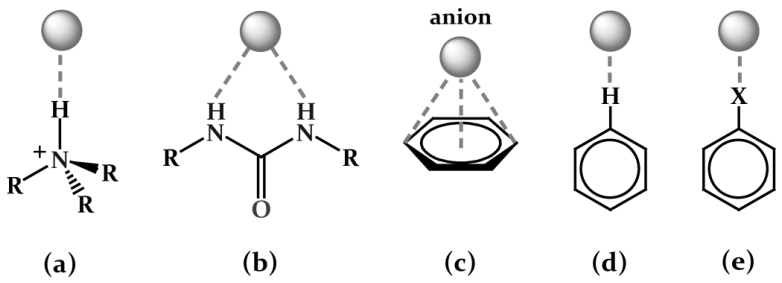

Scheme 1.3 Anion binding by different types of noncovalent interactions; (a) electrostatic N−H···A⁻ interaction by an ammonium cation; (b) complementary N−H···A⁻ interaction by a urea function; (c) anion–π interaction; (d) C−H···A⁻ interaction by an aryl function and (e) C−X···A⁻ halogen bonding by a halocarbon (X = F⁻, Cl⁻, Br⁻ and I⁻).

in defining the notions of complementarity for a given anion and can aid to the design of optimal anion-binding host structures.[21]

The most effective way to bind anions consists in taking advantage of their negative charge and accordingly, ammonium and quaternary ammonium receptors have been the principal receptor of choice since, they ensure an adequate electrostatic attraction reinforced by hydrogen bond contacts with the coordinated anions.[22] However, pyrrole, indole, amide and urea/thiourea functions have been the subject of intensive investigations for its performance in the construction of neutral anion receptors *via* favourable hydrogen bonding interactions.[23] However, if the −NH protons are acidic enough, in particular when an electron-withdrawing substituent is introduced into the receptor molecule, deprotonation may occur in the presence of a highly basic anion, such as fluoride and acetate.[24]

1.5 Anion coordination and anion directed assembly of multi-armed acyclic receptors

Although Nature exemplify how proteins can selectively and efficiently bind anions by weak intermolecular forces, the development of novel artificial receptors for the selective recognition of anions in solid state still remains a challenging task, with hydrogen bonds being fundamental in determining binding selectivity *via* topological complementarity. Anions generally have very high solvation energies that must be compensated by the host for effective anion recognition and complexation. Among the numerous design choices, multi-armed acyclic receptors have been especially of interest because of their potential ability to encapsulate the anions, such as nitrate, phosphate, and sulphate. The binding ability multi-armed acyclic receptors vary with the attached functionality unit, since functional groups modify the hydrogen bonding capability.

1.5a Anion receptors complete based on halogen-bond donor groups

Mark S. Taylor and his co-workers has reported a series of urea-based anion receptors based on the combined act of hydrogen and halogen bonding.[25] They showed that cooperation between two distinct noncovalent interactions leads to unusual effects on receptor selectivity. Theoretical study revealed that simple urea receptor (**1a)** with incorporation of two halogen bond donor sites (Fig. 1.2) switched selectivity from oxyanions to halides (Fig. 1.2).

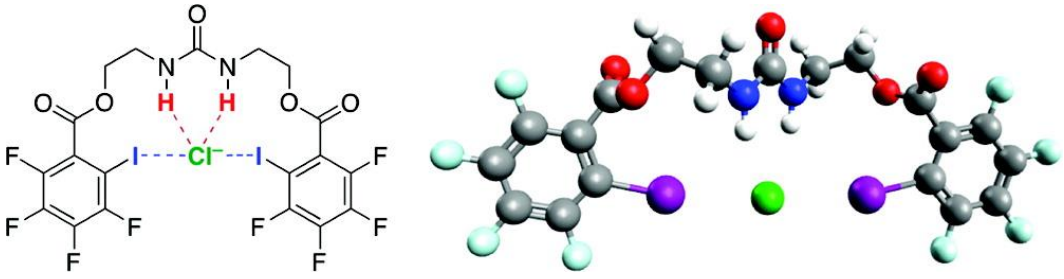

Figure 1.2 Structure of the combined hydrogen and halogen bonded chloride complex of the receptor **1a** calculated by DFT.

A rare example of a heteroditopic ion pair receptor (Fig. 1.3a) has been reported by Resnati and Metrangolo et al.[26] where the anion part has been pure taken care by halogen bonding. The tripodal ion-pair receptor has been established to dissociate the ion pair NaI through simultaneous binding of I^- and Na^+ by two different recognition arrays of atoms (Fig. 1.3b). They carried out detail NMR study on two receptors with and without halogen bonding donor groups and evidenced that the boosting effect of XB-mediated anion binding on the cation complexation. From ESI-MS/MS experiments, the selectivity for the halides in solution has been found to be higher for I^- over Br^- and Cl^- ions.

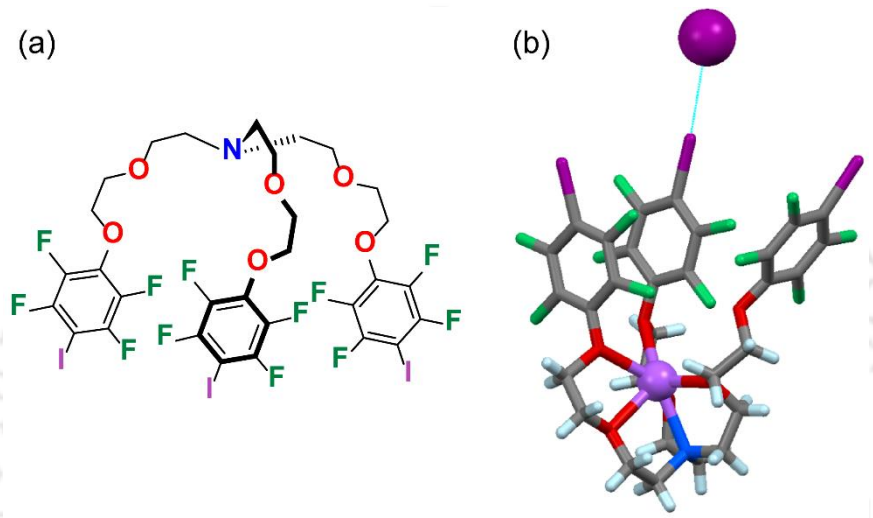

Figure 1.3 (a) Molecular structure of the tripodal heteroditopic ion-pair receptor receptor **1b** and (b) single-crystal X-ray structure of the complex of the receptor **1b** with NaI.

1.5b Tripodal amine receptors

Tren-based tripodal amine receptors have been shown to coordinate with anions of different dimensionality in its triprotonated form. Hossain et al. have shown example of anion binding by a tren based tripodal amine receptor having thiophene as terminal group (2a).

2a has been has been shown to encapsulate a nitrate anion in a selective orientation, forming a C_3 symmetric complex, $[(H_3\mathbf{2a})(NO_3^-)_3]$.[27] The anion is coordinated to three protonated secondary amines with six N−H···O hydrogen bonds in a plane perpendicular to the principal rotation axis passing through the bridgehead nitrogen of the protonated receptor and the nitrogen of the encapsulated nitrate (Figure 1.4b). On the other hand, in the structure of the iodide complex $[(H_3\mathbf{2a})(I^-)_3]$, an iodide anion is bound above the quasi-planar tripod with the three arms pointing outward in a trigonal-planar-like arrangement (Figure 1.4c). ^{1}H NMR titration studies showed that the triprotonated receptor forms a 1:1 complex with nitrate yielding a binding constant of K = 315 M^{-1} in chloroform and showing a moderate selectivity over halides. Thus, the attached aryl terminals in the receptor designing could play an important role towards the formation of different microenvironment for selective anion binding and encapsulation.

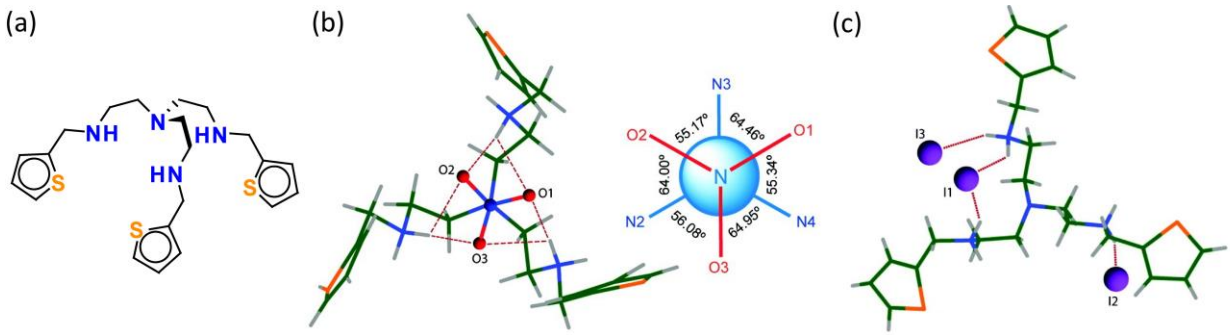

Figure 1.4 (a) Molecular structure of the tripodal amine host **2a** (b) X-ray structure of the $[H_3\mathbf{2a}(NO_3)]^{2+}$ complex (**2a**) showing one encapsulated nitrate with six NH···O bonds in binding mode and (c) X-ray structure of the $[H_3\mathbf{2a}](I)_3$ complex showing hydrogen-bonded iodide.

1.5c Tripodal amide receptors

Anion binding properties of tris(amide) receptor **3a** (Fig. 1.5a) with the π–acidic 3,5-dinitrophenyl-based substituents have been extensively studied by Das et al. in solution as well as in solid state. **3a** behaves as a selective chemosensor for F^- ion (Fig. 1.5b) by strong anion–π CT interaction and thereby, exhibits solvatochromism (Fig. 1.5c, d) in different aprotic solvents.[28] Interestingly, the receptor showed a distinct behaviour towards complexation of F^- anion when tetrabutylammonium fluoride (*n*-TBAF)[28a] and potassium fluoride (KF) salts were individually employed for recognition of F^- with **3a**.[28b] Single crystal X-ray diffraction analyses showed that an F^- anion is bound within the receptor cavity by strong N–H···F^- and C–H···F^-

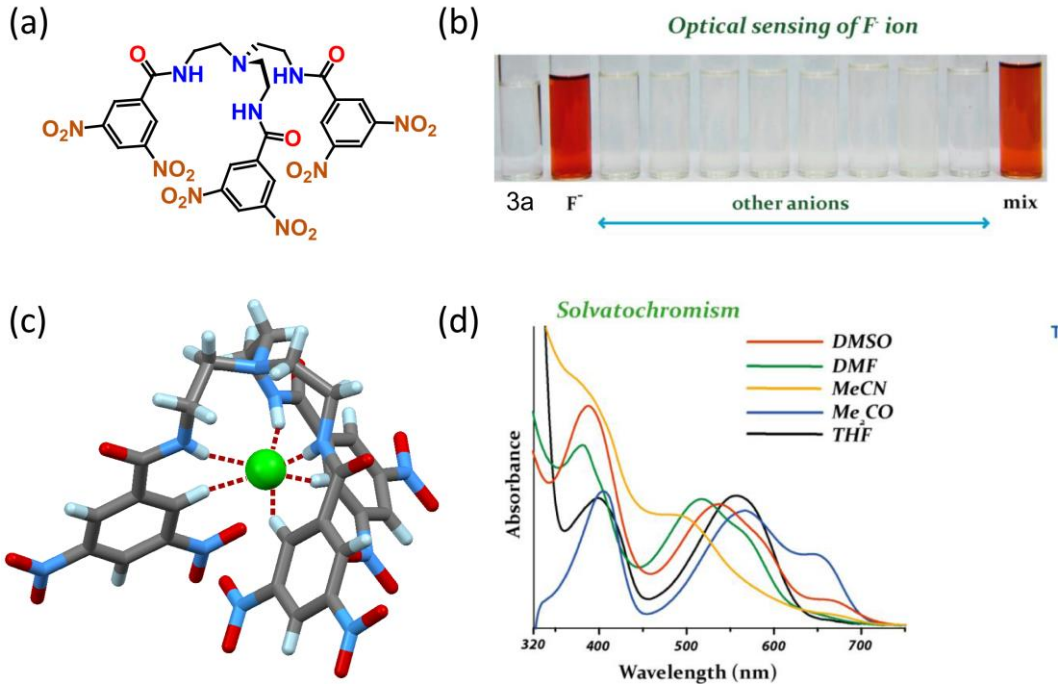

Figure 1.5 (a) Molecular structure of the tripodal amine host **3a**, (b) colour changes observed upon addition of anions (25 equiv.) to DMSO solutions of **3a**, (c) Crystal structure of the F^- encapsulated complex of receptor **3a** (d) changes in the UV/Vis spectrum of **3a** in various aprotic solvents upon addition of excess TBAF (Solvatomorphism).

hydrogen bonds irrespective of solvent of crystallization, when *n*-TBAF was employed as an F^- source. In case of other anions (Cl^-, Br^-, ClO_4^- and HSO_4^-) X-ray crystallography results showed that, anion binding with the protonated receptor is attributable entirely to N–H···A^- and C–H···A^- interactions in all the isolated complexes and in none of the cases anion encapsulation inside the receptor cavity was observed.[28c]

1.5d Tripodal urea and thiourea receptors

Since the pioneering work of Wilcox[29] and Hamilton[30] that showed that urea moieties can act as appropriate binding sites for anions, particularly oxoanions, a variety of acyclic receptors containing urea and thiourea subunits have been developed and applied for anion complexation and sensing over the past years. In particular, urea and thiourea functions can establish two directional hydrogen bonds with the planar anions (e.g., AcO^- and HCO_3^-) or chelate a spherical anion (e.g., halides). Furthermore, survey of tripodal anion receptors showed the dominant utility of urea and thiourea functionality over other classes of hydrogen bond donors.

Anion binding properties of tripodal urea and thiourea receptors **4a, 4b** and **5a, 5b** were studied using ^{1}H-NMR experiments. In both the cases, a 1:1 complex stoichiometry was suggested upon binding of a dihydrogen phosphate anion *via* six hydrogen bonds inside the tripodal cavity. However, based on the experimental results, Gale et al. has suggested that the phenyl substituted thiourea receptor **5b** is capable of both acting as a chloride/nitrate antiport and more significantly of transporting the more hydrophilic bicarbonate anion *via* a chloride/bicarbonate antiport mechanism than its urea analogue **4b**.[31] The crystal structures of the carbonate complex (Fig. 1.6b) of **5b** revealed that two receptor molecules are oriented in a face-to-face fashion and encapsulate a carbonate anion in the centre *via* twelve strong hydrogen bonding interaction.[31]

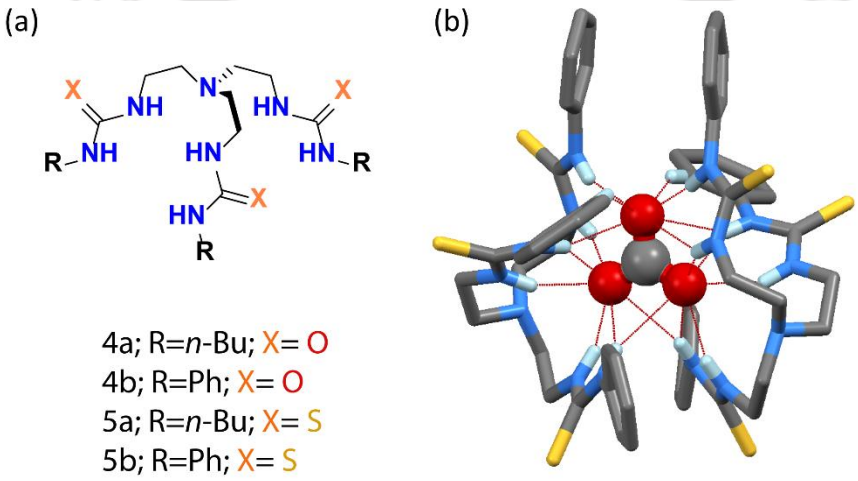

Figure 1.6 (a) Molecular structure of the tripodal urea/thiourea hosts **4a**-**5b**, (b) X-ray structure of the carbonate complex of receptor **5b**.

An 2:1 host-guest mode of sulphate binding within the cage of two inversion-symmetric molecules of receptor (**4d**) has been reported Das et al[32] where sulfate anion is stabilized *via* 12 N−H···O hydrogen bonds with six urea functions (Fig. 1.7b). Receptor **4d** also possesses the ability to uptake aerial CO_2 and stabilize as CO_3^{2-} inside its dimeric capsular assembly (Fig. 1.7c). Another interesting example of 1:1 hydrated sulfate encapsulation by the urea receptor **4c** has been shown by Ganguly, Das and coworker.[33] Structural analysis of the sulfate complex of **4c** showed that, all three urea functions are involved in N−H···O hydrogen bonding with a SO_4^{2-} which is further hydrogen bonded to three water molecules resulting in a coordination number of nine for the encapsulated sulphate. The concurrent interactions of three lattice water molecules with two encapsulated sulfate anions by O···H−O−H···O hydrogen bonds generates a rugby ball shaped sulfate–water–sulfate (SO_4^{2-}–$(H_2O)_3$–SO_4^{2-}) adduct held inside a pseudo dimeric assembly of receptor **4c** (Fig. 1.7d).

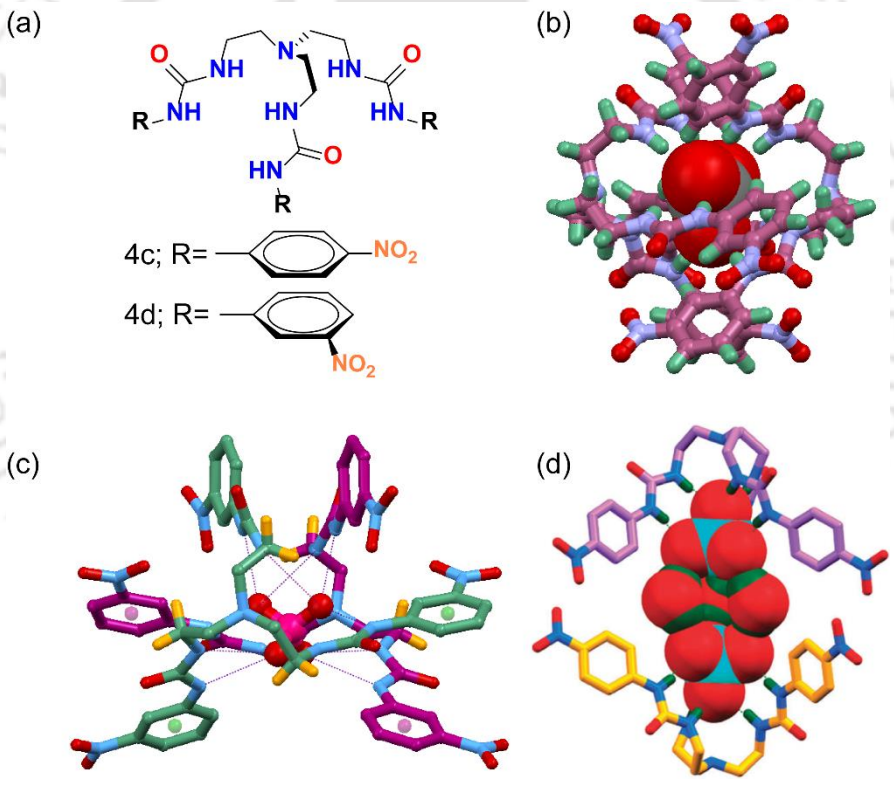

Figure 1.7 (a) Molecular structure of the tripodal urea hosts **4c** and **4d** and X-ray structure of the (b) carbonate encapsulated dimeric capsular complex of receptor **6f,** (c) sulphate encapsulated dimeric capsular complex of receptor **4d** and (d) rugby ball shaped sulfate–water–sulfate (SO_4^{2-}–$(H_2O)_3$–SO_4^{2-}) adduct encapsulated pseudodimeric capsular complex of receptor **4c.** Give the designation of the hosts in the fig. R=p-nitro, m-nitro

Structural analysis of the crystals of the dihydrogen phosphate complexes of **4e** showed that a pseudodimeric capsular assembly trapped a $H_2PO_4^-$ dimer where seven H-bonding interactions had been experienced by each $H_2PO_4^-$ ion[34] (Fig. 1.8b). But, the addition of 2 equivalents TBAOH in to the DMSO solution of the dihydrogen phosphate complexes of **4e** results 2:1

receptor-HPO_4^{2-}complex in solid state (Fig. 1.8c). The charge dependent anion binding discrepancy of phosphates in solid state has been further demonstrated by simple acid/base treatment *via* solution state ^{31}P-NMR studies.

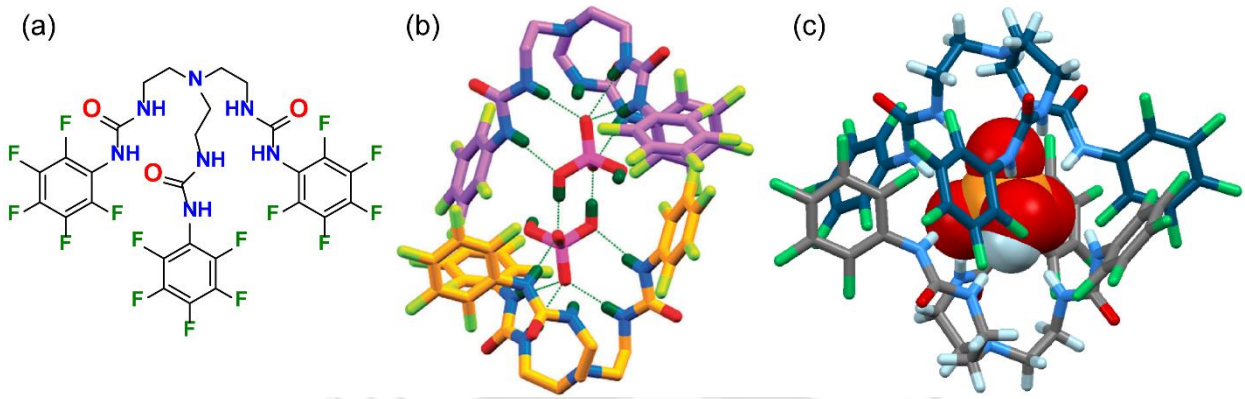

Figure 1.8 (a) Molecular structure of the tripodal urea hosts **4e** and X-ray structure of the (b) $(H_2PO_4^-)_2$ encapsulated pseudodimeric capsular complex and (c) HPO_4^{2-} encapsulated dimeric capsular complex of receptor **4e**.

1.6 Ion-pair receptor chemistry

Ion-pair receptors have potential applications in various fields, such as salt solubilisation, salt extraction and transmembrane ion transport. In spite of their prospective applications, the number of well characterized ion-pair receptors which might permit a greater level of control over these processes remains limited.[35] This could reflect a combination of synthetic challenges to design ion-pair receptors and experimental complexities associated with tracking multiple ionic species in solution as well as the high inherent thermodynamic lability of many ion-pairs in solution.

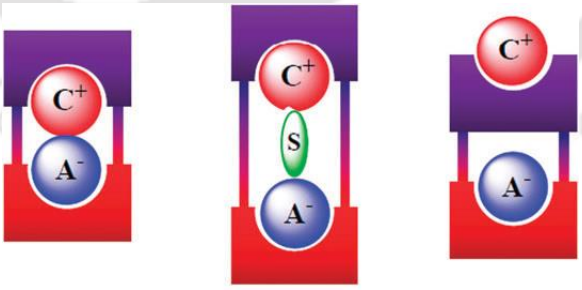

Scheme 1.6 Limiting ion-pair interactions relevant to receptor-mediated ion-pair recognition: (a) Contact; (b) Solvent-bridged, and (c) Host separated. In this schematic, the anion is shown as ''A^-'', the cation as ''C^+'', and the solvent is represented as ''S''. This scheme is reproduced from reference 35

The majority of reported ion-pair receptors rely either on lone pair electron donors including crown ethers or π-electron donors, such as functionalized calixarenes for cation recognition.[36] Since the pioneering discovery by Pedersen,[37] cyclic polyethers (crown ethers) have been used to stabilize low-dimensional structures of alkali metal salts. In most cases, alkali metal ions are

coordinated by the crown ether and linked by water molecules, resulting in one-dimensional structures[38] which exhibit transport properties for ions and water molecules. Moreover, when the metal ion is too large to reside in the crown ether cavity, one-dimensional structures are formed in a side-on fashion.[39]

This combination was successful in liquid–liquid extraction of KF and KCl from aqueous media. Single crystal X-ray structure analysis shows that crown-ether bound K^+ ion is coordinated from both sides by carbonyl O-atom and thereby self-assembles into 1D coordination polymers upon ion-pair recognition[41] (Fig, 1.9c).

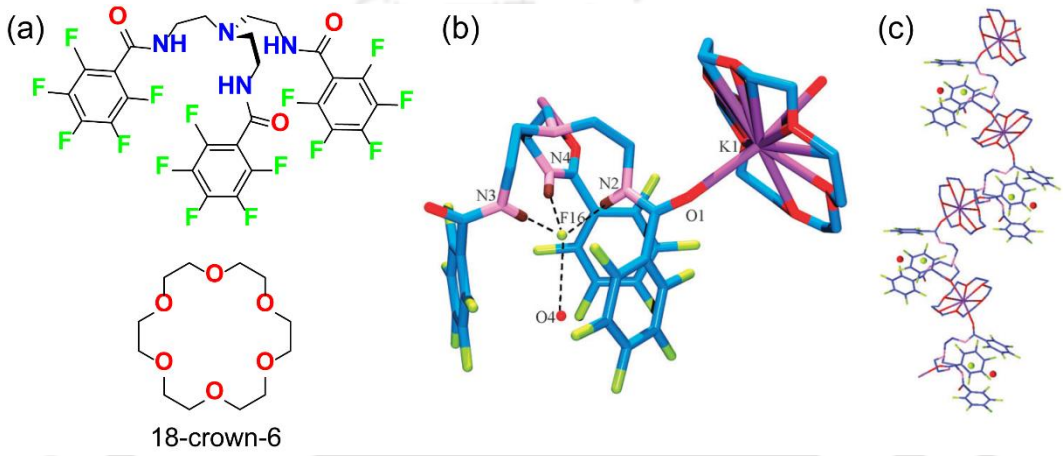

Figure 1.9 (a) Molecular structure of the tripodal amide hosts **3b** and Single crystal X-ray structure of (b) monomeric unit and (b) a 1-D polymer representation of the dual-host complex.

1.7 Objective of the thesis

In general, acyclic receptors with appropriately positioned binding sites can recognize anions and ion-pairs both in solid and solutions and also assist the self-assembly process. In anion receptor chemistry, tris(2-aminoethyl)amine based tripodal receptors have shown their high potential towards anion assisted capsule and pseudo-capsule formation. It was found that the attached aryl terminals and position of the substituents in the aryl ring play an important key role towards the formation of different microenvironment for selective anion binding and encapsulation and hence the architecture the resulting complex. The anion binding functions in the receptors are of utmost concern as they play the driving role towards anion stabilization. Anions generally have very high solvation energies that must be compensated for by the host for effective anion recognition. Usually, oxyanions like sulphate, phosphates and carbonate requires higher coordination number for their sound stabilization. In particular, urea and thiourea functions can establish two directional hydrogen bonds with the planar anions (e.g., AcO^- and HCO_3^-) or chelate a spherical anion (e.g., halides). Thus, it is the design of sophisticated three-dimensional architectures that is essential to fully encapsulate the anions by creating a highly

specific anion-binding pocket/cavity. Urea functionalized tripodal scaffolds offer a flexible and structurally preorganized cavity, which has been widely employed in the binding and recognition of anions because of their favorable conformation for multiple hydrogen bonds that favors the formation of a stable host/guest complex.[42]

The objective of the thesis is to explore the molecular self-assembly in the course of anion and ion-pair coordination chemistry of some newly synthesized simple and some less reported tripodal acyclic urea functionalised receptors bearing specific terminal aryl functions.

The recognition and binding of anions and ion-pairs, and anions and their role towards formation of molecular assembly is definitely a field which can expand considerably and bring immense advances in specialised applications such as: (a) removal and extraction toxic anions and salts from water, (b) drug delivery applications, (c) trapping reactive intermediates inside the molecular cavity, (d) membrane transport, (e) solubilize insoluble anions/salts and (f) Extraction of salts.

References

1. J. W. Steed and J. L. Atwood, *Supramolecular chemistry*, John Wiley and Sons, Ltd; **1997**, 1−6.
2. D. J. Cram, *Angew. Chem., Int. Ed*., **1986**, *25*, 1039.
3. T. Steiner, Hydrogen Bond in the Solid State. *Angew. Chem., Int. Ed.*, **2002**, *41*, 48.
4. (*a*) G. A. Jeffrey, *An Introduction to Hydrogen Bonding*, Oxford University Press, Oxford, **1997**. (*b*) P. Metrangolo and G. Resnati, in *Halogen Bonding In Encyclopedia of Supramolecular Chemistry*, ed. J. L. Atwood and J. W. Steed, Marcel Dekker Inc, New York, **2004**.
5. P. Metrangolo, F. Meyer, T. Pilati, G.Resnati and G. Terraneo, *Angew. Chem. Int. Ed.*, **2008**, *47*, 6114.
6. (*a*) K. Gao, N. S. Goroff, *J. Am. Chem. Soc.*, **2000**, *122*, 9320. (*b*) B. Borgen, O. Hassel, C. Romming, *Acta Chem. Scand.*, **1962**, *16*, 2469. (*c*) A. Sun, N. S. Goroff, J. W. Lauher, *Science*, **2006**, *312*, 1030.
7. (*a*) F. Guthrie, *J. Chem. Soc.*, **1863**, *16*, 239. (*b*) W. H. Seamon, J. W. Mallet, *Chem. News.*, **1881**, *44*, 188.
8. H. A. Benesi and J. H. Hildebrand, *J. Am. Chem. Soc.*, **1949**, *71*, 2703.
9. O. Hassel, *Science*, **1970**, *170*, 497.
10. (*a*) G. Resnati, T. Pilati, R. Liantonio and F. Meyer, *J. Polym. Sci., Part A: Polym. Chem.*, **2007**, *45*, 1 and references therein. (*b*) H. L. Nguyen, P. N. Horton, M. B. Hursthouse, A. C. Legon and D. W. Bruce, *J. Am. Chem. Soc.*, **2004**, *126*, 16. (*c*) J. Xu, X. Liu, J. K.-P. Ng, T. Lin and C. He, *J. Mater. Chem.*, **2006**, *16*, 3540.

11. (*a*) M. Fourmigue and P. Batail, *Chem. Rev.*, **2004**, *104*, 5379. (*b*) M. Fourmigue, in Halogen Bonding Fundamentals and Applications, ed. P. Metrangolo and G. Resnati, Springer, Berlin, **2008**, pp. 181–208.
12. (*a*) J. A. R. P. Sarma, F. H. Allen, V. J. Hoy, J. A. K. Howard, R. Thaimattam, K. Biradha and G. R. Desiraju, *Chem. Commun.*, **1997**, 101. (*b*) P. K. Thallapally, G. R. Desiraju, M. Bagieu-Beucher, R. Masse, C. Bourgogne and J. F. Nicoud, *Chem. Commun.*, **2002**, 1052.
13. (*a*) T. Caronna, R. Liantonio, T. A. Logothetis, P. Metrangolo, T. Pilati and G. Resnati, *J. Am. Chem. Soc.*, **2004**, *126*, 4500. (*b*) H. L. Nguyen, P. N. Horton, M. B. Hursthouse, A. C. Legon and D. W. Bruce, *J. Am. Chem. Soc.*, **2004**, *125*, 16. (*c*) A. Sun, N. S. Goroff and J. W. Lauher, *Science*, **2006**, *312*, 1030. (*d*) P. Metrangolo, Y. Carcenac, M. Lahtinen, T. Pilati, K. Rissanen, A. Vij and G. Resnati, *Science*, **2009**, *323*, 1461.
14. (*a*) Y. Lu, T. Shi, Y. Wang, H. Yang, X. Yan, X. Luo, H. Jiang and W. Zhu, *J. Med. Chem.*, **2009**, *52*, 2854. (*b*) C. Bissantz, B. Kuhn and M. Stahl, *J. Med. Chem.*, **2010**, *53*, 5061.
15. (*a*) Z. Wang, H. Luecke, N. Yao and F. A. Quiocho, *Nat. Struct. Biol.*, **1997**, *4*, 519. (*b*) J. W. Pflugrath and F. A. Quiocho, *Nature*, **1985**, *314*, 257. (*c*) C. J. Avers, *Molecular Cell Biology*., Addison-Wesley: Reading, **1986**.
16. J. L. Sessler, P. A. Gale and W. S. Cho, *Anion Receptor Chemistry*, The Royal Society of Chemistry, Cambridge, UK, **2006**.
17. P. Auffinger, F. A. Hays, E. Westhof and P. S. Ho, *Proc. Natl. Acad. Sci.*, U. S. A., **2004**, *101*, 16789.
18. A. Bianchi, K. Bowman-James and E. Garcia-Espana, *Supramolecular Chemistry of Anions*, Wiley-VCH, New York, **1997**.
19. B. A. Moyer and P. V. Bonnesen, *Physical factors in anion separations, In Supramolecular Chemistry of Anions*; Wiley-VCH: New York, **1997**; chapter 1.
20. D. J. Mercer and S. J. Loeb, *Chem. Soc. Rev.*, **2010**, *39*, 3612.
21. K. Bowman-James, *Acc. Chem. Res.*, **2005**, 38, 671.
22. (*a*) H. -J. Schneider and A. K. Yatsimirsky, *Chem. Soc. Rev.*, **2008**, *37*, 263. (*b*) E. Garcia-Espana, P. Diaz, J. M. Llinares and A. Bianchi, *Coord. Chem. Rev.*, **2006**, *250*, 2952. (*c*) S. O. Kang, M. A. Hossain and K. Bowman-James, *Coord. Chem. Rev.*, **2006**, *250*, 3038.
23. (*a*) C. Caltagirone and P. A. Gale, *Chem. Soc. Rev.*, **2009**, *38*, 520. (*b*) P. A. Gale, *Acc. Chem. Res.*, **2006,** *39*, 465. (*c*) A-F. Li, J-H. Wang, F. Wang and Y-B. Jiang, *Chem. Soc. Rev.*, **2010**, *39*, 3729.
24. (*a*) T. Gunnlaugsson, P. E. Kruger, P. Jensen, F. M. Pfeffer and G. M. Hussey, *Tetrahedron Lett.*, **2003**, *44*, 8909. (*b*) S. Camiolo, P. A. Gale, M. B. Hursthouse and M. E. Light, *Org. Biomol. Chem.*, **2003**, *1*, 741. (*c*) V. Amendola, D. Esteban-Gomez, L. Fabbrizzi and M. Licchelli, *Acc. Chem. Res.*, **2006**, *39*, *343*.
25. M. G. Chudzinski, C. A. McClary and M. S. Taylor, *J. Am. Chem. Soc.*, **2011**, *133*, 10559.
26. A. Mele, P. Metrangolo, H. Neukirch, T. Pilati and G. Resnati, *J. Am. Chem. Soc.*, **2005**, *127*, 14972.

27. M. Isiklan, M. A. Saeed, A. Pramanik, B. M. Wong, F. R. Fronczek, and M. A. Hossain, *Cryst. Growth Des.*, **2011**, *11*, 959.
28. (*a*) S. K. Dey and G. Das, *Chem. Commun.*, **2011**, *47*, 4983. (*b*) S. K. Dey and G. Das, *Cryst. Eng. Comm.*, **2012**, *14*, 5305. (*c*) S. K. Dey and G. Das, *Cryst. Growth Des*., **2011**, *11*, 4463.
29. P. J. Smith, M. V. Reddington and C. S. Wilcox, *Tetrahedron Lett*., **1992**, *33*, 6085.
30. E. Fan, S. A. Van Arman, S. Kincaid and A. D. Hamilton, *J. Am. Chem. Soc*., **1993**, *115*, 369.
31. N. Busschaert, P. A. Gale, C. J. E. Haynes, M. E. Light, S. J. Moore, C. C. Tong, J. T. Davis and W. A. Harrell, Jr., *Chem. Commun*., **2010**, *46*, 6252.
32. S. K. Dey, R. Chutia and G. Das, *Inorg. Chem*., **2012**, *51*, 1727.
33. D. A. Jose, D. K. Kumar, B. Ganguly and A. Das, *Inorg. Chem*., **2007**, *46*, 5817.
34. (*a*) P. S. Lakshminarayanan, I. Ravikumar, E. Suresh and P. Ghosh, *Chem. Commun*., **2007**, 5214. (*b*) B. Akhuli, I. Ravikumar, and P. Ghosh, *Chem. Sci.*, **2012**, *3*, 1522.
35. S. K. Kim and J. L. Sessler, *Chem. Soc. Rev.*, **2010**, *39*, 3784.
36. (*a*) G. W. Gokel, W. M. Leevy and M. E. Weber, Chem. Rev., **2004**, *104*, 2723. (*b*) A. Ikeda and S. Shinkai, *Chem. Rev.*, **1997**, *97*, 1713. (*c*) J. S. Kim and D. T. Quang, *Chem. Rev*., **2007**, *107*, 3780.
37. C. J. Pedersen, *J. Am. Chem. Soc.*, **1967**, *89*, 7017.
38. K. M. Fromm, *Coord. Chem. Rev.*, **2008**, *252*, 856.
39. M. D. Brown, J. M. Dyke, F. Ferrante, W. Levason, J. S. Ogden and M. Webster, *Chem.–Eur. J.*, **2006**, *12*, 2620.
40. (*a*) M. M. Murad, T. Hayashita, K. Shigemori, S. Nishizawa and N. Teramae, Anal. Sci., **1999**, *15*, 1185. (*b*) K. Kavallieratos, R. A. Sachleben, G. J. V. Berkel and B. A. Moyer, *Chem. Commun.*, **2000**, 187. (*c*) K. Kavallieratos, A. Danby, G. J. V. Berkel, M. A. Kelly, R. A. Sachleben, B. A. Moyer and K. Bowman-James, *Anal. Chem.*, **2000**, *72*, 5258. (*d*) G. Cafeo, G. Gattuso, F. H. Kohnke, A. Notti, S. Occhipinti, S. Pappalardo and M. F. Parisi, *Angew. Chem., Int. Ed.*, **2002**, *41*, 2122.
41. I. Ravikumar, S. Saha and P. Ghosh, Chem. Commun., **2011**, *47*, 4721.
42. (*a*) R. Custelcean, B. A. Moyer and B. P. Hay, *Chem. Commun.*, **2005**, *47*, 5971. (*b*) N. Busschaert, M. Wenzel, M. E. Light, P. Iglesias-Hernandez, R. Perez-Tomas and P. A. Gale, P. A. *J. Am. Chem. Soc.*, **2011**, *133*, 14136.

Chapter 2

Experimental Methods

&

Characterization

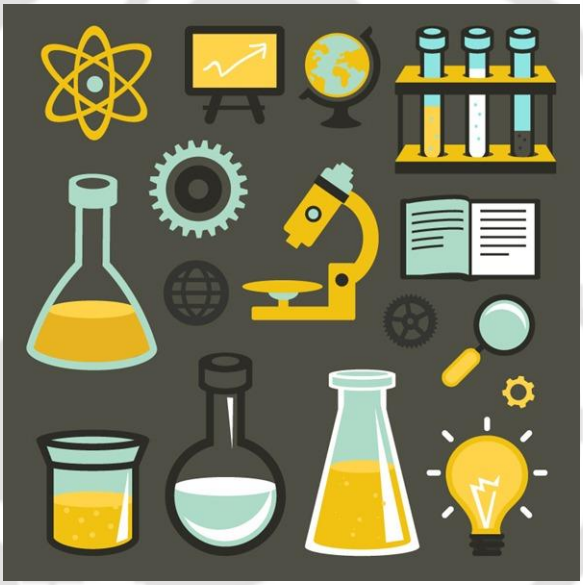

In this chapter, a detailed report of the various reagents used in the synthesis of acyclic receptors **L_1-L_5** (Scheme 2.1), their synthetic procedures, crystallization details and specifications of instruments/equipment employed in the characterization of synthesized receptors and their various complexes with anions are presented.

2.1 Materials

All reagents and solvents were obtained from commercial sources and used as received without further purification. Tris(2-aminoethyl)amine (tren), 2-nitrophenylisocyanate, 3-nitrophenylisocyanate, 4-nitrophenylisocyanate, 4-iodophenylisocyanate, and 4-bromophenyl isocyanate were purchased from Sigma-Aldrich (U.S.A) All quaternary ammonium salts were purchased from Sigma-Aldrich (U.S.A) whereas, inorganic and organic salts such as H_3PO_4, terephthalic acid were obtained either from Merck or LOBA chemicals (India). All sodium, potassium salts and deuterated solvent DMSO-d_6 were purchased from Merck chemicals (India) and used as received. Solvents for synthesis and crystallization experiments were purchased either from Merck or LOBA chemicals (India) and dried using standard procedures, wherever mentioned in the synthetic procedures.

2.2 Experimental methods

^{1}H, NMR and 2D NOESY NMR spectra were recorded on a Varian FT-400 MHz instrument and a Bruker 600 MHz. Instrument chemical shifts were recorded in parts per million (ppm) on the scale using tetramethylsilane (TMS) or residual solvent peak as a reference. ^{13}C spectra were obtained at 100 MHz or 150 MHz at 298 K. FT-IR spectra were recorded on a Perkin-Elmer-Spectrum One FT-IR spectrometer with KBr disks in the range 4000-450 cm^{-1}. Powder X-ray diffraction patterns of dried crystalline powder were recorded using a Bruker-D8 Advance X-ray diffractometer with Cu-$K\alpha$ radiation at λ = 0.15418 nm. Thermal analysis (TGA) of dried samples was performed using an SDTA 851-E TGA thermal analyser (*Mettler Toledo*) with a heating rate of 5-10^{o}C/min in a N_2 atmosphere. The absorption spectra were recorded on a Perkin-Elmer Lambda-25/35 UV-Visible spectrophotometer with a quartz cuvette.

Association constants (log *K* or *K*) of anions with receptors (**L_1-L_3** and **L_5**) were obtained by ^{1}H NMR titrations of the receptor with tetraethyl ammonium (TEA) or tetrabutyl ammonium (TBA) salts of anions in DMSO-d_6 at 298 K. The initial concentration of the receptor solution was 5 mM/10 mM. Aliquots of anions were added from the stock solutions up to 1:10 host-guest stoichiometry. The residual solvent peak in DMSO-d_6 (2.50 ppm) was used as an internal reference, and each titration was performed with at least 10-15 measurements.

For **L_1** and **L_2**, WinEQNMR2 software was used to calculate the binding constants (*K*) values.[1]

For $\mathbf{L_3}$ and $\mathbf{L_5}$, following equation was used to determine the association constant (K) values.

$\Delta\delta = \{([A]_0 + [\mathbf{L}]_0 + 1/K) +/- (([A]_0 + [\mathbf{L}]_0 + 1/K)^2 - 4[\mathbf{L}]_0[A]_0)^{1/2}\} \Delta\delta_{max}/2[\mathbf{L}]_0$

Where, **L** = receptor and A = anion. An error limit in log K was less than 15%.

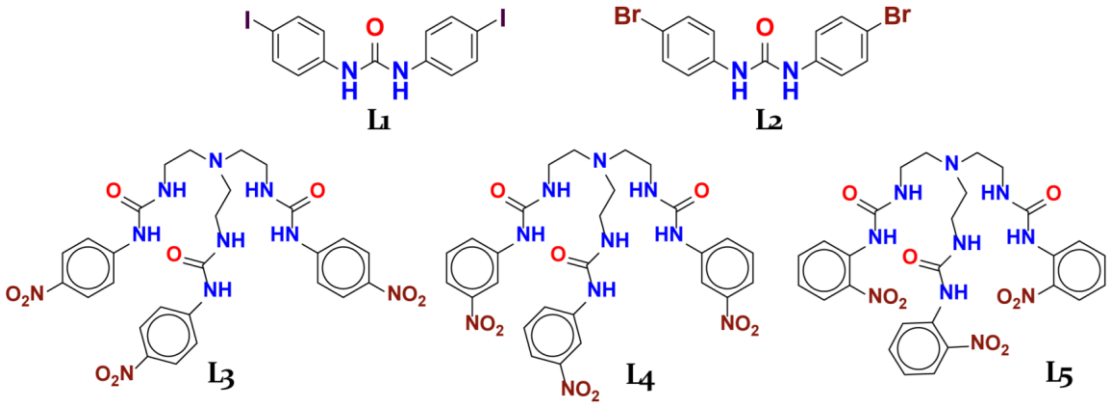

Scheme 2.1 Molecular structures of the receptors ($\mathbf{L_1}$-$\mathbf{L_5}$).

2.3 Single crystal X-ray crystallography

In each case, a crystal of suitable size was selected from the mother liquor and immersed in silicone oil, and it was mounted on the tip of a glass fiber and cemented using epoxy resin. The intensity data were collected using a Bruker SMART APEX-II CCD diffractometer, equipped with a fine focus 1.75 kW sealed tube Mo-K_α radiation (λ = 0.71073 Å) at 298(3) K, with increasing ω (width of 0.3° per frame) at a scan speed of 5 s/ frame. The SMART software was used for data acquisition. Data integration and reduction were undertaken with SAINT and XPREP software.[2] Multi-scan empirical absorption corrections were applied to the data using the program SADABS.[3] Structures were solved by direct methods using SHELXS-97[4] and refined with full-matrix least-squares on F^2 using SHELXL-97.[5] All non-hydrogen atoms were refined anisotropically and hydrogen atoms attached to all carbon atoms were geometrically fixed and the positional and temperature factors are refined isotropically. Hydrogen atoms attached with the urea nitrogen atoms were located from electron Fourier map and refined isotropically. Usually, temperature factors of hydrogen atoms attached to carbon atoms are refined by restraints -1.2 or -1.5 U_{iso} (C), although the isotropic free refinement is also acceptable. Structural illustrations have been drawn with MERCURY 2.3[6] and MERCURY-3.0.[7] for Windows. PLATON-was performed to refine the caged cluster complex **3e** to simplify the complex with a large volume 25630 Å^3 symmetrically. The high wR2 value (38%) for complex **3e** may be due to the disorder in the *n*-TBA cations and comparatively poor data quality because of the rapid loss of solvent molecules (MeCN) and the situation did not improve even after recrystallization and fresh data collection. Disorder in the *n*-TBA units was modelled using standard crystallographic methods including constraints, restraints and rigid bodies to modify

the disorder in the *n*-TBA units. PART instruction has been also used in the complexes of $\mathbf{L_1}$ and $\mathbf{L_2}$ whenever necessary. However, PART instruction in the case of complex **3e** to modify the disorder in the *n*-TBA units but found to be not so fruitful. All the crystallographic data have been deposited to the CCDC. Parameters for data collection and crystallographic refinement details of the receptors and their various anion and/or ion-pair complexes are summarized in the respective chapters.

2.4 Synthesis and characterization of receptors, (L_1-L_3 and L_5)

2.4.1 1,3-bis(4-iodophenyl)urea (L_1)

Symmetric receptor $\mathbf{L_1}$ has been synthesized in quantitative yield by the equimolar reaction of the aromatic amine with the corresponding phenylisocyanate. 4-iodophenylisocyanate (0.490g or 2 mmol) was dissolved in dry tetrahydrofuran (THF) in a 50 mL round bottomed flask and 4-iodoaniline (0.438g or 2 mmol) dissolved in dry THF was added was added drop-wise (using a dropping funnel) over a period of half hour with constant stirring at room temperature. The resulting solution mixture was stirred overnight at room temperature. The colourless precipitate formed, was filtered off and washed with 10 ml of dichloromethane (DCM) and then 10 ml of methanol a couple of times to remove the unreacted reagents. The precipitate thus collected was dried in air and characterized by NMR, FT-IR, ESI-MS and single crystal X-ray diffraction analyses. Yield: 87%.

^{1}H NMR (DMSO-d_6, 400 MHz): δ (ppm) at 298 K, 7.28 (d, 4H, ArH), 7.59 (d, 4H, ArH), 8.832 (s, 2H, −NH). ^{13}C NMR (150 MHz, DMSO-d_6): δ (ppm) 84.98 (2C, ArH), 120.67 (4C, ArH), 137.43 (4C, ArH), 139.49 (2C, ArH), 152.30 (1C, CvO). ESI-Mass: m/z = 463.07 $[M]^+$. FT-IR (ν, cm^{-1}): 1005 (C−I), 1236 (C−N), 1549 (C=C), 1637 (−C=O), 3301 (N−H).

2.4.2 1,3-bis(4-bromophenyl)urea (L_2)

Receptor $\mathbf{L_2}$ was synthesized in the same way as $\mathbf{L_1}$ using 4-bromophenylisocyanate and 4-bromoaniline in quantitative yield.

^{1}H NMR (DMSO-d_6, 600 MHz): δ (ppm) at 298 K, 7.417 (d, 4H, ArH), 7.435 (d, 4H, ArH), 8.829 (s, 2H, –NH). ^{13}C NMR (150 MHz, DMSO-d_6): δ (ppm) 113.609 (2C, ArH), 120.457 (4C, ArH), 131.675 (4C, ArH), 139.027 (2C, ArH), 152.434 (1C, C=O). ESI-Mass: m/z = 369.06 $[M]^+$. FT-IR (ν, cm^{-1}): 1070 (C−Br), 1236 (C−N), 1555 (C=C), 1641 (−C=O), 3299 (N−H).

2.4.3 Tris(2-aminoethyl)-4-nitrophenylurea (L_3)

Reaction of tris(2-aminoethyl)amine, (tren) with 4-nitrophenyl isocyanate in a 1:3 molar ratio at room temperature yielded the tris(urea) receptor, $\mathbf{L_3}$ in quantitative yield. 2.460 g (15 mmol) of 3-nitrophenyl isocyanate was dissolved in 30 mL of dry tetrahydrofuran (THF) in a 100 mL

round bottomed flask and 0.730 ml (5 mmol) of tris(2-aminoethyl)amine (tren) dissolved in 10 ml of dry THF was added drop-wise (using a dropping funnel) over a period of 1 hour with constant stirring at room temperature. The resulting solution mixture was stirred overnight at room temperature when a pale yellow precipitate was formed. Then, the volume of the solvent (THF) was reduced to around 10 ml under *vacuum* and the obtained solid product was filtered off and washed with 10 ml of dichloromethane (DCM) a couple of times to remove the unreacted reagents. The pale yellow precipitate thus collected was dried in air and characterized by NMR, FT-IR, ESI-MS and single crystal X-ray diffraction analyses. Yield: 82%.

^{1}H NMR (DMSO-d_6, Varian-400 MHz): at 298 K, δ (ppm), 2.62 (t, 6H, −NCH_2), 3.23 (t, 6H, −$NHCH_2$), 6.44 (s, 3H, −NH_a), 7.57 (d, 6H, ArH), 8.08 (d, 6H, ArH), 9.37 (s, 3H, −NH_b).

2.4.4 Tris(2-aminoethyl)-2-nitrophenylurea (L_5)

Receptor **L_5** was synthesized in the same way as **L_3** using tris(2-aminoethyl)amine, (tren) and 2-nitrophenylisocyanate in a 1:3 molar ratio at room temperature. Yield 80%.

^{1}H NMR (DMSO-d_6 Varian-400 MHz): at 298 K, δ (ppm), 2.63 (t, 6H, −NCH_2), 3.21 (t, 6H, −$NHCH_2$), 7.084 (t, 3H, ArH), 7.457 (s, 3H, −NH_a), 7.573 (t, 3H, ArH), 7.99 (d, 3H, ArH), 8.24 (d, 3H, ArH) 9.355 (s, 3H, −NH_b).

2.5 Synthesis and characterization of anion complexes of the receptors L_1-L_5 and ion-pair complex of the receptor L_3

2.5.1 Complexes of the receptor L_1

Bicarbonate-complex, (*n*-TBA)[L_1·HCO_3^-], (1a). Colorless block-shaped crystals of bicarbonate complex **1a**, suitable for single-crystal X-ray diffraction analysis were obtained by charging an excess (10 equiv.) of n-tetrabutylammonium fluoride (*n*-TBAF) into a 5 mL MeCN solution of **L_1** (46.4 mg, 0.1 mmol). After the addition of *n*-TBAF, the initially insoluble **L_1** gets dissolved in MeCN and the solution was stirred for about 30 min at room temperature and filtered in a test tube for slow evaporation. After 4–5 days, the isolated yield of 1a was 92%. Mp: 140 °C.

^{1}H NMR (DMSO-d_6, Bruker-600 MHz) at 298 K, δ (ppm) 1.011 (t, 12H, n-TBA−CH_3), 1.28 (q, 8H, n-TBA−CH_2), 1.533 (q, 8H, *n*-TBA−CH_2), 3.125 (t, 8H, n-TBA−N^+CH_2), 7.57 (d, 4H, ArH), 7.520 (d, 4H, ArH), 10.67 (s, 2H, −NH). ^{13}C NMR (DMSO-d_6, Bruker-150 MHz) at 298 K, δ (ppm), 13.59 (4C, *n*-TBA−CH_3), 19.29 (4C, *n*-TBA−CH_2), 23.15 (4C, *n*-TBA−CH_2), 57.64 (4C, n-TBA−N^+−CH_2), 84.12 (2C, ArH), 120.15 (4C, ArH), 137.21 (4C, ArH), 140.46 (2C, ArH), 153.05 (1C, C=O), and 182.12 (1C, HCO_3^- anion), FT-IR (ν, cm^{-1}): 822 (HCO_3^-), 1231 (C−N), 1537 (CvC), 1577 (C−O), 1697 (−C=O), 2960 (C−H), 3420 (N−H), 3511 (O−H).

Acetate-complex, (*n*-TBA)[$L_1 \cdot CH_3COO^-$] (1b). Acetate-complex **1b** was obtained by adding an excess of *n*-tetrabutylammonium acetate into a 5 mL MeCN solution of $\mathbf{L_1}$ (46.4 mg, 0.1 mmol).

In the same fashion, after the addition of acetate salt, the initially insoluble $\mathbf{L_1}$ gets dissolved in MeCN and the solution was stirred for about 30 min at room temperature and filtered in a test tube. The slow evaporation of the filtrate at room temperature yielded colorless crystals suitable for single crystal X-ray crystallographic analysis within 8–10 days. The isolated yield of **1b** was 70%. Mp: 178 °C.

^{1}H NMR ($CDCl_3$, Varian-400 MHz) at 298 K, δ (ppm), 0.93 (t, 12H, n-TBA−CH_3), 1.294 (q, 8H, *n*-TBA−CH_2), 1.43 (t, 8H, *n*-TBA–CH_2), 2.029 (s, Acetate−CH_3), 2.987 (t, 8H, *n*-TBA−N^+CH_2), 7.485 (d, 4H, ArH), 7.53 (d, 4H, ArH), 11.67 (s, 2H, −NH). ^{13}C NMR (DMSO-d_6, Bruker-150 MHz) at 298 K, δ (ppm) 13.57 (4C, *n*-TBA−CH_3), 19.27 (4C, *n*-TBA−CH_2), 23.12 (4C, *n*-TBA−CH_2), 24.73 (1C, Acetate–CH_3) 57.61 (4C, *n*-TBA−N^+CH_2), 84.17 (2C, ArH), 120.59 (4C, ArH), 137.21 (4C, ArH), 140.43 (2C, ArH), 152.97 (1C, C=O) and 176.53 (acetate−COO^-). FT-IR (ν, cm^{-1}): 642 (−COO deformation), 823 (−COO^-), 1003 (C−I), 1235 (C−N), 1553 (C=C), 1634 (−C=O), 2961 (C−H), 3301 (N−H).

2.5.2 Complexes of the receptor L_2

Hexafluorosilicate-Complex, 2(*n*-TBA)[$L_2.SiF_6^{2-}$], (2a). The SiF_6^{2-} complex **2a** of $\mathbf{L_2}$ was obtained during the similar attempt as in the case of complex **1a**, but with a complete different result. After the addition an excess of n-tetrabutylammonium fluoride (*n*-TBAF) into a 5 mL MeCN solution of $\mathbf{L_2}$ (37 mg, 0.1 mmol) contained in a glass vial, the solution was stirred for about 30 minute at room temperature and filtered in a test tube. Slow evaporation of the filtrate at room temperature yielded colorless crystals suitable for single crystal X-ray crystallographic analysis within 7−8 days. Isolated yield of **2a** was 65%.Mp: 133 °C.

^{1}H NMR (DMSO-d_6, Bruker-600 MHz) at 298 K, δ (ppm) 0.922 (t, 12H, *n*-TBA−CH_3), 1.30 (s, 8H, *n*-TBA−CH_2), 1.55 (p, 8H, *n*-TBA−CH_2), 3.143 (s, 8H, *n*-TBA−N^+CH_2), 7.374 (d, 4H, ArH), 7.52 (d, 4H, ArH), 11.043 (s, 2H, −NH).^{13}C NMR (DMSO-d_6, Bruker-150 MHz) at 298 K, δ (ppm) 13.54 (4C, *n*-TBA−CH_3), 19.27 (4C, *n*-TBA−CH_2), 23.14 (4C, *n*-TBA−CH_2), 57.64 (4C, *n*-TBA−N^+CH_2), 112.69 (2C, ArH), 120.14 (4C, ArH), 131.31 (4C, ArH), 140.44 (2C, ArH) and 153.41 (1C, C=O). FT-IR (ν, cm^{-1}): 740(SiF_6^{2-}), 1008(C−Br), 1227 (C−N), 1648 (−C=O), 2962 (C−H), 3422 (N−H).

Acetate-complex, (*n*-TBA)[$L_2 \cdot CH_3COO^-$], (2b). Acetate-complex **2b** was obtained in the same way as complex **1b**. Mp: 118 °C.

^{1}H NMR (DMSO-d_6, Bruker-600 MHz) at 298 K, δ (ppm), 0.91 (t, 12H, *n*-TBA−CH_3), 1.293 (q, 8H, *n*-TBA−CH_2), 1.541 (s, 8H, *n*-TBA−CH_2), 1.799 (s, acetate−CH_3), 3.132 (s, 8H, *n*-TBA−N^+CH_2), 7.384 (d, 4H, ArH), 7.547 (d, 4H, ArH), 11.39 (s, 2H, −NH). ^{13}C NMR (DMSO-d_6, Bruker-150 MHz) at 298 K. δ

(ppm) 13.57 (4C, *n*-TBA−CH_3), 19.29 (4C, *n*-TBA−CH_2), 23.15 (4C, *n*-TBA−CH_2), 24.74 (1C, acetate−CH_3), 57.65 (4C, *n* TBA−N^+CH_2), 112.49 (2C, ArH), 120.15 (4C, ArH), 131.31 (4C, ArH), 140.46 (2C, ArH), 153.44 (1C, C=O) and 176.53 (acetate−COO^-). FT-IR (ν, cm^{-1}): 642 (−COO deformation), 829 (−COO^-), 1070 (C−Br), 1236 (C−N), 1564 (C=C), 1634 (−C=O), 2962 (C−H), 3305 (N−H).

2.5.3 Complexes of the receptor L_3

Carbonate complex, 2(TEA)[2L_3(CO_3^{2-})], (3a). Carbonate-encapsulated complex **3a** was obtained as suitable crystals for X-ray diffraction analysis by stirring a DMSO solution containing the receptor **L_3** and excess (TEA)HCO_3 for about 30 min at room temperature and filtered in a test tube for slow evaporation. The colorless crystals thus obtained were isolated by filtration and dried at room temperature by pressing between the filter papers before characterization by NMR and FT-IR analyses. Isolated yield: 72% based on **L_3** after 2 weeks of exposure to unmodified atmosphere.

^{1}H NMR (DMSO-d_6, 400 MHz): δ (ppm) 1.11 (t, 24H, TEA−CH_3), 2.47−2.51 (t, 12H, −NCH_2), 3.14 (t, 12H, −$NHCH_2$), 7.53 (d, 12H, ArH), 7.80 (d, 12H, ArH), 7.96 (s, 6H, urea−NH_a), 10.88 (s, 6H, urea−NH_b). ^{13}C NMR (100 MHz, DMSO-d_6): δ (ppm) 7.05 (×8C, TEA−CH3), 37.13 (×6C, −NCH_2), 51.37 (×8C, TEA−CH_2), 53.34 (×6C, −$NHCH_2$), 116.65 (×12C, Ar), 124.5 (×12C, Ar), 139.74 (×6C, Ar), 147.85 (×6C, Ar), 154.84 (×6C, −C=O), 172.01 (CO_3^{2-}). FT-IR (υ cm^{-1}): 1108 (C=O, CO_3^{2-}), 1324 (NO_2-sym.), 1523 (NO_2-asym.), 1707 (C=O), 2968 (C−H), 3327 (N−H).

Terephthalate Complex, 2(*n*-TBA)[2L_3($C_8H_4O_4^{2-}$)], (3b).Terephthalate complex **3b** was obtained as suitable crystals for X-ray diffraction analysis from a DMF solution mixture of **L_3** charged with an excess of a 1:2 solution mixture of terephthalic acid and TBA(OH). A 3 mL DMF solution mixture of terephthalic acid and TBA(OH) (5 equiv. of 1:2 mixture) was stirred for about 15 min before adding to a 5 mL DMF solution of **L_3**. Slow evaporation of the solution at room temperature yielded colorless crystals of **3b** within a duration of 2 weeks. Isolated yield: 76% based on **L_3** after 3−4 weeks of exposure to unmodified atmosphere.

^{1}H NMR (DMSO-d_6, 400 MHz): δ (ppm) 0.78 (t, 24H, *n*-TBA−CH_3), 1.15 (q, 16H, *n*-TBA−CH_2), 1.41 (s, 16H, *n*-TBA−CH_2), 2.50 (s, 12H, −NCH_2), 3.02 (t, 16H, *n*-TBA−N^+CH_2), 3.11 (t, 12H, −$NHCH_2$), 7.38 (s, 6H, urea−NH_a), 7.52 (d, 12H, ArH), 7.92 (d, 12H, ArH), 10.364 (s, 6H, urea−NH_b). 13C NMR (100 MHz, DMSO-d_6): δ (ppm) 13.67 (×8C, TBA−CH3), 19.43 (×8C, TBA−CH2), 23.29 (×8C, TBA−CH_2), 37.36 (×6C, −NCH_2), 53.71 (×6C, −$NHCH_2$), 57.80 (×8C, TBA−N^+CH_2), 116.88 (×12C, Ar), 125.18 (×12C, Ar), 128.82 (×4C, Ar), 139.95 (×2C, Ar), 140.23 (×6C, Ar), 147.98 (×6C, Ar), 155.07 (×6C, −C=O), 172.35 (−COO^-). FTIR (υ cm^{-1}): 1107 (C−O; −COO^-), 1330 (NO_2-sym.), 1502−1557 (NO_2-asym.), 1705 (−C=O), 2963 (C−H), 3321 (N−H).

Fluoride complex, *n*-TBA[$L_3(F^-)$], (3c). Fluoride-encapsulated complex **3c** was obtained as crystalline precipitate by stirring a DMSO solution containing the receptor $\mathbf{L_3}$ and excess *n*-TBAF for about 30 min at room temperature and filtered in a test tube for slow evaporation. Isolated yield: 48% based on $\mathbf{L_3}$ after 10 days of exposure to unmodified atmosphere.

^{1}H NMR (DMSO-d_6, 400 MHz): δ (ppm) 0.885 (t, 12H, *n*-TBA−CH_3), 1.26 (q, 8H, *n*-TBA−CH_2), 1.50 (t, 8H, *n*-TBA−CH_2), 2.49 (s, 6H, −NCH_2), 3.12 (t, 8H, *n*-TBA−N^+CH_2), 3.21 (s, 6H, −$NHCH_2$), 7.29 (s, 3H, urea–NH_a), 7.64 (d, 6H, ArH), 8.08(d, 6H, ArH), 11.16 (s, 6H, urea–NH_b); ^{19}F NMR (DMSO-d_6, 400 MHz): δ (ppm) -122.06 (s, fluoride); ^{13}C NMR (DMSO-d_6, 100 MHz): δ (ppm), 13.45 (×4C, *n*-TBA−CH_3), 19.22 (×4C, *n*-TBA−CH_2), 23.09 (×4C, *n*-TBA−CH_2), 35.58 (×3C, −NCH_2), 50.513 (×3C, −$NHCH_2$), 57.58 (×4C, *n*-TBA−N^+CH_2), 116.33 (×6C, Ar), 125.26 (×6C, Ar), 140.00 (×3C Ar), 147.79 (×3C Ar), 154.77 (×3C, −C=O).

Dual-host complex, [$2L_3.2L_C(2K^+)(CO_3^{2-})$], (3d): On the basis of complex **3a**, the stoichiometry for this three component complexation reaction has been taken in a ratio of 2 : 2 : 1 = $\mathbf{L_3}$: $\mathbf{L_C}$: K_2CO_3. 13.82 mg (0.1 mmol) of K_2CO_3 was added into a 10 ml DMSO solution of $\mathbf{L_3}$ and $\mathbf{L_C}$ mixture, containing 128 mg (0.2 mmol) of $\mathbf{L_3}$ and 52.82 mg (0.2 mmol) of $\mathbf{L_C}$. The resulting solution was stirred vigorously for about an hour at 60˚C. The solution was then allowed to cool at room temperature and filtered. Slow evaporation of the filtrate at room temperature yielded good quality colourless crystals suitable for single crystal X-ray crystallography analysis. Isolated yield: 45% based on $\mathbf{L_3}$ after ~15 days. m.p. 176ºC.

^{1}H NMR (DMSO-d_6, 400 MHz) δ (ppm), 2.47-2.51(t, 12H, −NCH_2), 3.14(t, 12H, −$NHCH_2$), 3.50 (s, 48H, crown ether−CH_2), 7.53 (d, 12H, ArCH), 7.80 (d, 12H, ArCH), 7.94 (s, 6H, urea−NH_a), 10.88 (s, 6H, urea–NH_b); ^{13}C NMR (100 MHz, DMSO-d_6): δ (ppm) 37.18 (×6C, –NCH_2), 53.39 (×6C, −$NHCH_2$), 69.51 (×24C, crown-ether −CH_2), 116.73 (×12C, Ar CC−NH), 124.5 (×12C, Ar CC−NO_2), 139.8 (×6C Ar C−NH), 147.88 (×6C Ar C−NO_2), 154.9 (×6C, −C=O), 172.04 (CO_3^{2-}); FT-IR (υ cm^{-1}): 851 (δ OCO; CO_3^{2-}), 1107 (υ C−O), 1237 (C−N), 1327 (NO_2-sym.), 1523 (NO_2-asym.), 1705 (−C=O), 3326 (N−H).

Phosphate cluster caged complex 6(n-TBA)[$4L_3(H_2PO_4^-)(HPO_4^{2-})_2$] (3e): Caged cluster complex (**3e)** was obtained as suitable crystals for X-ray diffraction analysis by stirring a 20 ml MeCN solution containing the receptor $\mathbf{L_3}$ and excess excess (*n*-TBA)H_2PO_4 for about 30 min at room temperature and filtered in a test tube for slow evaporation. The very light yellow crystals thus obtained were isolated by filtration and dried at room temperature by pressing between the filter papers before characterization by NMR and FT-IR analyses. Isolated yield: 54 % based on $\mathbf{L_3}$ after 1 weeks of exposure to unmodified atmosphere.

^{1}H NMR (DMSO-d_6, 400 MHz): δ (ppm) 0.893 (t, 24H, *n*-TBA−CH_3), 1.275 (q, 16H, *n*-TBA−CH_2), 1.514 (t, 16H, *n*-TBA−CH_2), 2.451 (s, 12H, −NCH_2), 3.110-3.132 (t, 16H, *n*-TBA−N^+CH_2) and (t, 12H, −$NHCH_2$), 7.735 (d, 12H, ArH), 7.84 (d, 12H, ArH), 8.042 (s, 6H, urea−NH_a), 10.495 (s, 6H, urea−NH_b); ^{13}C NMR (100 MHz, DMSO-d_6): δ (ppm) 13.50 (×12C, *n*-TBA–CH_3), 19.259 (×12C, *n*-TBA–CH_2), 23.13 (×12C, *n*-TBA−CH_2), 37.677 (×6C, −NCH_2), 54.42 (×6C, −$NHCH_2$), 57.636 (×12C, *n*-TBA−N^+CH_2), 116.92 (×12C, Ar), 124.513 (×12C, Ar), 139.736 (×6C, Ar), 148.13 (×6C, Ar), 155.09 (×6C, −C=O); ^{31}P NMR (242 MHz, DMSO-d_6): δ (ppm) 7.96; FT-IR (υ cm^{-1}): 1111, 1330, 1503, 1580, 1714, 2928, 3360; melting point: 192 °C.

Anion-acid cluster complex $[(L_3H)^+(H_2PO_4^-{\cdot}H_3PO_4)DMSO{\cdot}H_2O]$ (3f): Complex **3f** was obtained by adding 0.5 mL of 49% orthophosphoric acid (H_3PO_4) to a 5 mL DMSO solution of $\mathbf{L_3}$ and stirred for about 20-30 minutes at room temperature. The resulting solution, in a test tube was allowed to slowly evaporate at room temperature, which yielded light yellow crystals suitable for X-ray crystallography analysis within 8–10 days. Yield of **2**: 66% based on $\mathbf{L_3}$.

^{1}H NMR (600 MHz, DMSO-d_6) δ ppm 2.86 (s, 6H, −NCH_2), 3.31 (d, 6H, −NCH_2CH_2), 6.84 (s, 3H, −NH_a), 7.582-7.597 (d, 6H, ArH), 7.995-8.01 (d, 6H, ArH), 9.758 (s, 3H, −NH_b); ^{13}C NMR (150 MHz, DMSO-d_6): δ (ppm) 36.38 (×3C, −NCH_2), 53.593 (×3C, −$NHCH_2$), 116.884 (×6C, Ar), 124.9 (×6C, Ar), 140.335 (×3C, Ar), 147.145 (×3C, Ar), 154.9 (×3C, −C=O); ^{31}P NMR (242 MHz, DMSO-d_6) δ 0.54 ppm; FT-IR (KBr, υ cm^{-1}): 990, 1247, 1360, 1451, 1678, 1814, 3400.

Fluoride encapsulated complex, TEA$[L_3F^-]$ (3g): Complex **3g** was obtained as suitable crystals for X-ray diffraction analysis upon slow evaporation of a 15 mL MeCN solution of $\mathbf{L_3}$ in presence of excess TEAF. The crystals thus obtained were isolated by filtration and dried at room temperature by pressing between the filter papers before characterization by NMR and FT-IR analyses. Isolated yield: 72 % based on $\mathbf{L_3}$ after 1 weeks of exposure to unmodified atmosphere.

^{1}H NMR (600 MHz, DMSO-d_6) δ ppm 2.08 (s, 12H, TEA−CH_3), 2.497 (s, 8H, TEA−CH_2), 2.624 (t, 6H, −NCH_2), 3.21 (t, 6H, −NCH_2CH_2), 7.203 (s, 3H, −NH_a), 7.573-7.589 (d, 6H, ArH), 7.825-7.841 (d, 6H, ArH), 10.852 (s, 3H, −NH_b); ^{13}C NMR (150 MHz, DMSO-d_6): δ (ppm) 30.69 (×4C, TEA–CH_3), 37.24 (×3C, −NCH_2), 40.43 (×4C, TEA−CH_2), 54.24 (×3C, −$NHCH_2$), 116.77 (×6C, Ar), 125.08 (×6C, Ar), 140.33 (×3C, Ar), 147.18 (×3C, Ar), 154.53 (×3C, −C=O); ^{19}F NMR (600 MHz, DMSO-d_6) δ ppm -88.16; FT-IR (KBr, υ cm^{-1}): 1111, 1221, 1330, 1511, 1565, 1707, 2928, 3335.

Phosphate encapsulated complex 3(*n*-TBA)$[2L_3(PO_4^{3-})]$, (3h): To an acetonitrile solution (20 ml) of $\mathbf{L_3}$, an excess of $(n\text{-TBA})_3PO_4$ [which has been prepared separately from $(n\text{-TBA}^+)H_2PO_4^-$+{2(*n*-$TBA^+$)}$OH^-$] has been added and stirred for half an hour and then filtered

Slow evaporation of the filtrate solution yielded a light yellow crystalline complex 3(*n*-TBA)[2$\mathbf{L_3}$(PO_4^{3-})] (**3h**) in a low quantitative yield after 12-15 days. Yield of **3h**: 38% based on $\mathbf{L_3}$.

^{1}H NMR (DMSO-d_6, 600 MHz): δ (ppm) 0.912 (t, 36H, *n*-TBA–CH_3), 1.290 (q, 24H, *n*-TBA−CH_2), 1.541 (t, 24H, *n*-TBA−CH_2), 2.457 (s, 12H, −NCH_2), 3.027 (s, 12H, −$NHCH_2$), 3.141 (t, 24H, *n*-TBA–N^+CH_2), 7.576 (d, 12H, ArH), 7.469 (d, 12H, ArH), 10.023 (s, 6H, urea−NH_a), 13.105 (s, 6H, urea−NH_b); ^{13}C NMR (150 MHz, DMSO-d_6): δ (ppm) 13.54 (×12C, *n*-TBA−CH_3), 19.27 (×12C, *n*-TBA−CH_2), 23.13 (×12C, *n*-TBA−CH_2), 38.22 (×6C, −NCH_2), 55.47 (×6C, −$NHCH_2$), 57.63 (×12C, *n*-TBA−N^+CH_2), 116.74 (×12C, Ar), 123.99 (×12C, Ar), 138.51 (×6C, Ar), 149.95 (×6C, Ar), 155.22 (×6C, −C=O); ^{31}P NMR (242 MHz, DMSO-d_6): δ (ppm) 8.14; FT-IR (υ cm^{-1}): 1107, 1250, 1324, 1505, 1561, 1697, 2960, 3426; Melting point: 143 ˚C.

2.5.4 Complexes of the receptor $\mathbf{L_4}$

Hydrogenphosphate complex 2(*n*-TBA)[2$\mathbf{L_4}$($\mathbf{HPO_4^{2-}}$)] (4a): Hydrogen phosphate complex, **4a** was obtained as suitable crystals for X-ray diffraction analysis from a DMF solution mixture of $\mathbf{L_4}$ charged with an excess of a 1:1 solution mixture of *n*-TBA(H_2PO_4) and *n*-TBA(OH). The solution mixture was stirred for about 15 minute before allowed to crystallize at room temperature. Isolated yield: 52 % based on $\mathbf{L_4}$ after 2-3 weeks of exposure to unmodified atmosphere.

^{1}H NMR (DMSO-d_6, 400 MHz): δ (ppm) 0.87 (t, 24H, *n*-TBA−CH_3), 1.24 (q, 16H, *n*-TBA−CH_2), 1.49 (q, 16H, *n*-TBA−CH_2), 2.52 (s, 12H, −NCH_2), 3.10 (t, 16H, *n*-TBA−N^+CH_2), 3.16 (t, 12H, −$NHCH_2$), 7.07 (t, 6H, ArH), 7.40 (d, 6H, ArH), 7.51 (d, 6H, ArH), 7.67 (s, 6H, urea−NH_a), 8.15 (s, 6H, ArH), 10.47 (s, 6H, urea−NH_b); ^{31}P NMR (DMSO-d_6, 400 MHz): δ (ppm), 20.98 (s, HPO_4^{2-}); FT-IR (υ cm^{-1}): 1348 (NO_2-sym.), 1525 (NO_2 -asym.), 1690 (C=O), 2964 (C−H), 3394 (N−H).

Terephthalate complex 3*n*-TBA[$\mathbf{L_4}$($\mathbf{C_8H_4O_4^{2-}}$)$_{1.5}$] (4b): Similar to terephthalate complex **3b**, complex **2b** was obtained as suitable crystals for X-ray diffraction analysis from a DMF solution mixture of $\mathbf{L_4}$ charged with an excess (5 equiv.) of a 1:2 solution mixture of terephthalic acid and *n*-TBA(OH). Isolated yield: 77 % based on $\mathbf{L_4}$ after 2 weeks of exposure to unmodified atmosphere.

^{1}H NMR (DMSO-d_6, 400 MHz): δ (ppm), 0.87 (t, 36H, *n*-TBA−CH_3), 1.27 (q, 24H, *n*-TBA−CH_2), 1.49 (s, 24H, *n*-TBA−CH_2), 2.54 (s, 6H, −NCH_2), 3.10 (q, 24H, *n*-TBA–N^+CH_2), 3.20 (t, 6H, −$NHCH_2$), 7.36 (t, 3H, ArH), 7.61 (d, 3H, ArH), 7.69 (d, 3H, ArH), 7.87 (s, 4H, ArH, terephthalate), 7.96 (s, 3H, urea−NH_a), 8.57 (s, 3H, ArH), 10.81 (s, 3H, urea−NH_b); ^{13}C NMR (100 MHz, DMSO-d_6): δ (ppm) 13.46 (×12C, *n*-TBA−CH_3), 19.19 (×12C, TBA−CH_2), 23.07 (×12C, *n*-TBA−CH_2), 37.22 (×3C, −NCH_2), 53.56 (×3C, −$NHCH_2$), 57.57 (×12C, *n*-TBA−N^+CH_2), 111.22 (×3C, Ar), 114.57 (×3C, Ar), 123.44 (×3C, Ar),

128.12 (×6C,Ar), 129.50 (×3C, Ar), 140.53 (×3C,Ar), 142.97 (×3C,Ar), 148.10 (×3C,Ar), 155.75 (×3C, C=O), 170.61 (−COO^-); FT-IR (υ cm^{-1}): 1330 (NO_2 -*sym.*), 1530 (NO_2-asym.), 1694 (C=O), 2964 (C−H).

References

1. M. J. Hynes, EQNMR: A computer program for the calculation of stability constants from nuclear magnetic resonance chemical shift data, *J. Chem. Soc., Dalton Trans.*, **1993**, 311.
2. *SMART, SAINT and XPREP*; *Siemens Analytical X-ray Instruments Inc*.: Madison, WI, **1995**.
3. G. M. Sheldrick, SADABS: *Software for Empirical Absorption Correction*; University of Gottingen, Institute fur Anorganische Chemieder Universitat: Tammanstrasse 4, D-3400, Gottingen, Germany, **1999-2003**.
4. G.M. Sheldrick, *SHELXS-97*; University of Gottingen: Germany, **1997**.
5. G. M. Sheldrick, *SHELXL-97*: *Program for Crystal Structure Refinement*; University of Gottingen, Gottingen, Germany, **1997**.
6. Mercury 2.3, Supplied with Cambridge Structural Database; CCDC, Cambridge, U.K., **2007**.
7. Mercury 2.3 Supplied with Cambridge Structural Database; CCDC: Cambridge, U.K., **2011-2012**.

Chapter 3

Aerial CO_2 Uptake by a Simple Urea Receptor: Concert Act of Hydrogen and Halogen Bonding

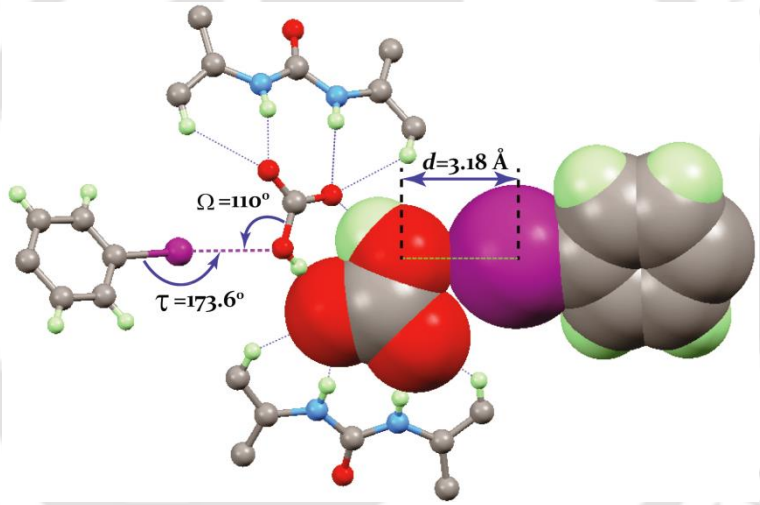

3.1 Background and Focus of the Chapter

Albert Einstein once said," Look deep into nature, and then you will understand everything better." Yes, the only miracle and absolute truth is nature. As the brainiest creature we, the human being should take care best of our own.

A major environmental issue of utmost concern is the significant rise in the CO_2 concentration in the atmosphere caused by increased consumption of fossil fuels and the overgrowing number of automobiles, industries, etc., which eventually demands the efficient fixation and activation of atmospheric CO_2 into green chemicals.[1] Therefore, mitigation by emissions reduction and recovery of CO_2 from industrial and natural sources is of utmost concern rather than adaptation to its effects or building systems resilient to its effects.

Nature recycles this greenhouse gas (CO_2) efficiently by photosynthetic cycle. But again it is the so called human being shrinks this process by deforestation on various purposes and handshakes to global warming. Capturing CO_2, although not generally employed on a large scale, is a well-studied process. The separation of CO_2 from gas streams can be achieved by diverse separation techniques based on different physical and chemical processes, including absorption into a liquid solution, adsorption onto suitable solids, cryogenic separation, and permeation through membranes.[2] Microporous aluminosilicates, activated carbons, and metal-organic frameworks (MOFs) have also widely been employed to capture and store CO_2 utilizing the effective conversion of CO_2 into green chemicals for the synthesis of specific chemical intermediates.[3] However, in light of supramolecular chemistry, efficient fixation of aerial CO_2 as carbonate/bicarbonate can be achieved with artificial H-bonding receptors in the presence of hydroxide and fluoride ions.[4] Gale *et al.* have also demonstrated CO_2 capture as carbamates (alkylammonium/alkylcarbamate) by a series of urea-based receptors in the presence of aliphatic amines (CO_2 scrubbers) bubbled with CO_2 in dimethyl sulfoxide (DMSO).[5]

While hydrogen bonding (HB) is a full-blown tool in molecular as well as anion recognition, the parallel non-covalent mate to HB, halogen bonding (XB) is still adolescent from this point of view, though XB has been sensibly approached in recently developed anion recognition.[6, 7] Recently, a series of urea-based anion receptors bearing one or two halogen bond donors has been designed to probe the potential for anion recognition through combinations of hydrogen and halogen bonding by Taylor et al.[6e] Supramolecular anion host systems utilizing both (HB & XB) with defined functions yet is a challenging prospect.

This chapter describes the evidence of fluoride-ion-induced uptake of atmospheric CO_2 stabilize as HCO_3^- anion (air-stable crystals) by a structurally simple acyclic 1,3-bis(4-iodophenyl)urea receptor, $\mathbf{L_1}$ (scheme 3.1).[8] The *in situ* formed HCO_3^- complex (**1a**) is stabilized by a concert act

of hydrogen and halogen bonding donated by the receptors. To the best of our knowledge, 1,3-bis(4-iodophenyl)urea is the simplest of anion receptors that displays a concert act of hydrogen and halogen bonding to stabilize aerial CO_2 as HCO_3^-. Further evidence of the potentiality of $\mathbf{L_1}$ as a halogen bond donor is unanimous as confirmed by single crystal analysis of the acetate (CH_3COO^-) complex of $\mathbf{L_1}$ (**1b**). Following the trend in strength of halogen bond formation *viz.*, −I > −Br > −Cl,[9] we have examined the structural aspects of anion binding with the 1,3-bis(4-bromophenyl)urea as a control receptor, $\mathbf{L_2}$ (scheme 3.1). The $\mathbf{L_2}$-fluoride solution resulted a complex with octahedral SiF_6^{2-} anion where the coordination environment of the anion is merely governed by multiple N−H···F (anion) interactions. The fluoride induce uptake of areal CO_2 only for $\mathbf{L_1}$ is due to the unique ability of $\mathbf{L_1}$ to form both HB bond and XB with anionic guest simultaneously. The most decisive evidence supporting the ability of $\mathbf{L_1}$ to form XB is obtained via crystallizing the acetate complex of $\mathbf{L_2}$, where the receptor $\mathbf{L_2}$ has been found to form only form HB interactions with acetate anion.

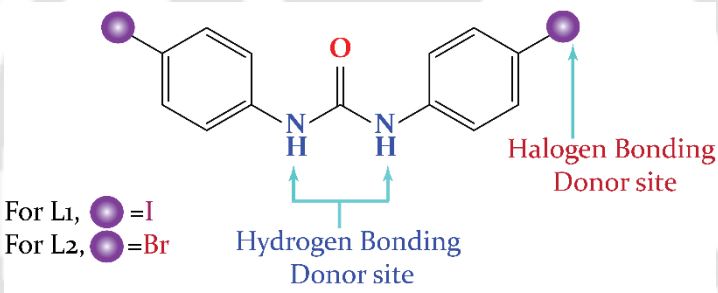

Scheme 3.1 Molecular Structure of the Receptors $\mathbf{L_1}$ and $\mathbf{L_2}$.

3.2 Crystal structure of receptors $\mathbf{L_1}$ and $\mathbf{L_2}$

Single crystals of $\mathbf{L_1}$ and $\mathbf{L_2}$ suitable for single crystal XRD analysis were obtained from DMSO and both crystallize monoclinic system with centrosymmetric space group C2/*c*. Structural analysis showed weak π-stacking interactions between the receptor molecules that are N−H···O

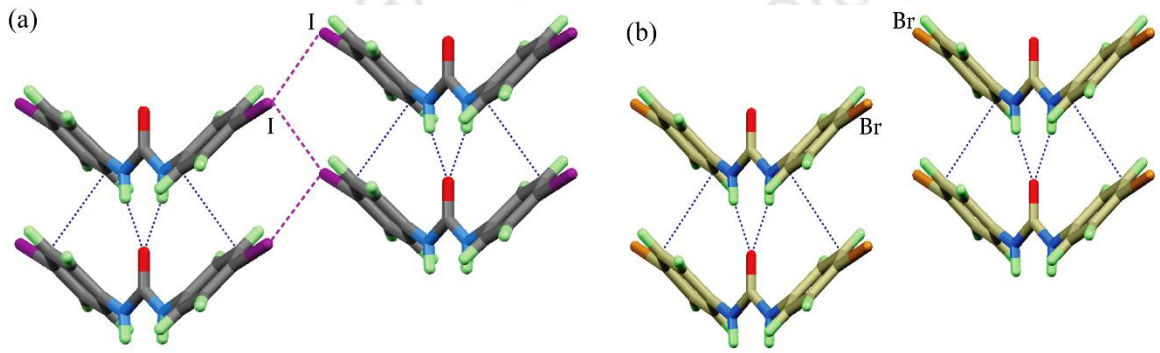

Figure 3.1 (a) X-ray structure of $\mathbf{L_1}$ shows the urea tape hydrogen bond motif along with π-stacking and I···I interactions, and (b) X-ray structure of $\mathbf{L_2}$ showing the urea tape hydrogen bond motif along with π-stacking interactions.

hydrogen bonded with one another. The π-stacked urea tapes are interlinked with one another by halogen-halogen (I···I) interactions in **L_1**, whereas **L_2** in spite of having similar π- stacked tape motif lacks halogen-halogen (Br···Br) interaction. Thus, from the structural features it can be presumed that **L_1** has the possibility for special noncovalent feature.

3.3 Structural aspects of anion binding with L_1 and L_2

Structural information obtained from single crystal X-ray analyses of the anion complexes can provide insight into the proper binding topology of different anions Efforts were made to explore the solid-state binding properties of **L_1** and **L_2** with different anions, by charging excess quaternary ammonium [*n*-TBA (tetrabutylammonium)/TEA (tetraethylammonium)] salt of anions to the individual receptor solutions in aprotic solvents such as MeCN or DMSO and allowed to crystallize at room temperature. The addition of F^-, HCO_3^- and CH_3COO^- solubilize the otherwise insoluble receptors **L_1** and **L_2** in MeCN, indicating explore worthy host–guest chemistry. Under identical condition, both **L_1** and **L_2** crystallised out with different in-situ generated anionic guests in presence of excess fluoride where **L_1** showed off the halogen bonding ability (complex **1a**), but **L_2** didn't (complex 2**a**). Treatment of both the hosts with excess acetate anion found to be decisive as **L_1** continues its halogen bonding in the acetate complex (**1b**)**,** while **L_2** didn't (**2b**).

3.3.1 Aerial CO_2 uptake as hydrogen & halogen bonded HCO_3 dimer (1a)

Interestingly, single crystals of HCO_3^- complex *n*-TBA[**L_1**·HCO_3] (**1a**) was obtained upon slow evaporation of the F^- containing MeCN solution of receptor **L_1**. The source of HCO_3^- is the atmosphere where hydroxide ion generated in situ from the basic receptor-F^- solution dissolves aerial CO_2 into HCO_3^-.

$$2F^- + H_2O \longrightarrow OH^- + HF_2^-$$
$$OH^- + CO_2 \longrightarrow HCO_3^-$$

The anion binding topology of this complex (**1a**) revealed the involvement of both hydrogen and halogen bonding in a concert act to stabilize the guest. The *in situ* generated bicarbonate complex crystallized in the monoclinic system with C_2 space group, from an acetonitrile solution of **L_1** containing excess fluoride ions. Structural elucidation revealed a 1:1 complex stoichiometry and dimeric association between two receptor coordinated HCO_3^- anions. Each urea bound HCO_3^- anion donates and accepts an O−H···O hydrogen bond (1.796 Å) to/from another urea bound HCO_3^- ion, giving rise to a dimeric anion complex. The $–COO^-$ fragment of a HCO_3^- anion is hydrogen bonded to the urea–NH groups with a donor- acceptor (N−H···O)

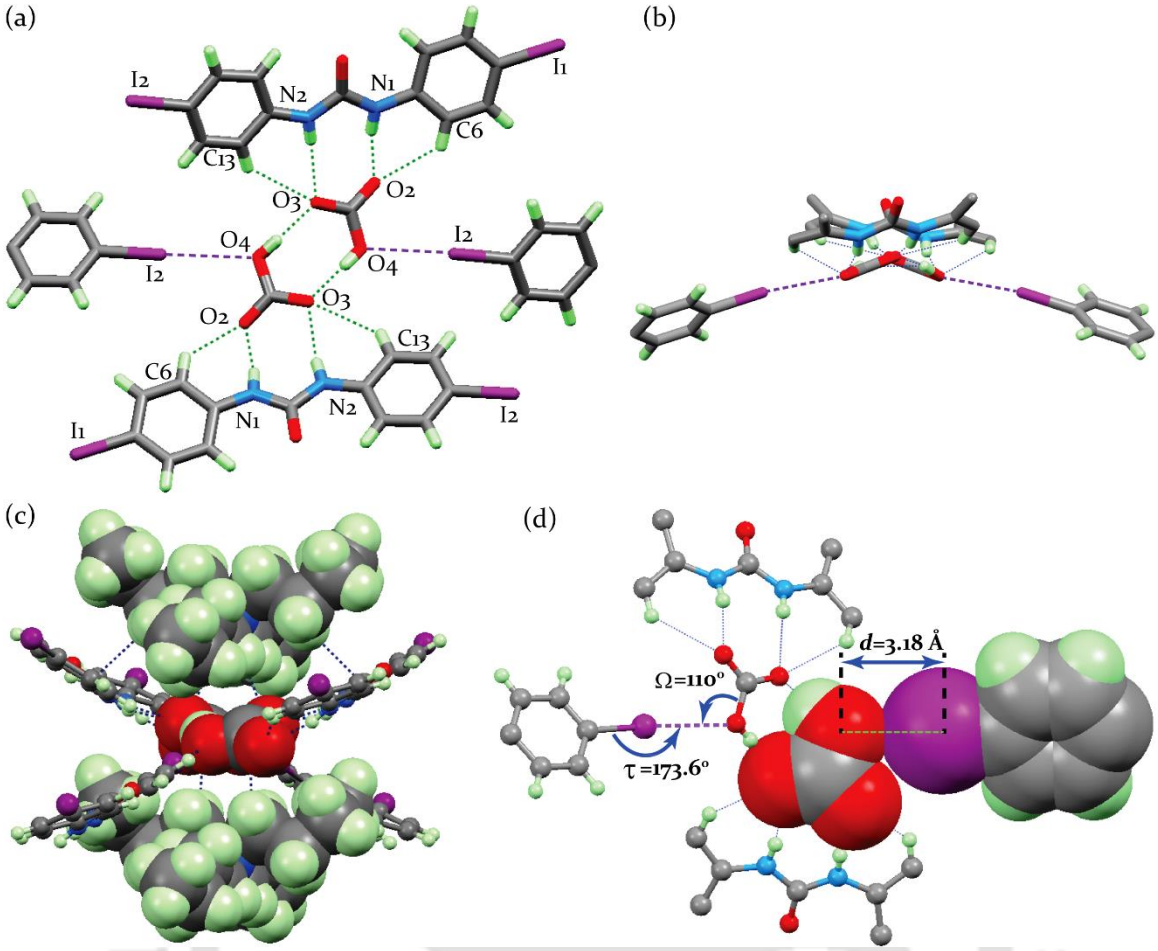

Figure 3.2 Ball-and-stick representation of complex **1a** depicting (a) the hydrogen and halogen bonding contacts on HCO_3^-− dimer as viewed down the crystallographic b-axis, (b) the tetrahedral spatial orientation of the HCO_3^- dimer in as viewed down the crystallographic c-axis. (c) ball-and-stick (host) and spacefill (guest) representation depicting the aliphatic C–H···O and C–H···π interactions from the *n*-TBA cations to the dimeric anion and receptors and (d) a magnified view of the coordination environment of the complex highlighting halogen bonding distances and angles respectively (*n*-TBA cations are omitted for clarity of the presentation, where necessary).

distance of 1.921(5) and 2.104(4) Å for O2 and O3, respectively. Additionally, HCO_3^- oxygen O2 and O3 is hydrogen bonded to an aryl –CH proton (*ortho* w.r.t. to urea function) with a donor-acceptor (C−H···O) distance of 2.571(4) and 2.644(4) Å, respectively. Conspicuous, the –OH group of HCO_3^- anion accepts one strong C−I···O halogen bond from the iodophenyl ring of an adjacent anion bound receptor molecule. Thus, each HCO_3^- anion is coordinated to a receptor by four hydrogen bonds and to another by a halogen bond, which implies that a HCO_3^- dimer is coordinated to four receptor molecules via two distinct types of noncovalent interactions (Fig. 3.1a). The HCO_3^- dimer is located below the hydrogen bond donor and above the halogen bond donor platform. The spatial position of the HCO_3^- dimer looks as if the dimer is hanging by holding the hydrogen bonding threads which is supported by two halogen bonding pillars from the bottom (Fig. 3.1b). In other words, it is the halogen bonds that pulled the HCO_3^- dimer out of the more common hydrogen bonded planar structure, as observed in the case of HCO_3^- complex of 1,3-bis(4-nitrophenyl)urea reported by Fabbrizzi *et al.*[10] Furthermore, the exposed

area at the top and bottom created due to the tetrahedral like environment around the bicarbonate dimer are capped by the *n*-TBA cations *via* contact ion-pairing (C−H···Anion interactions) and C−H···π interactions with the phenyl rings to form a compact enclosed system surrounding the in situ generated anion (Fig 3.1c). The melting point of the complex was found to be ~140 °C indicating good air stability.

The halogen bonding contact (I2···O4) in complex **1a** has a distance of 3.183(4) Å (Fig. 3a), which corresponds to 9% shortening of the sum of their van der Waals radii (3.50 Å) (The van der Waals radii of O and I are 1.52 and 1.98 Å).[11] Parthasarathy *et al.* has reported the crystallographic evidence of directional preferences of intermolecular forces around halogen atoms[12] where they have shown that nucleophiles in general tend to approach the C−X bond in a "head-on" fashion with Γ≈165(8)˚ for C−I bond. Similar results were obtained by Allen *et al.*[13a] and Glaser *et al.*[13b] In complex **1a** the iodophenyl unit is "head-on" with the HCO_3^- oxygen at an angle ∠(C−I2···O4) of Γ=173.6˚(2) close to 180° [∠(C−O4···I2) angle Ω=110.0(3)˚, Fig. 3.1d]. The details of the halogen bonding contacts and angles are listed in Table 3.1.

In Fabbrizzi's case,[10] the presence of electron withdrawing nitro chromophore, resulted in a fluoride ion induced –NH deprotonation with the subsequent absorption of atmospheric CO_2 in moist THF. The structural elucidation of that HCO_3^- complex also showed dimeric association of urea bound HCO_3^- anions along with crystallized water molecules H-bonded to a HCO_3^- oxygen atom. However, in the present case, the urea bound HCO_3^- dimer is additionally stabilized by a pair of halogen bonding interactions to which gives rise to a distinct directional coordination environment for the guest.

3.3.2 Acetate-complex of receptor L_1 (1b)

The acetate-complex, *n*-TBA[$\mathbf{L_1}$·CH_3COO] (**1b**) was obtained as suitable crystals for XRD analysis upon slow evaporation of a MeCN solution of $\mathbf{L_1}$ and excess (TBA)CH_3COO. Complex **1b** crystallizes in the monoclinic system with the P_21/c space group, where each acetate oxygen atom is hydrogen bonded to a receptor molecule by a pair of N–H···O and aryl C–H···O bonds. A correlation of the N–H···O angle versus the N–H···O distance shows that both the N–H···O hydrogen bonds are in the very strong hydrogen- bonding interaction regions of *d*(H···O) < 2.5 Å and *d*(D···O) < 3.2 Å (Annexure 3, Table A3.2). Furthermore, each acetate oxygen atom interacts with a neighbouring receptor molecule by accepting a halogen bond each from two different iodophenyl rings. The halogen bonding contacts (I···O) in this complex were calculated to be *d*(I1···O2) = 3.144 Å and *d*(I2···O3) = 3.482 Å (Fig. 3.3b), which correspond to 11% and 1% shortening of the sum of their van der Waals radii (3.5 Å). The ∠(C–I···O) angles were

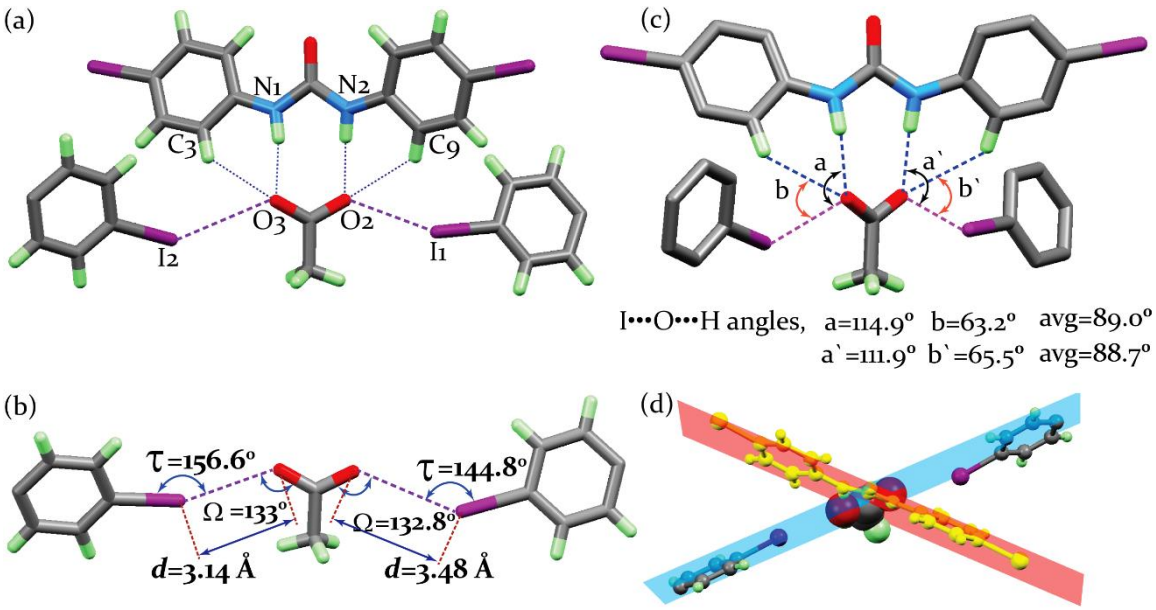

Figure 3.3 Ball-and-stick representation of complex **1b** depicting (a) the hydrogen and halogen bonding contacts on CH_3COO^- anion along the crystallographic a-axis, (b) halogen bonding distances and angles, (c) orthogonal relationship between hydrogen and halogen bonds, and (d) a magnified view depicting the planarity of acetate anion with the halogen bond donating iodophenyl rings (light blue coloured plane) and not with the hydrogen bonded urea function (light pink coloured plane) (*n*-TBA cations are omitted for clarity of the presentation).

Table 3.1 Detail of Halogen Bonding Contacts in the Complexes **1a** and **1b**.

complex	**1a**	**1b**	**1b**
C–I···O	C11–I2···O4	C1–I1···O2	C11–I2···O3
d(I···O)/Å	3.187(4)	3.144(4)	3.482(5)
d(C–I···O)/Å	5.272(6)	5.143(4)	5.339(5)
I···O [%][a]	90.8%	89.8%	99%
∠C–I···O/deg (Γ)	173.6(2)	156.60(8)	144.77(8)
∠C–O(A^-)···I/deg (Ω)	110.0(3)	132.8(4)	133.4(4)

measured to be Γ=156.6(8)° and Γ=144.77(8)° for the I1···O2 and I2···O3 halogen bonds, respectively. The details of the halogen bonding contacts and angles are listed in Table 3.1. In complex **1b**, the acetate anion resides in the plane of the XB donating iodophenyl rings, rather than the HB donating urea function (Fig. 3.3d), showcasing the effect of XB on the H-bonded urea–acetate complex, unlike the most common urea–acetate cases.[14] Recently, Ho and co-workers have reported that the halogen bonds can adopt an orthogonal (perpendicular) geometry and they are energetically independent of the hydrogen bonds that share a common acceptor atom.[15] Based on their calculations on biomolecules, they found that in most of the cases, the X···O···H angle lies in the range of ±(85–89)°. Our attempt to analyse the orthogonality of the halogen bonds in the acetate complex (**1b**), we find that the –NH related I···O···H angles are in

the range of 110–115° and –CH related I···O···H angles are in the range of 63–66°. Thus, it may be assumed that the halogen bonds are maintaining an orthogonal relationship to the –NH and –CH hydrogen bonds with an average angle of ±89° (Fig. 3.3c).

3.3.3 Hexafluorosilicate-Complex of receptor L_2 (2a)

The *in situ* generated SiF_6^{2-}complex 2*n*-TBA[$\mathbf{L_2}$-SiF_6^{2-}], (**2a**) crystallized in the monoclinic system with $P2_1/c$ space group, from an acetonitrile solution of $\mathbf{L_2}$ containing excess fluoride ions. It is to be mentioned that, complexes **1a** and **2a** were obtained under identical crystallization conditions, but with entirely different compositions. The SiF_6^{2-} anions might have generated from the reaction of fluoride ions with the glass surfaces (SiO_2) during the crystallization process. To be ensured about the source of silicon, we carried out the same crystallization experiment in a plastic container under similar conditions. However, no solid products were obtained to ascertain the composition. Whereas, crystallization experiment in a plastic vial employing $\mathbf{L_1}$ and excess fluoride ions in MeCN solution resulted in exclusive formation of the bicarbonate complex, **1a**. Thus, a subtle variation in the electronic properties of 1,3-bis(4-halophenyl)urea receptors resulted in a drastic change in their anion recognition properties.

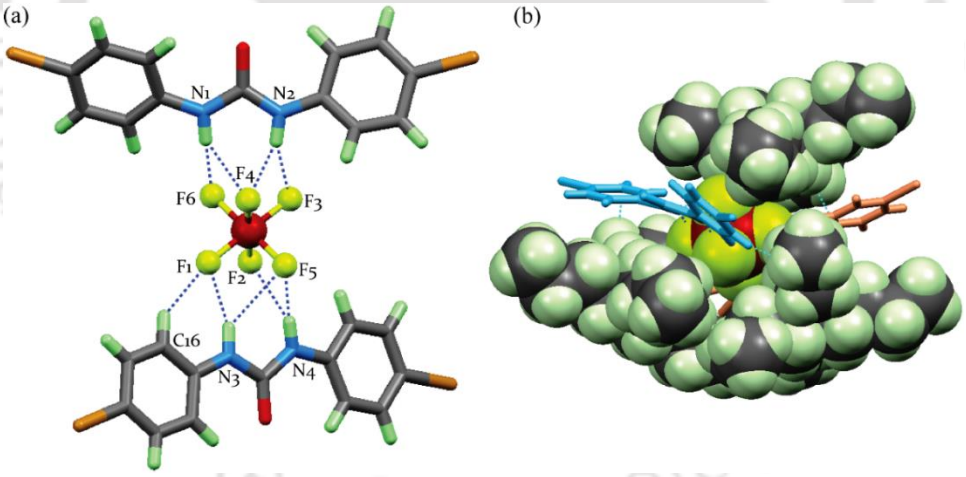

Figure 3.4 (a) Ball-and-stick representation depicting the H-bonding contacts on SiF_6^{2-} anion and (b) ball-and-stick (host) and spacefill (guest) representation depicting the aliphatic C–H···F and C–H···π interactions from the *n*-TBA cations of complex **2a**.

Structural elucidation revealed that an octahedral SiF_6^{2-} anion is hydrogen bonded to the urea functions of two receptor molecules, where each urea moiety is in interaction with three fluoride atoms of a triangular face of the octahedral anion (Fig 3.4a). A correlation of the N−H···F angle versus the N−H···F distance shows that out of the eight N−H···F hydrogen bonds, seven are in the strong hydrogen bonding interaction region of d(H···F) < 2.5 Å and d(N···F) < 3.2 Å (Annexure 3, Table A3.2). Additionally, one of the *ortho*-aryl protons also participates in the stabilization of the octahedral anion complex.

3.3.4 Acetate-complex of receptor L_2 (2b)

In Identical condition to **1b**, complex **2b**, *n*-TBA[$\mathbf{L_2}$·CH_3COO] crystallized in the monoclinic system with the P_21/c space group with a 1 : 1 complex stoichiometry. However, there are significant differences in the acetate coordination on switching from the 1,3-bis(4-iodophenyl)urea to 1,3-bis(4-bromophenyl) urea.

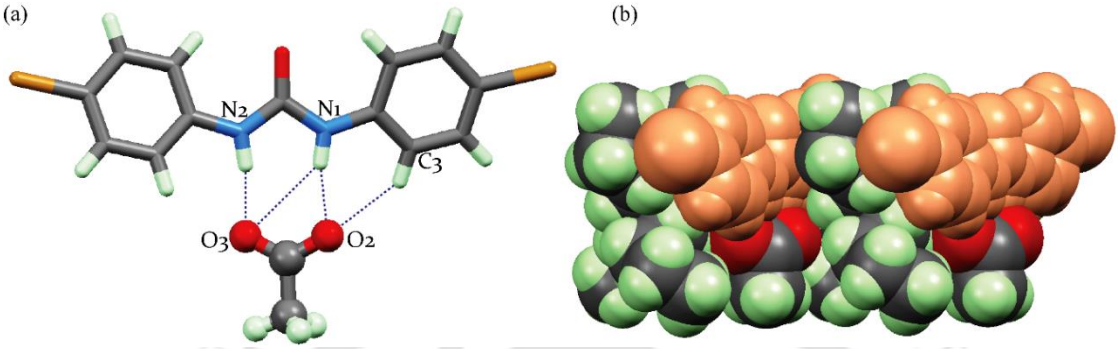

Figure 3.5 (a) Ball-and-stick representation depicting the H-bonding contacts on AcO^- anion (*n*-TBA cations are omitted for clarity of the presentation) and (b) Spacefill representation depicting *n*-TBA cations separated host-guest complex units of complex **2b**.

In complex **2b**, each acetate oxygen atom behaves as a bifurcated hydrogen bond acceptor, where oxygen O2 is hydrogen bonded to a –NH proton and an aryl –CH proton, and oxygen O3 is hydrogen bonded to both urea –NH protons (Fig. 3.5a). However, in complex **1b**, a pair of halogen bonds (I···O) provides added stabilization to the hydrogen bonded acetate anion. Such a feature showcasing halogen bond formation with the anion was found to be absent in complex **2b**. Moreover, the urea bound acetate complex is sandwiched between two *n*-TBA cations (Fig 3.5b) by forming several C–H···O interactions, thereby getting some extra stability in its solid-state. Further, the lack of halogen bonding in **2b** left it to be planar unlike complex **1a.**

3.4 Solution-state anion binding studies

Analysis of the ^{1}H NMR (DMSO-d_6) spectrum of HCO_3^- complex, **1a** showed appreciable downfield shift and concomitant broadening of the urea −NH resonance with $\Delta\delta$ = 1.84 ppm, indicating strong solution-state binding of HCO_3^- with the urea function (Annexure 3, Fig A3.9). The strong interaction of HCO_3^- has also been confirmed by monitoring the differences in the chemical shifts of ^{13}C NMR signals of TEA (tetraethylammonium) salt of HCO_3^- and complex **1a**. TEA(HCO_3) in DMSO-d_6 showed a sharp ^{13}C NMR resonance at 158.91 ppm, whereas in complex **1a** the HCO_3^- resonance showed at 182.12 ppm showing a large downfield shift of 23.27 ppm (Figure 3.6). The solution-state anion binding properties of $\mathbf{L_1}$ and $\mathbf{L_2}$ were investigated by qualitative as well as quantitative ^{1}H NMR experiments in DMSO-d_6 using the quaternary ammonium (*n*-TBA/TEA) salt of monovalent anions such as F^-, Cl^-, Br^-, I^-, HCO_3^-, CH_3COO^-, NO_3^-, $H_2PO_4^-$ and HSO_4^-. Figure 3.7a and 3.7b show the chemical shift changes

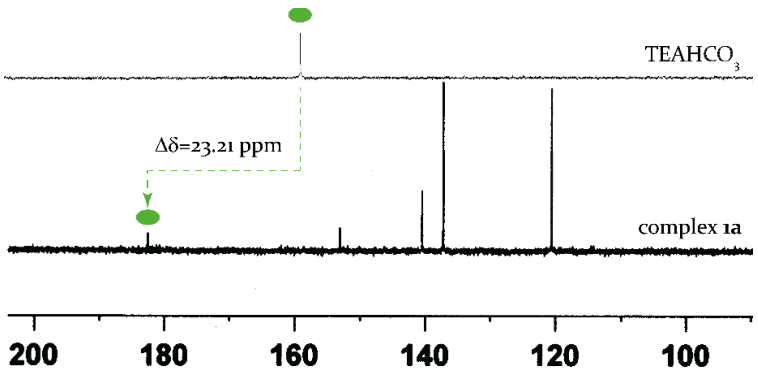

Figure 3.6 Partial ^{13}C NMR spectrum of complex **1a** (below) showing the huge downfield shift of the HCO_3^- resonance relative to the (TEA)HCO_3 salt (above).

observed upon one equivalent addition of different anions to the individual solutions of $\mathbf{L_1}$ and $\mathbf{L_2}$, respectively, in DMSO-d_6. The most significant change has been observed for the urea –NH proton in the presence of F^-, HCO_3^-, and CH_3COO^- indicating that the –NH function acts as the primary site for anion recognition. The ^1H NMR titration of $\mathbf{L_1}$ with a standard HCO_3^- solution, a large downfield shift of urea –NH resonance w.r.t. the urea group) were observed. Tracking the shift of the –NH resonance, the binding constant (log K_a) for HCO_3^- was (WinEQNMR2) calculated to be 5.16 with 1 : 1 host/guest stoichiometry, which is in agreement with Job's plot analysis (Annexure 3, Fig. A3.1). However, the best fitted curve obtained from WinEQNMR2 was for a mixture of 1 : 1 and 1 : 2 host/guest stoichiometry. Similarly, the titration data for F^- yielded a log K_a value of 4.95 (Annexure 3, Fig. A3.3) for 1:1 stoichiometry. The highest downfield shift of –NH resonance has been observed with acetate anion with Δδ= 2.73 ppm. The binding constant (log K_a) for CH_3COO^- was calculated to be 3.69 with 1:1 host/guest stoichiometry (Annexure 3, Fig. A3.2). The titration of $\mathbf{L_2}$ with F^- and CH_3COO^- showed a huge downfield shift of the –NH resonance with Δδ=2.32 ppm and 2.27 ppm for F^- and CH_3COO^-

Table 3.2 Association constants in log $K_a(M^{-1})$ of $\mathbf{L_1}$ and $\mathbf{L_2}$ with different anions in DMSO-d_6 at 298 K, calculated using WinEQNMR2.

Receptor	Anions (TBA/TEA salts)	log K_a	
		Log K_{11} (1:1=host:guest complex)	Log K_{12} (1:2=host:guest complex)
$\mathbf{L_1}$	F^-	4.95	8.37
$\mathbf{L_1}$	AcO^-	3.69	6.34
$\mathbf{L_1}$	HCO_3^-	5.16	9.06
$\mathbf{L_2}$	F^-	4.40	8.24
$\mathbf{L_2}$	AcO^-	3.66	6.53
$\mathbf{L_2}$	HCO_3^-	3.32	6.79

and CH_3COO^-, respectively. However, the titration with HCO_3^- resulted in a comparatively respectively. However, the titration with HCO_3^- resulted in a comparatively lesser shift of $\Delta\delta$=1.14 ppm for –NH resonance of **L_2**, which is ~1.00 ppm less than that of **L_1**. In all the three cases, the host/guest stoichiometry was found to be 1:1, which is in agreement with the Job's plot analyses (Annexure 3, Fig. A3.4, A3.5 and A3.6) and the binding constants (log *K*) were calculated to be 4.40, 3.66 and 3.32 for F^-, CH_3COO^- and HCO_3^-, respectively (Table 3.2). However, in all the cases, WinEQNMR2[16] has given the best fit curve for the equilibrium mixture of 1:1 and 1:2 host/guest stoichiometries. Other halides (Cl^-, Br^-, I^-) and oxyanions (NO_3^-, $H_2PO_4^-$, HSO_4^-) hardly had any effect on the urea –NH resonance, indicating very weak interactions with **L_1** and **L_2**. We have also checked the UV/Vis absorption properties of both the receptors in the presence of all the common anions in excess. Except for F^-, CH_3COO^- and HCO_3^- ions, both the receptors showed no response towards the other anions in a dilute MeCN solution. With F^-, CH_3COO^- and HCO_3^-, both the receptors get red shifted, supporting the solid-state evidences. We have checked both the receptors with excess of each of the anions, where **L_1** gets red shifted by 10 nm with F^- as well as AcO^- and 8 nm with HCO_3^- (Annexure 3, Fig. A3.7). Similarly, **L_2** gets red shifted by 10 nm with F^- and 5 nm with HCO_3^- as well as AcO^- (Annexure 3, Fig. A3.8).

3.5 Conclusion

In the 1,3-bis(4-nitrophenyl)urea compound, electron withdrawing nitro groups render the urea protons sufficiently acidic to get deprotonated in the presence of fluoride ions, and they eventually can capture CO_2 as HCO_3^- hydrogen bonded to the urea receptor.[9] As anticipated, the utilization of 1,3-bis(4-iodophenyl)urea (**L_1**) decreases the possibility of fluoride ion induced urea deprotonation due to the less electronegative character of iodine. However, **L_1** showcases the exciting property of fluoride ion induced CO_2 capture as HCO_3^- complex (**1a**) stabilized by a combined act of hydrogen and halogen bonding. However, in a control experiment, 1,3- bis(4-bromophenyl)urea (**L_2**) crystallized as hydrogen bonded SiF_6^{2-} complex in the presence of excess fluoride ions, suggesting its impotency to act as a CO_2 scrubber. The proficiency of **L_1** as a halogen bond donor has also been authenticated in the crystal structures of the free receptor and acetate complex 1b. The inability of **L_2** to form halogen bonds with anions has also been confirmed by the structural elucidation of its hydrogen bonded acetate complex **2b**, suggesting that it is the combined act of hydrogen and halogen bonding that prompted the CO_2 uptake from a fluoride containing solution of 1,3-bis(4-iodophenyl)urea. Overall, we have shown that a subtle variation in the electronic properties of 1,3-bis(4-halophenyl)urea receptors resulted in a drastic change in their anion recognition properties in solution as well as solid-state.

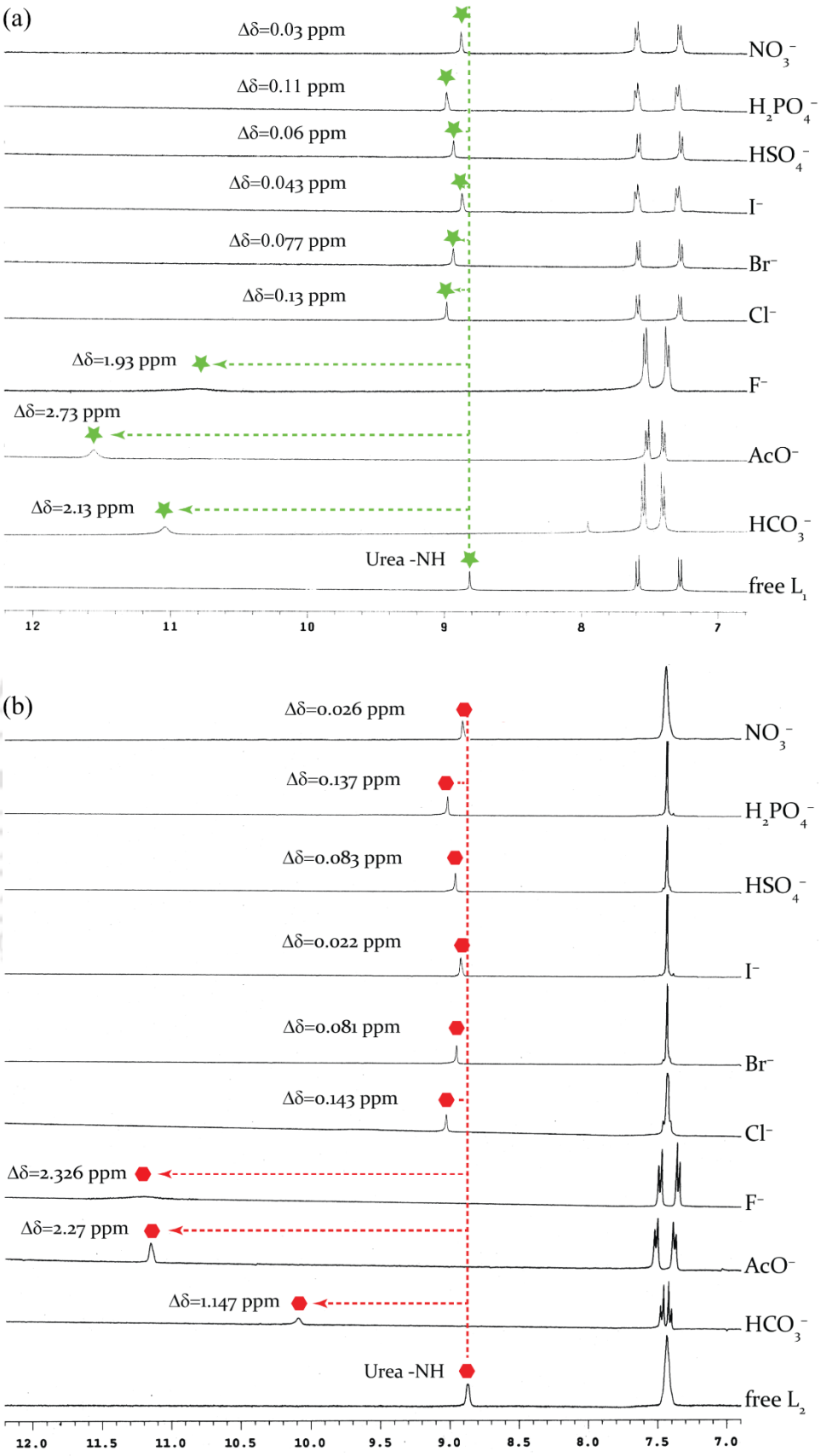

Figure 3.8 Partial ^{1}H NMR spectra (400 MHz, DMSO-d_6) of (a) $\mathbf{L_1}$ and (b) $\mathbf{L_2}$ with the maximum observable shifts of urea –NH resonance upon the addition of 1 equivalent of HCO_3^-, CH_3COO^-, F^-, Cl^-, Br^-, I^-, $HSO_4^-H_2PO_4^-$ and NO_3^- as their TEA/*n*-TBA salts.

References

1. (*a*) Climate Change, **2007**: Synthesis Report, International Panel on Climate Change; Cambridge University Press: Cambridge, U.K., 2007. (*b*) D. S. Jenkinson, D. E. Adams and A. Wild, *Nature*, **1991**, *351*, 304. (*c*) K. Caldeira, A. K. Jain and M. I. Hoffert, *Science*, **2003**, *299*, 2052.
2. (*a*) A. Kohl and R. Nielsen, *Gas Purification*, 5th ed.; Gulf Publishing Co.; Houston, **1997**. (*b*) G. A. Olah, A. Goeppert, and G. K. S. Prakash, *J. Org. Chem.*, **2009**, *74*, 487.
3. (*a*) J. L. C. Rowsell, E. C. Spencer, J. Eckert, A. K. Howard and O. M. Yaghi, *Science*, **2005**, *309*, 1350. (*b*) R. Banerjee, A. Phan, B. Wang, C. Knobler, H. Furukawa, M. O'Keeffe and O. M. Yaghi, *Science*, **2008**, *319*, 939. (*c*) G. A. Olah, *Angew. Chem., Int. Ed.*, **2005**, *44*, 2636. (*d*) E. Garcia-Espana, P. Gavina, J. Latorre, C. Soriano and B. Verdejo, *J. Am. Chem. Soc.*, **2004**, *126*, 5082.
4. (*a*) A. Pramanik, M. E. Khansari, D. R.; Powell, R. FronczekF and M. A. Hossain. *Org. Lett.*, *Org. Lett.*, **2014**, *16* (2), 366. (*b*) T. Gunnlaugsson, P. E. Kruger, P. Jensen, F. M. Pfeffer and G. M. Hussey, *Tetrahedron Lett*. **2003**, *44*, 8909. (*c*) S. J. Brooks, S. E. Garcia-Garrido, M. E. Light, P. A. Cole and P. A. Gale, *Chem. Eur. J.*, **2007**, *13*, 3320. *(d)* S. J. Brooks, P. A. Gale and M. E. Light, *Chem. Commun.*, **2006**, 4344. (*e*) S. K. Dey, R. Chutia and G. Das, *Inorg. Chem.*, **2012**, *51*, 1727.
5. (*a*) P. R. Edwards, J. R. Hiscock and P. A. Gale, *Tetrahedron Lett*., 2009, *50*, 4922. (*b*) P. R. Edwards, J. R. Hiscock and P. A. Gale and M. E. Light, *Org. Biomol. Chem.*, **2010**, *8*, 100.
6. (*a*) M. G. Sarwar, B. Dragisic, L. J. Salsberg, C. Gouliaras and M. S. Taylor, *J. Am. Chem. Soc*., **2010**, *132*, 1646. (*b*) M. G. Sarwar, B. Dragisic, S. Sagoo and M. S. Taylor *Angew. Chem., Int. Ed*., **2010**, *49*, 1674. (*c*) E. Dimitrijevic, O. Kvak and M. S. Taylor M. S. *Chem. Commun*., **2010**, *46*, 9025. (*d*) T. M. Beale, M. G. Chudzinski, M. G. Sarwar and M. S. Taylor, *Chem. Soc. Rev.* **2013**, *42*, 1667.
7. (*a*) A. Mele, P. Metrangolo, H. Neukirch, T. Pilati and G. Resnati, *J. Am. Chem. Soc*., **2005**, *127*, 14972. (*b*) A. Caballero, N. G. White and P. D. Beer, *Angew. Chem., Int. Ed*., **2011**, *50*, 1845.
8. R. Chutia and G. Das, *Dalton Trans*., **2014**, *43*, 15628.
9. (*a*) P. Metrangolo, H. Neukirch, T. Pilati and G. Resnati, *Acc. Chem. Res*., **2005**, *38*, 386. (*b*) P. Politzer, P. Lane, M. C. Concha, Y. Ma and J. S. Murray, *J. Mol. Model.*, **2007**, *13*, 305.
10. M. Boiocchi, L. D. Boca, D. E. Gomez, L. Fabbrizzi, M. Licchelli, and E. Monzani, *J. Am. Chem. Soc.*, **2004**, *126*, 16507.
11. A. Bondi, *J. Phys. Chem.*, **1964**, *68*, 441.
12. N. Ramasubbu, R. Parthasarathy and P. Murray-Rust, *J. Am. Chem. Soc.*, **1986**, *108*, 4308.
13. (*a*) J. P. M. Lommerse, A. J. Stone, R. Taylor and F. H. Allen, *J. Am. Chem. Soc.*, **1996**, *118*, 3108. (*b*) R. Glaser, N. Chen, H. Wu, N. Knotts and M. Kaupp, *J. Am. Chem. Soc.*, **2004**, *126*, 4412.
14. I. L. Kirby, M. B. Pitak, M. Wenzel, C. Wilson, H. A. Sparkes, S. J. Coles and P. A. Gale, *CrystEngComm*, **2013**, *15*, 9003.
15. A. R. Voth, P. Khuu, K. Oishi and P. S. Ho, *Nat. Chem*., **2009**, *1*, 74.
16. M. J. Hynes, *J. Chem. Soc.*, *Dalton Trans*. **1993,** 311.

Annexure 3

Table A3.1 Crystallographic parameters and refinement details of receptors **L_1**, **L_2**, complexes **1a**, **2a**, **2a** and **2b**

Parameters	**L_1**	**1a**	**1b**	**L_2**	**2a**	**2b**
CCDC	973820	973821	973822	973823	973824	973825
Formula	$C_{13}H_{10}I_2N_2O$	$C_{30}H_{47}I_2N_3O_4$	$C_{31}H_{49}I_2N_3O_3$	$C_{13}H_{10}Br_2N_2O$	$C_{58}H_{92}Br_4F_6N_6O_2Si$	$C_{31}H_{49}Br_2N_3O_3$
Fw	464.03	767.51	765.53	370.03	1367.07	671.53
Crystal system	Monoclinic	Monoclinic	Monoclinic	Monoclinic	Monoclinic	Monoclinic
Space group	C_2/c	C_2	P_21/c	C_2/c	P 21/c	P_21/c
a/Å	29.2420(9)	23.9471(7)	8.8809(3)	28.0636(16)	15.4434(8)	9.5024(5)
b/Å	4.6414(10)	8.3931(2)	21.0697(6)	4.6085(3)	14.6392(8)	18.9054(10)
c/Å	10.1031(3)	17.0344(5)	18.9452(6)	10.0857(6)	33.471(2)	19.3877(13)
α/°	90.00	90.00	90.00	90.00	90.00	90.00
β/°	94.122(2)	96.4510(10)	97.815(2)	95.469(4)	116.731(6)	99.771(5)
γ/°	90.00	90.00	90.00	90.00	90.00	90.00
V/Å^3	1367.68(7)	3402.07(16)	3512.06(19)	1298.46(14)	6758.4(7)	3432.4(3)
Z	4	4	4	4	4	4
Dc/g cm^{-3}	2.254	1.498	1.448	1.893	1.344	1.299
μ Mo Kα/mm^{-1}	4.588	1.884	1.823	6.231	2.458	2.394
T/K	298(2)	298(2)	298(2)	298(2)	298(2)	298(2)
θ max.	28.30	23.64	23.12	26.00	24.76	23.23
Total no.of reflections	9542	19895	43647	8968	21949	15160
Independent reflections	1694	8369	8711	1596	17673	8817
Observed reflections	1541	4435	4605	1040	9665	5893
Parameters refined	83	384	358	83	727	426
R_1, $I > 2\sigma(I)$	0.0292	0.0421	0.0612	0.0377	0.0963	0.0590
wR_2, $I > 2\sigma(I)$	0.0996	0.1107	0.1786	0.1119	0.1630	0.1226
R_1, (all data)	0.0315	0.0604	0.1155	0.0697	0.3202	0.1794
wR_2 (all data)	0.1052	0.1203	0.2080	0.1397	0.2334	0.1652
GOF (F^2)	0.909	1.074	1.082	0.920	1.032	1.003

Table A3.2 Details of Hydrogen Bonding contacts in the Complexes **1a, 1b**, **2a** and **2b**

complex	D–H···A[a]	d(D···A)/Å	d(H···A)/Å	∠D–H···A/°
1a	N1–H···O2	2.761(7)	1.921(5)	165.2(4)
	N2–H···O3	2.909(6)	2.104(4)	155.4(3)
	C6–H···O2	3.292(7)	2.571(4)	134.6(4)
	C13–H···O3	3.382(6)	2.644(4)	136.8(4)
1b	N1–H···O3	2.835(6)	1.985(4)	169.3(3)
	N2–H···O2	2.833(5)	1.974(4)	175.8(3)
	C3–H···O3	3.384(8)	2.648(5)	136.4(4)
	C9–H···O2	3.449(7)	2.723(4)	135.4(4)
2a	N1–H···F6	3.072(9)	2.251(4)	159.2(5)
	N1–H···F4	3.02(1)	2.353(6)	134.4(5)
	N2–H···F4	2.83 (1)	2.044(5)	152.5(5)
	N2–H···F3	3.054(9)	2.324(4)	143.0(5)
	N3–H···F1	2.89(1)	2.056(6)	163.8(5)
	N3–H···F5	3.237(9)	2.556(4)	136.5(5)
	N4–H···F5	2.820(8)	1.987(5)	162.7(5)
	N4–H···F2	3.11(1)	2.464(6)	131.9(5)
	C16–H···F1	3.119(8)	2.323(5)	143.4(4)
2b	N1–H···O3	3.454(5)	2.728(4)	142.8(3)
	N2–H···O3	2.809 (5)	1.976(4)	162.5(3)
	N1–H···O2	2.778(5)	1.962(3)	157.8(3)
	C3–H···O2	3.315(7)	2.661(4)	128.0(3)

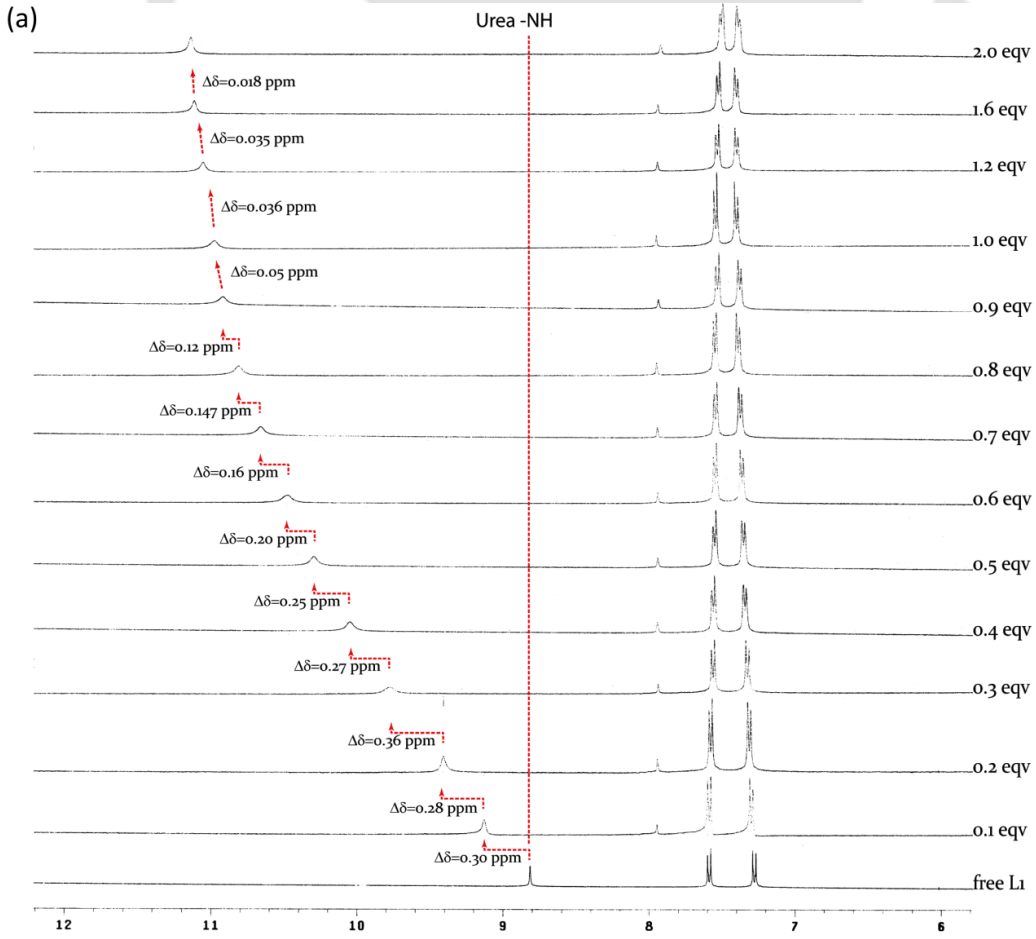

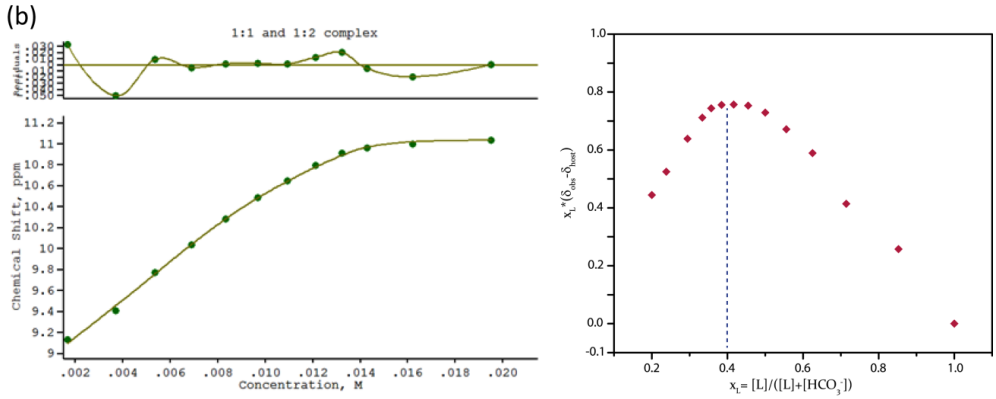

Figure A3.1 (a) Expanded partial ^{1}H NMR spectra of $\mathbf{L_1}$ upon titration with HCO_3^-(TEA) in DMSO-d_6 and (b) Fit plot obtained by WinEQNMR2 and corresponding Job's plot showing a maximum at 0.4 mole fraction of the receptor for the multiple equilibria existing between 1: 1 and 1 : 2 complexes in the determination of K_a using urea-NH resonance for $\mathbf{L_1}$ and bicarbonate anion.

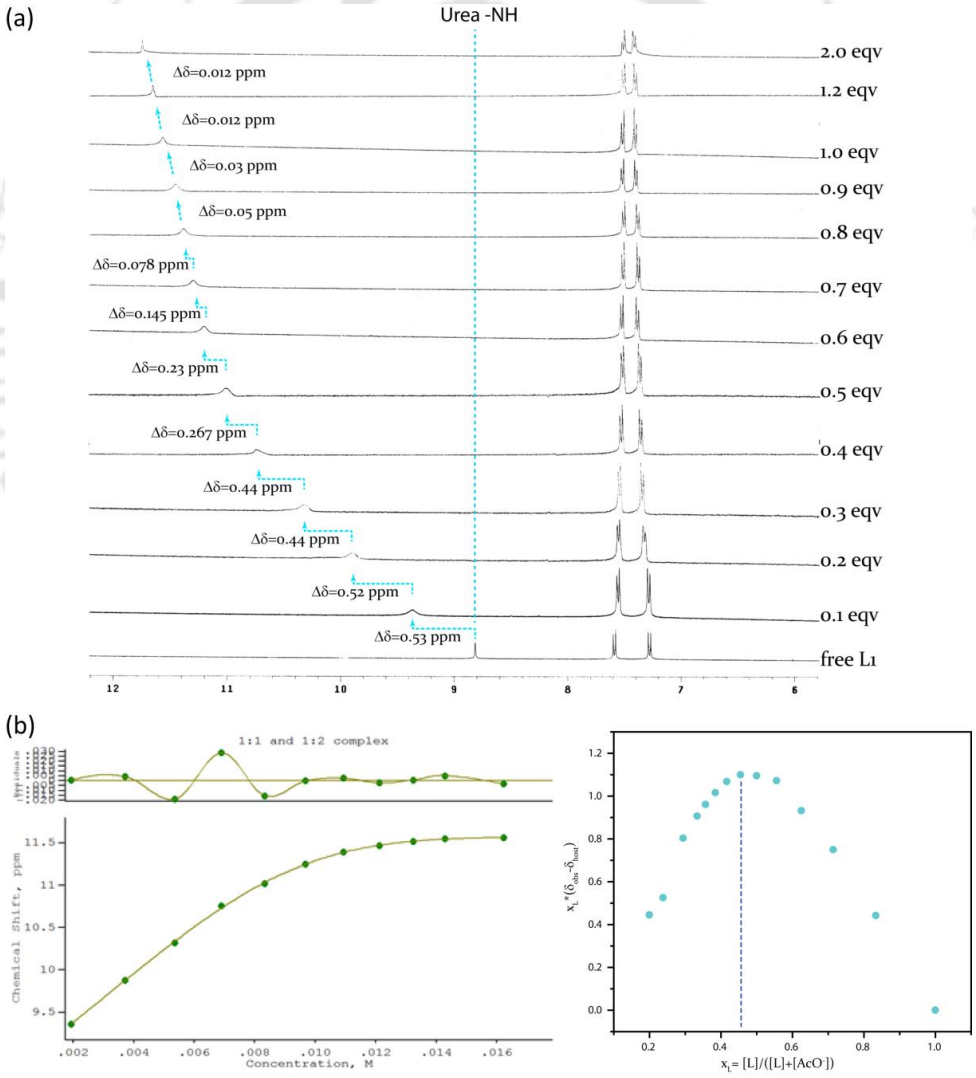

Figure A3.2 (a) Expanded partial ^{1}H NMR spectra of $\mathbf{L_1}$ upon titration with AcO^-(*n*-TBA) in DMSO-d_6 and (b) Fit plot obtained by WinEQNMR2 and corresponding Job's plot showing a maximum at 0.45 mole fraction of the receptor for the multiple equilibria existing between 1: 1 and 1 : 2 complexes in the determination of K_a using urea-NH resonance for $\mathbf{L_1}$ and acetate anion.

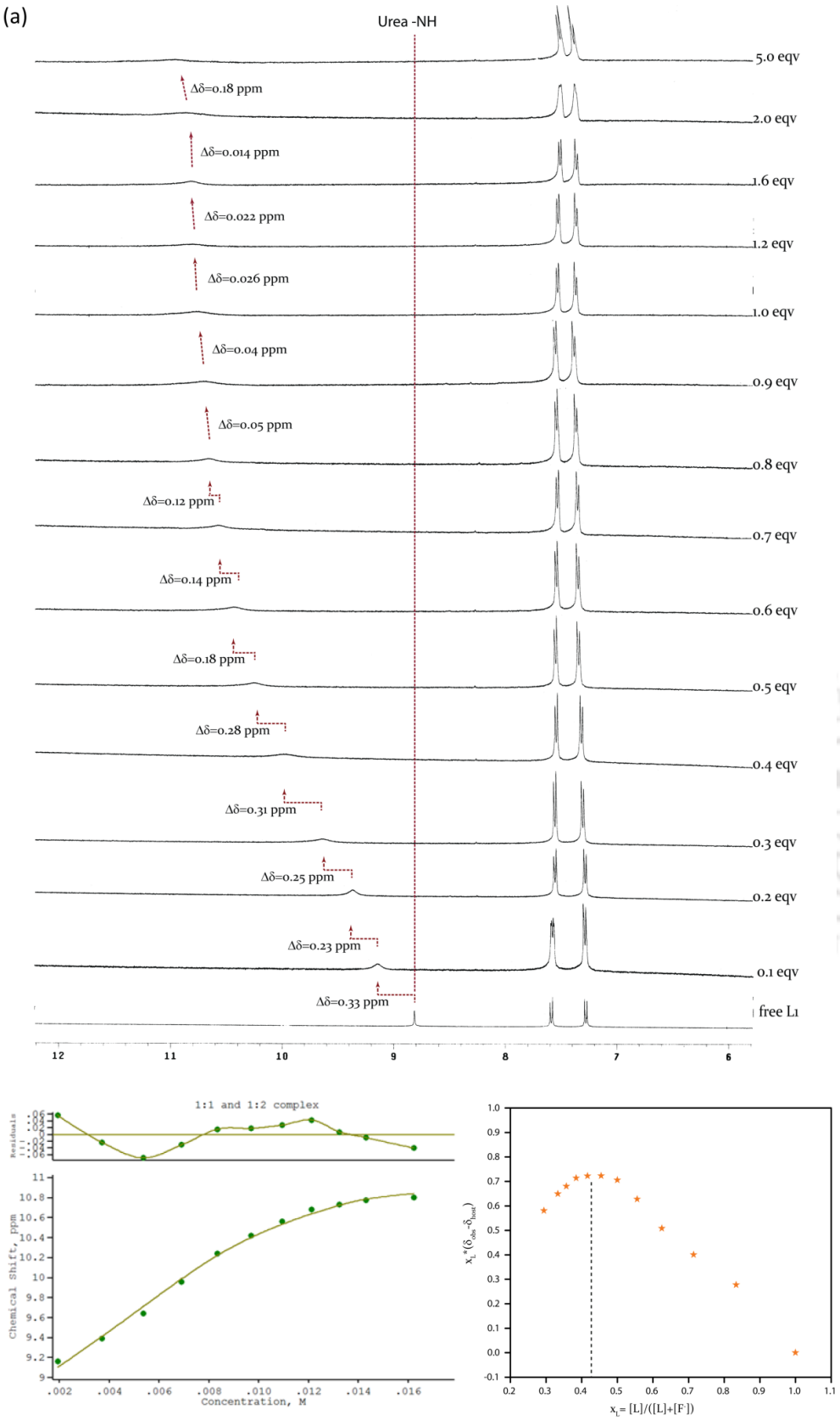

Figure A3.3 (a) Expanded partial ^{1}H NMR spectra of $\mathbf{L_1}$ upon titration with F^-(*n*-TBA) in DMSO-d_6 and (b) Fit plot obtained by WinEQNMR2 and corresponding Job's plot showing a maximum at 0.43 mole fraction of the receptor for the multiple equilibria existing between 1: 1 and 1 : 2 complexes in the determination of K_a using urea-NH resonance for $\mathbf{L_1}$ and fluoride anion.

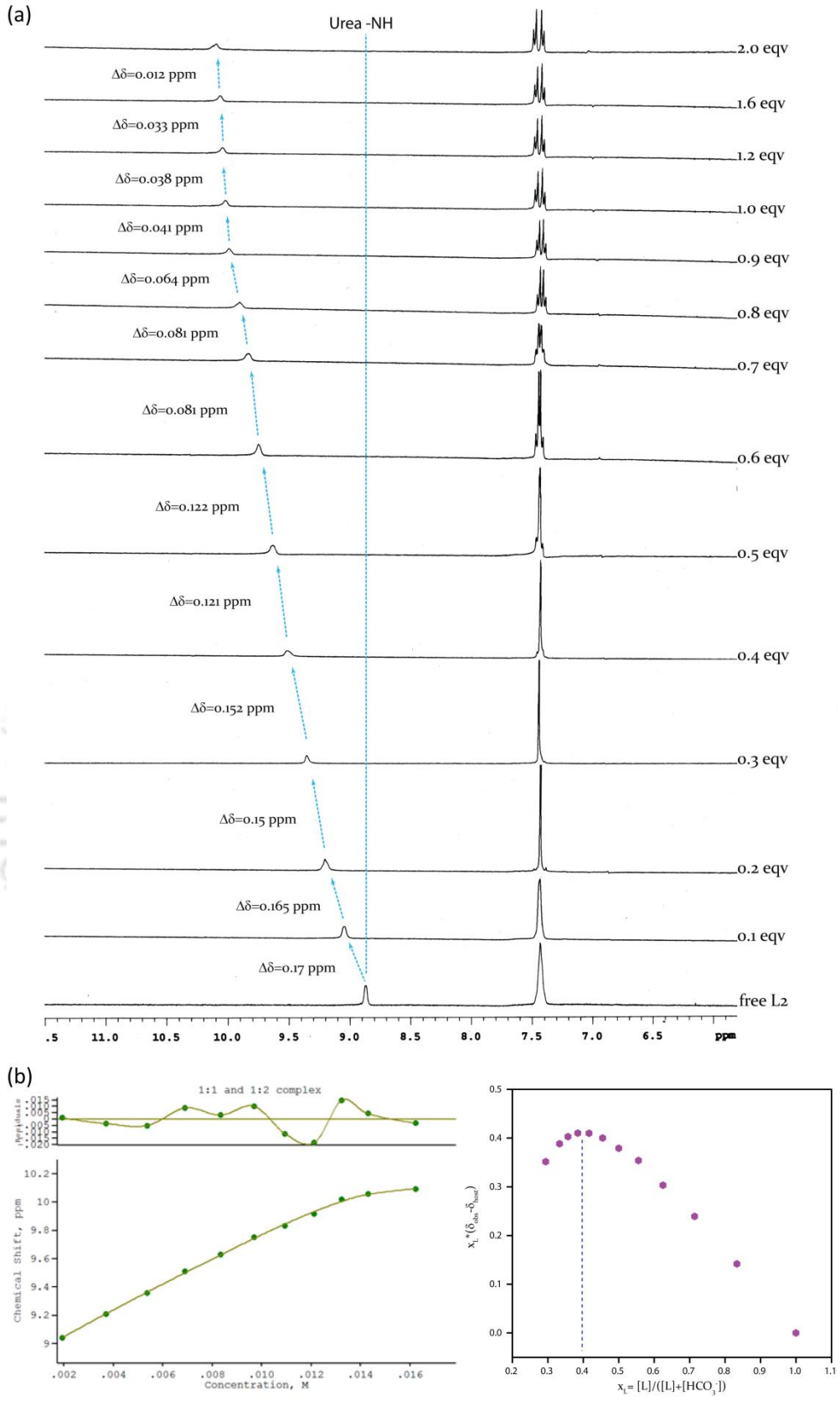

Figure A3.4 (a) Expanded partial ^{1}H NMR spectra of $\mathbf{L_2}$ upon titration with HCO_3^-(TEA) in DMSO-d_6 and (b) Fit plot obtained by WinEQNMR2 and corresponding Job's plot showing a maximum at 0.4 mole fraction of the receptor for the multiple equilibria existing between 1: 1 and 1 : 2 complexes in the determination of K_a using urea-NH resonance for $\mathbf{L_2}$ and bicarbonate anion.

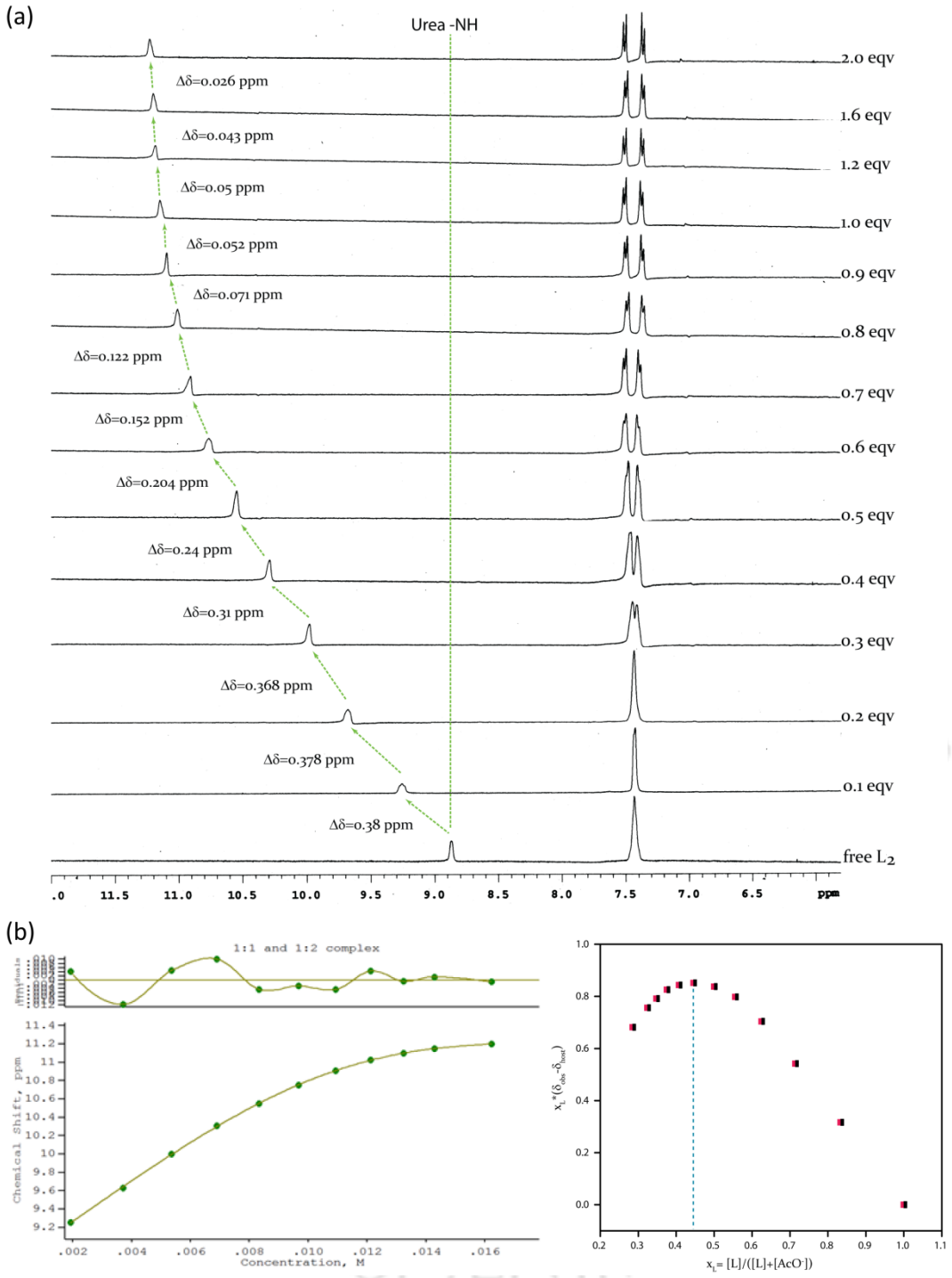

Figure A3.5 (a) Expanded partial ^{1}H NMR spectra of $\mathbf{L_2}$ upon titration with AcO^{-}(*n*-TBA) in DMSO-d_6 and (b) Fit plot obtained by WinEQNMR2 and corresponding Job's plot showing a maximum at 0.45 mole fraction of the receptor for the multiple equilibria existing between 1: 1 and 1 : 2 complexes in the determination of K_a using urea-NH resonance for $\mathbf{L_2}$ and acetate anion.

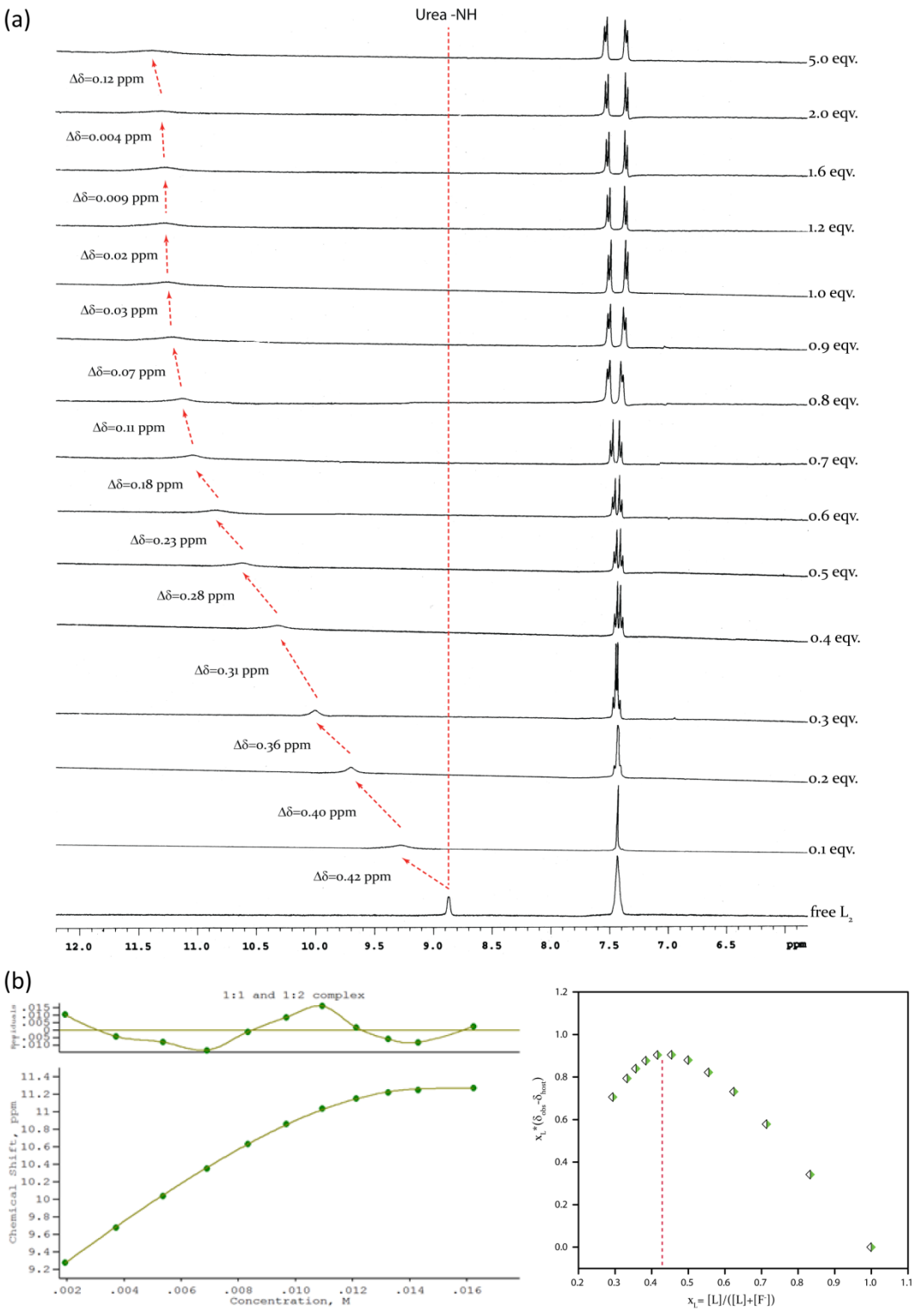

Figure A3.6 (a) Expanded partial ^{1}H NMR spectra of $\mathbf{L_2}$ upon titration with F^-(*n*-TBA) in DMSO-d_6 and (b) Fit plot obtained by WinEQNMR2 and corresponding Job's plot showing a maximum at 0.43 mole fraction of the receptor for the multiple equilibria existing between 1: 1 and 1 : 2 complexes in the determination of K_a using urea-NH resonance for $\mathbf{L_2}$ and fluoride anion.

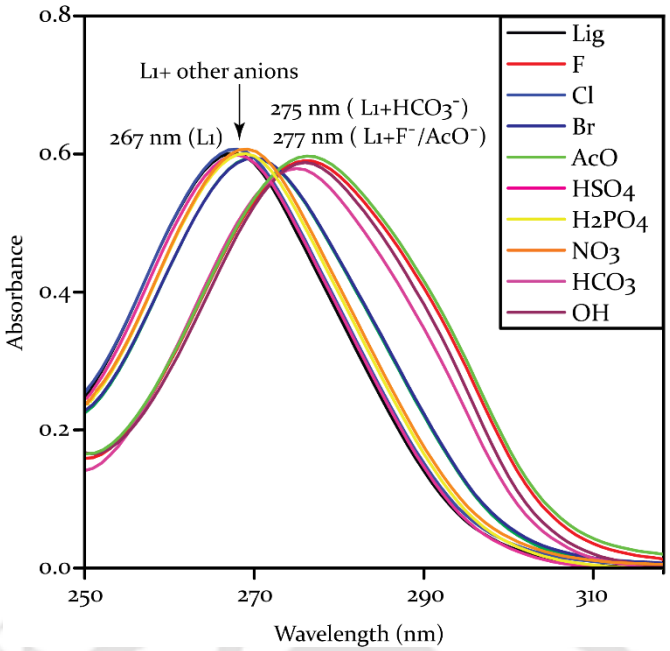

Figure A3.7 Changes in the UV/Vis spectrum of $\mathbf{L_1}$ in MeCN upon addition of *n*-TBA/TEA salts of anions (20 equiv.)

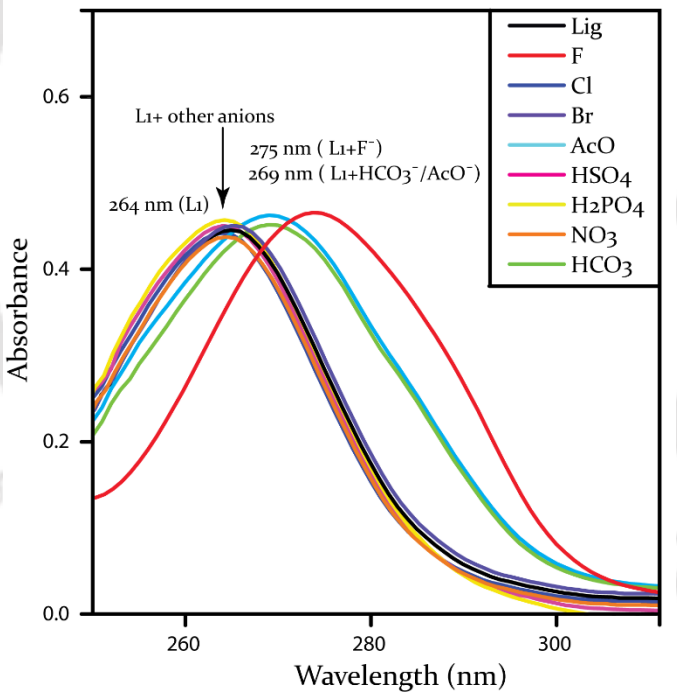

Figure A3.8 Changes in the UV/Vis spectrum of $\mathbf{L_2}$ in MeCN upon addition of *n*-TBA/TEA salts of anions (20 equiv.)

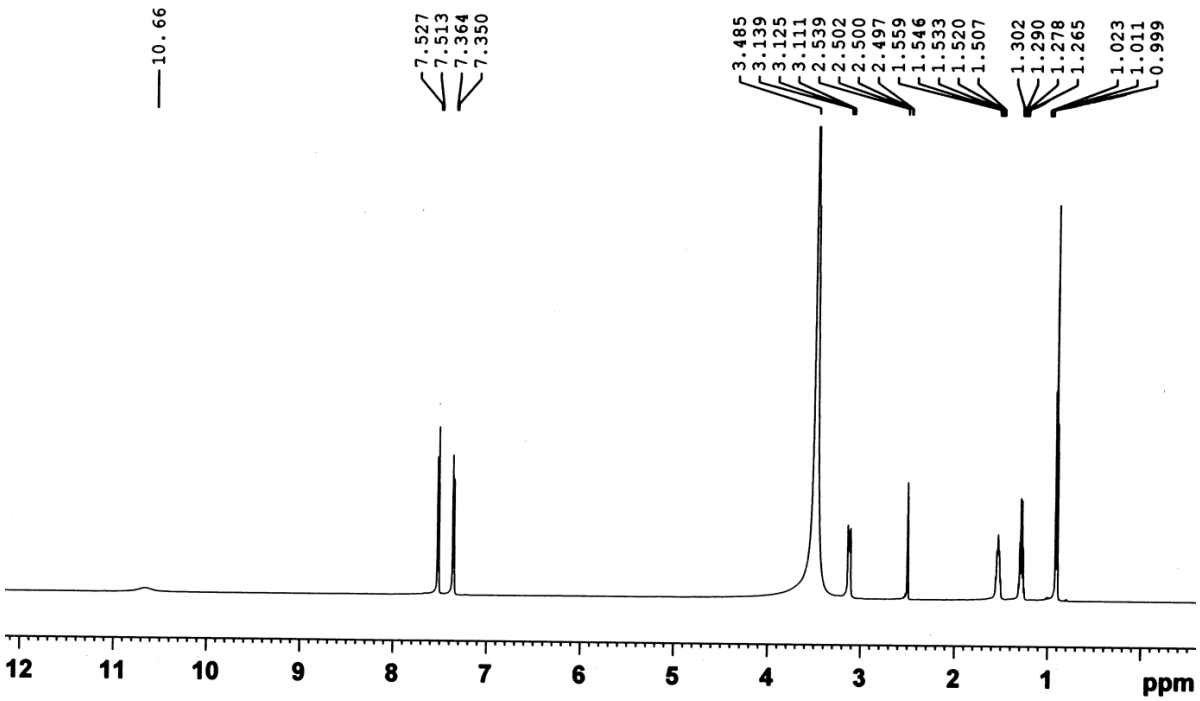

Figure A3.9 ^{1}H NMR spectrum of complex **1a** in DMSO-d_6 (Bruker-600 MHz) at 298 K.

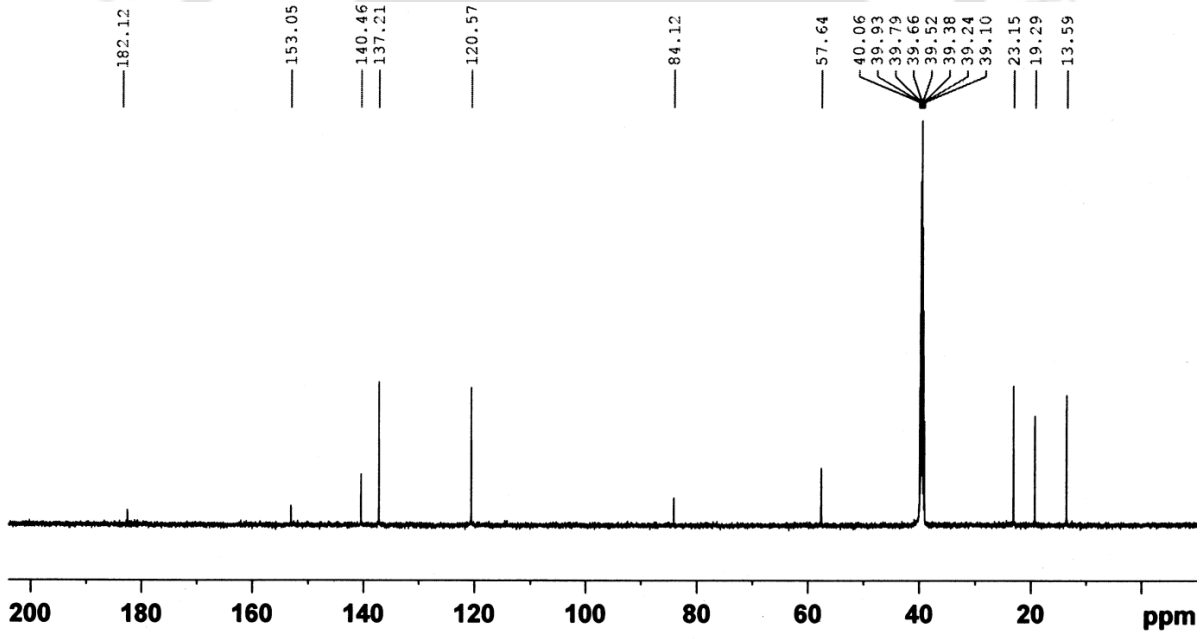

Figure A3.10 ^{13}C NMR spectrum of complex **1a** in DMSO-d_6 (Bruker-150 MHz) at 298 K.

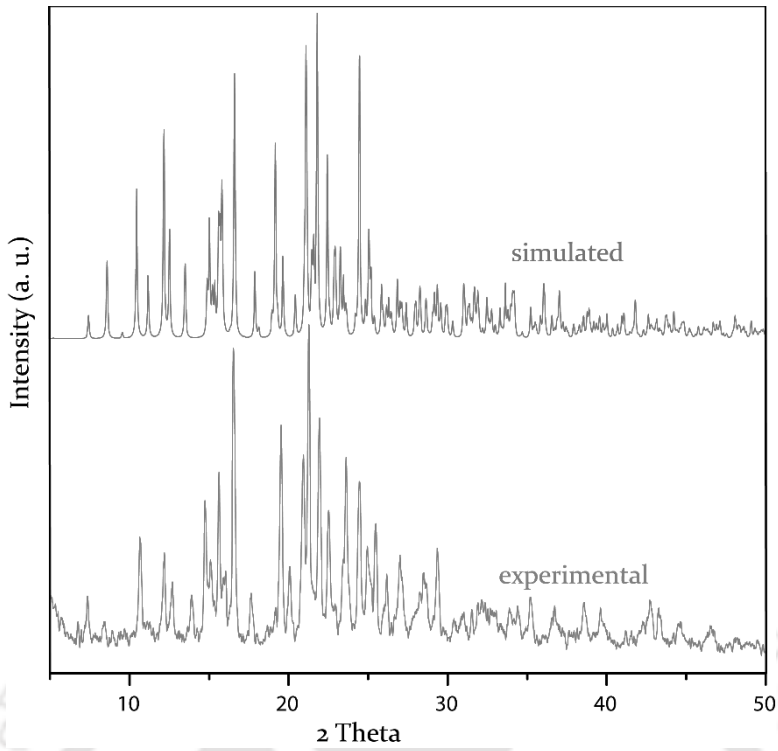

Figure A3.11 Powder X-ray diffraction patterns of isolated crystals of **1a:** experimental is in green colour and simulated pattern is in red colour.

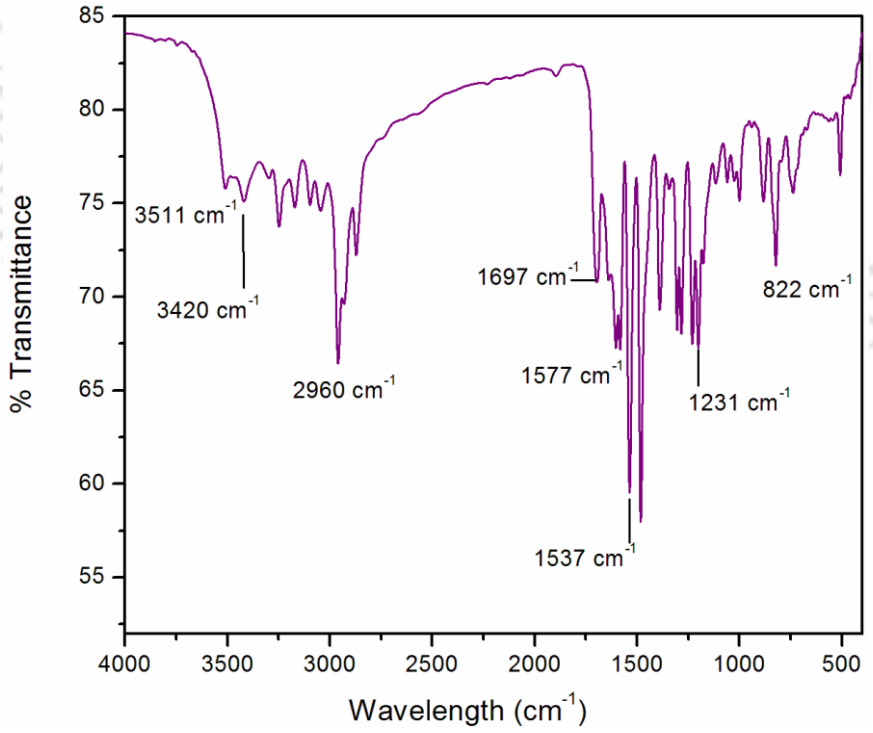

Figure A3.12 FT-IR spectrum of complex **1a** recorded in KBr pellet.

Chapter 4

Anion Binding and Encapsulation by a Set of Positional Isomeric Nitrophenyl Tris(urea) Receptors

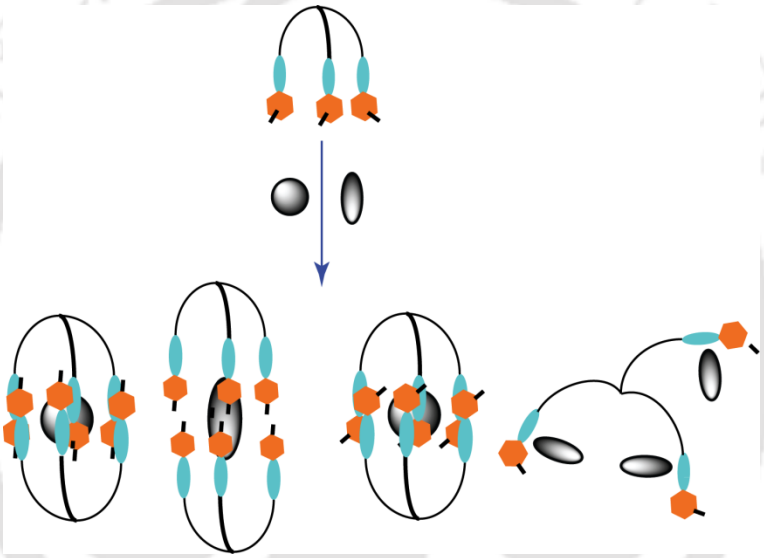

4.1 Background and Focus of the Chapter

Since the beginning of anion receptor chemistry, hydrogen bonding tripodal scaffolds has widely been employed for anion binding and encryption featuring receptor cavities, which can contract or expand in response to the incoming anionic guest species.[1] The binding ability of tripodal receptors for anionic guests varies with the appended peripheral functions, since both the position and the nature of functional groups modify the hydrogen bonding capability. Theoretical investigation by Hay *et al.* showed that the position of electron withdrawing substituents on the peripheral aryl moiety have significant consequences on the stability of anion complexes.[2] When two tripodal molecules with interior anion binding elements create a dimeric capsular assembly, there is a possibility to satisfy the higher coordination numbers required for the binding of multicharged oxoanions such as CO_3^{2-}, SO_4^{2-}, and PO_4^{3-}. Anions generally have very high free energies of solvation (e.g., $\Delta G_{hydration}$ of CO_3^{2-} and $H_2PO_4^-$ are –1315 and –465 kJ mol^{-1}) that must be compensated by the host for effective anion recognition.[3] Hydrogen bond donating tripodal receptors have shown a number of interesting properties, e.g., anion recognition in water,[4] encapsulation of anion-water clusters within dimeric capsular assembly,[5] fixation of aerial carbon dioxide (CO_2) as carbonate (CO_3^{2-}),[6] selective salt extraction from water,[7] and transmembrane anion transportation.[8]

This chapter is divided into two parts, where part A discusses the anion coordination and part B deals with ion-pair binding. Part A deals with a set of three nitrophenyl functionalized tripodal urea scaffolds, **L_3**, **L_4** and **L_5** (Scheme 4.1) and demonstrate the effect of positional isomerism in anion coordination.[9] Structural studies revealed oxyanion induced self-assembly of the para-isomer (**L_3**) into dimeric (pseudo)molecular capsule as observed in carbonate and terephthalate complexes (**3a** and **3b**), whereas the meta-isomer (**L_4**) can self-assemble into dimeric capsules only in presence of inorganic oxyanions, as observed in hydrogenphosphate complex (**4a**), and assemble into a 2D sheet-like structure in the presence of terephthalate dianion (**4b**). In contrast to **L_3** and **L_4** structural authentication of the *ortho*-isomer (**L_5**) in the presence of different oxyanions was not fruitful, and solution-state studies revealed that the receptor binds to oxyanions rather weakly in comparison to the *para*- and *meta*-isomers, as reflected from the apparent binding constant values of HCO_3^- and $H_2PO_4^{2-}$. However, F^- is bound almost equally by the three isomeric receptors. Furthermore, attempted crystallization of **L_3** in the presence of excess TBAF in DMSO yielded crystalline precipitate of F^- bound complex (**3c**), which was confirmed by ^{19}F and 2D-NOESY NMR analyses of the isolated complex. It is worth mentioning that the *meta*-isomer (**L_4**) has recently been established as a potential hydrogen bonding scaffold which can efficiently fix atmospheric CO_2 as air-stable crystals of CO_3^{2-}

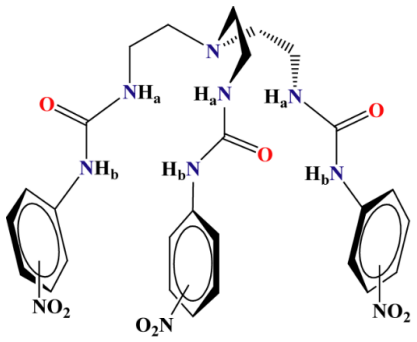

Scheme 4.1 Molecular structure of nitrophenyl appended tris(urea) receptors, $\mathbf{L_3}$ (*para*-isomer), $\mathbf{L_4}$ (*meta*-isomer) and $\mathbf{L_5}$ (*ortho*-isomer).

entrapped molecular capsule in DMSO solution induced by the presence of excess TBAF or an equivalent amount of TBAOH.[10]

Part B discusses an example of dual-host based ion-pair recognition. $\mathbf{L_3}$ in accompany with 18-crown-6-ether ($\mathbf{L_C}$) have also been structurally authenticated to self-assemble into a 1D coordination polymer in the presence of K_2CO_3 (**3d**).[11] In the integrated polymeric assembly, a carbonate anion is encapsulated within a dimeric assembly of the receptor $\mathbf{L_3}$ and one carbonyl oxygen and a nitro group from each tripodal unit of the dimeric assembly is coordinated to a potassium ion bound within the crown ether cavity.

4.2 Crystal structure of receptors $\mathbf{L_3}$

Single crystals of $\mathbf{L_3}$ suitable for X-ray diffraction analysis were obtained from dimethyl sulfoxide (DMSO) solution as [$\mathbf{L_3}$**.DMSO**], which crystallizes in the monoclinic space group P_21/c with Z = 4 (Annexure 4, table A4.1). Structural elucidation of the DMSO solvated crystal revealed that one of the urea functions from a tripodal sidearm is hydrogen bonded to lattice DMSO by relatively strong N−H···O hydrogen bonds, which is again involved in intra-molecular N−H···O hydrogen bonding with a second sidearm of the receptor (Fig. 4.1a). This intra-molecular hydrogen bonding between two arms of the tripodal ligand presumably assists one of the aryl rings of the hydrogen bonded tripodal arms to be in a π···π interaction (C2g···C3g = 3.831 Å) with the aryl ring of the third sidearm, which is not involved in any H-bonding interactions. Thus, the existence of intra-molecular N−H···O hydrogen bonding and aromatic π···π stacking restricts the opening of the flexible tripodal scaffold to an open conformation, which is very common and a stable conformation for this kind of tripodal ligand system. Additionally, multiple inter-molecular N−H···O hydrogen bonding interactions between the tripodal arms results in polymeric association of the receptor molecules bridged by lattice DMSO molecules. In the alternate layer, the ligands are oriented in the opposite direction. The DMSO molecules are arranged in a linear fashion through hydrophilic channels (Fig. 4.1b).

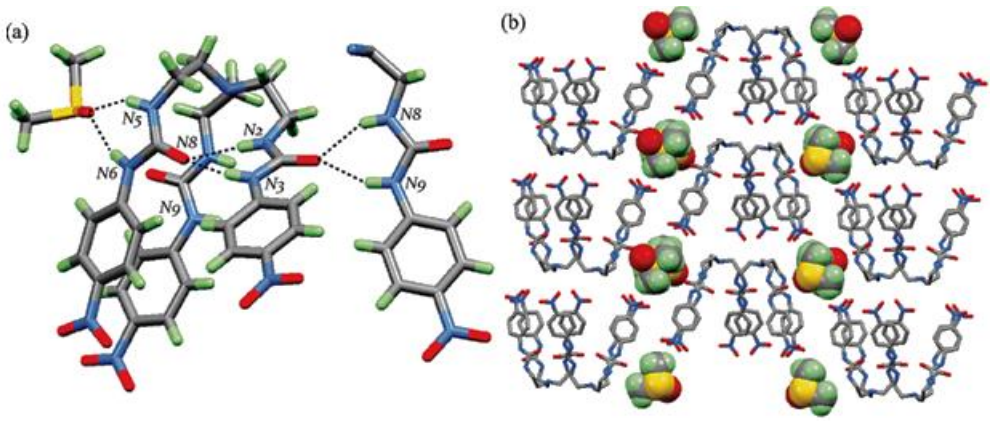

Figure 4.1 (a) Ball-and-stick representation of **L**$_3$.DMSO depicting inter-molecular N−H···O (carbonyl), N−H···O (DMSO) and intra-molecular N−H···O (carbonyl) interactions. (b) Packing diagram of **L**$_3$.DMSO viewed along the crystallographic c-axis.

Part A

4.3 Structural aspects of anion binding with L_3, L_4 and L_5

Structural information obtained from single crystal X-ray analyses of the anion complexes can provide insight into the binding differences of an anion with the isomeric receptors. From the perspective of anion receptor chemistry, crystallization has traditionally been a route to understand the structural insights of the anion complexes, which are then related to the observed selectivity in solution. We tried to explore the solid-state binding properties of **L**$_3$, **L**$_4$ and **L**$_5$ with different anions, by charging excess quaternary ammonium [*n*-TBA (tetrabutylammonium)/TEA (tetraethylammonium)] salt of anions to the individual receptor solutions in aprotic solvents such as MeCN, DMSO or DMF and allowed to crystallize at room temperature. Efforts were also made to crystalize the receptors with larger sized carboxylate (organic) oxyanions like benzoate phthalate, terephthalate and isophthalate as their in-situ generated *n*-TBA or TEA salts. However we were successful only with the terephthalate dianion, but fortunately for two of the receptors (*para*- and *meta*-isomers).

4.3.1 CO_3^{2-} -encapsulated dimeric capsule (3a)

The carbonate-encapsulated dimeric complex, 2TEA[2**L**$_3$(CO_3^{2-})] (**3a**) was obtained as suitable crystals for SC-XRD analysis upon slow evaporation of a 5 mL DMSO solution of **L**$_3$ in presence of excess (TEA)HCO_3. Structural elucidation revealed that the complex **3a** crystallizes in the monoclinic system with centrosymmetric space group C_2/c. Added HCO_3^- anion has been deprotonated in solution and is bound in the form of CO_3^{2-} by two inversion symmetric units of **L**$_3$ with an array of 14 N−H···O hydrogen bonds to the six urea functions, in the solid-state (Figure 4.2). A correlation of N−H···O angle vs N−H···O distance shows that 12 out of 14 hydrogen bonds are in the strong hydrogen bonding interaction region of d(H···O) ≤ 2.5 Å and

d(D···O) ≤ 3.2 Å (Annexure 4, Table A4.3), which indeed provide high stability to the dimeric molecular capsule. The inversion-symmetric molecules are flipped inward toward each other in a face-to-face fashion with a distance of 8.00(2) Å between the apical nitrogen atoms (Figure 4.2) and, thereby, generate a centrosymmetric molecular capsule self-assembled via multiple C−H···O H-bonds between each capsular unit. Such a solution state deprotonation of the protonated state of an anion namely, HCO_3^- and $H_2PO_4^-$, is common and results because of the formation of multiple H-bonding interactions with the receptor that lower the pK_a of the bound guest to the extent that it is deprotonated by the free guest species in solution.[12]

Structural comparison of **3a** (2TEA[2**L**$_3$(CO_3^{2-})]) with the reported carbonate-encapsulated complex of the *meta*-isomer (2TBA[2**L**$_4$(CO_3^{2-})])[11] revealed a couple of noteworthy features

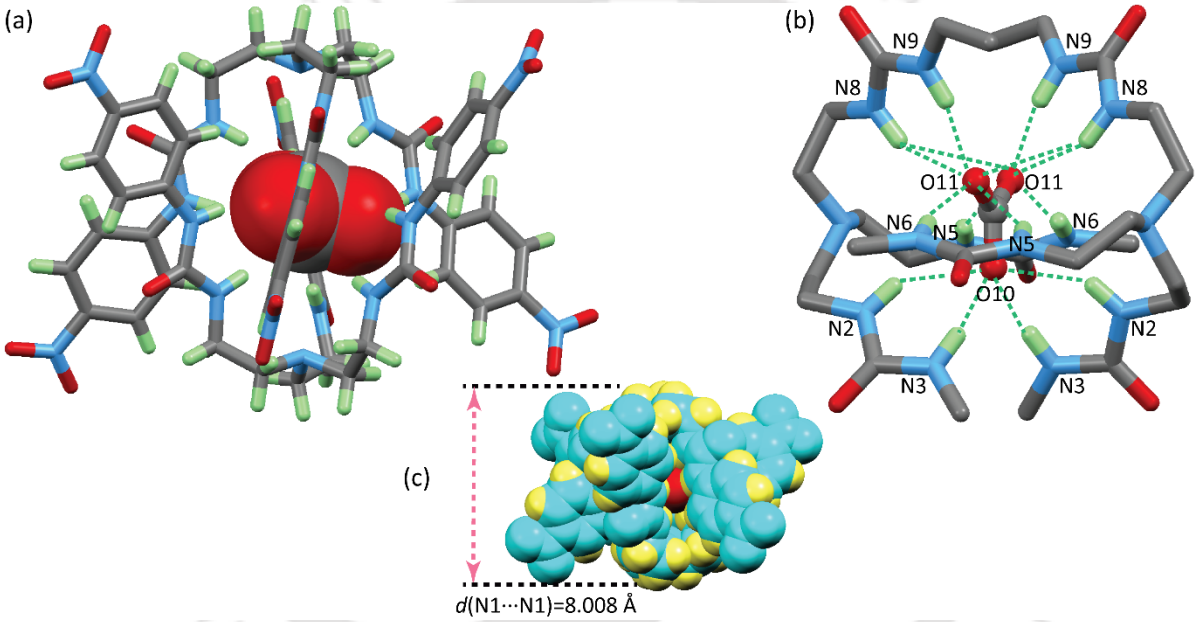

Figure 4.2 (a) X-ray structure of **3a** depicting the encapsulation of a CO_3^{2-} anion within a centrosymmetric capsule of **L**$_3$, (b) A magnified ball-and stick representation depicting the 14 H-bonding contacts on CO_3^{2-} within the dimeric capsule of **L**$_3$ in **3a** and (c) spacefill representation depicting full encapsulation of the anion (TEA cations and peripheral nitrophenyl groups are omitted for clarity).

that differentiate the binding of the CO_3^{2-}anion within the respective self-assembled dimeric capsules. Irrespective of the nature of the countercation (TEA/*n*-TBA), both the complexes crystallized in the same space group (C_2/c) with 14 hydrogen bonding contacts on the encapsulated CO_3^{2-}anion. In the carbonate complex of the *para*-isomer (**3a**), the anion is coordinated by 14 N−H···O hydrogen bonds, where a −NH (N8H) group from each receptor molecule of the capsule acts as a bifurcated H-bond donor to carbonate oxygen O11. However, in the carbonate complex of the *meta*-isomer, the binding occurs with the aid of 12 N−H···O H-bonds (one from each −NH group of the dimeric assembly) and 2 C−H···O H-bonds from an aryl function of each receptor unit (donated from the *para*-hydrogen with respect to the $-NO_2$

group) of the dimeric assembly having a capsular length of 9.05 Å.[11] Thus, substituting the *meta*-nitrophenyl terminal by its *para*-analogue in the tripodal urea scaffold resulted in a significant drop of 1.05 Å in the capsular size of the carbonate capsule **3a**, which is indeed a consequence of positional isomeric effect. The effect of positional isomerism has also been observed in the solid-state binding of sulfate by $\mathbf{L_3}$ and $\mathbf{L_4}$ where the former in the presence of sulfate ions resulted in a pseudodimeric capsule partially engulfing a SO_4^{2-}–$3H_2O$–SO_4^{2-} adduct, whereas the latter formed a sulfate encapsulated dimeric capsule. Thus, it is the anion that templates the formation of (pseudo)capsular self-assemblies in tripodal scaffolds and not the nature of the quaternary ammonium cations (TEA/*n*-TBA), which indeed have an overall effect in the crystal packing motif.

4.3.2 Terephthalate encapsulated pseudo-dimeric capsular complex (3b)

Terephthalate encapsulated pseudo-dimeric complex of $\mathbf{L_3}$, 2(*n*-TBA)[2$\mathbf{L_3}$($C_8H_4O_4^{2-}$)] (**3b**) was obtained as suitable crystals for SC-XRD analysis from a DMF solution (3 mL) mixture of $\mathbf{L_3}$ charged with an excess of a 1:2 solution mixture of terephthalic acid and TBA(OH). Slow evaporation of the solution at room temperature yielded colorless crystals of **3b** within a duration of 2 weeks. Structural elucidation revealed the formation of the 2:1 host-guest complex in **3b** that crystallizes in the triclinic system with *P*-1 space group. Each carboxylate group of a terephthalate dianion is coordinated to a receptor molecule by seven N–H···O hydrogen bonds to the three urea functions (Figure 4.3). A correlation of N–H···O angle vs N–H···O distance shows that five out of seven hydrogen bonds are in the strong hydrogen bonding interaction

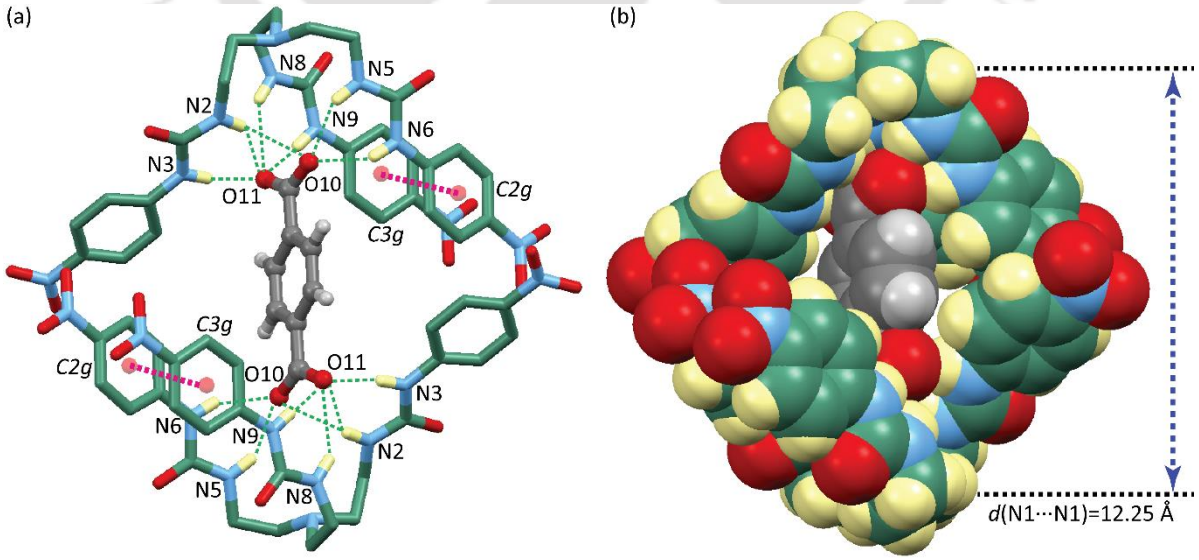

Figure 4.3 (a) X-ray structure of **3b** depicting the seven H-bonding contacts on each $-COO^-$ residue of terephthalate dianion and intramolecular π···π stacking in each receptor molecule of the dimeric capsule of $\mathbf{L_3}$ and (b) spacefill representation depicting the pseudo encapsulation of a terephthalate dianion (*n*-TBA countercations are omitted for clarity).

region of d(H···O) ≤ 2.5 Å and d(D···O) ≤ 3.2 Å (Annexure 4, Table A4.3). Carboxylate is bound more strongly to the $-NH_b$ protons of the receptor with an average hydrogen bond distance of 2.848 Å, whereas the $-NH_a$ protons interact with an average hydrogen bond distance of 3.157 Å. Additionally, two tripodal side arms of a receptor molecule are involved in π···π interaction with a distance of 3.824 Å between the centroids of each aromatic (C2g···C3g). Two inversion symmetric receptor molecules are flipped inward toward each other in a face-to-face fashion with a distance of 12.25(2) Å between the apical nitrogen atoms (Figure 4.3) and, thereby, generate a pseudo molecular capsule engulfing a terephthalate dianion. Additional stability to the crystals of **3b** is provided by intermolecular π-stacking interactions and C−H···O interactions between the adjacent anion bound receptor units.

4.3.3 Hydrogenphosphate Complex of L_4 (4a)

Dimeric capsular complex 2TBA[2$\mathbf{L_4}$(HPO_4^{2-})] (**4a)** of $\mathbf{L_4}$ encapsulating HPO_4^{2-} was obtained as suitable crystals for SC-XRD analysis by slow evaporation of a 3 ml DMF solution containing $\mathbf{L_4}$ charged with an excess of a 1:1 solution mixture of TBA(H_2PO_4) and TBA(OH). Complex **4a** crystallizes in the triclinic system with *P*-1 space group. The dihydrogen phosphate anion has deprotonated in presence of TBA(OH) and is bound in the form of HPO_4^{2-} by two units of receptor $\mathbf{L_4}$. One host molecule is coordinating in axial mode and the other in facial mode with an array of 13 N−H···O H-bonds to the six urea functions and 2 weak C−H···O H-bonds (Figure 4.4). A correlation of N−H···O angle vs. N−H···O distance shows that 10 out of

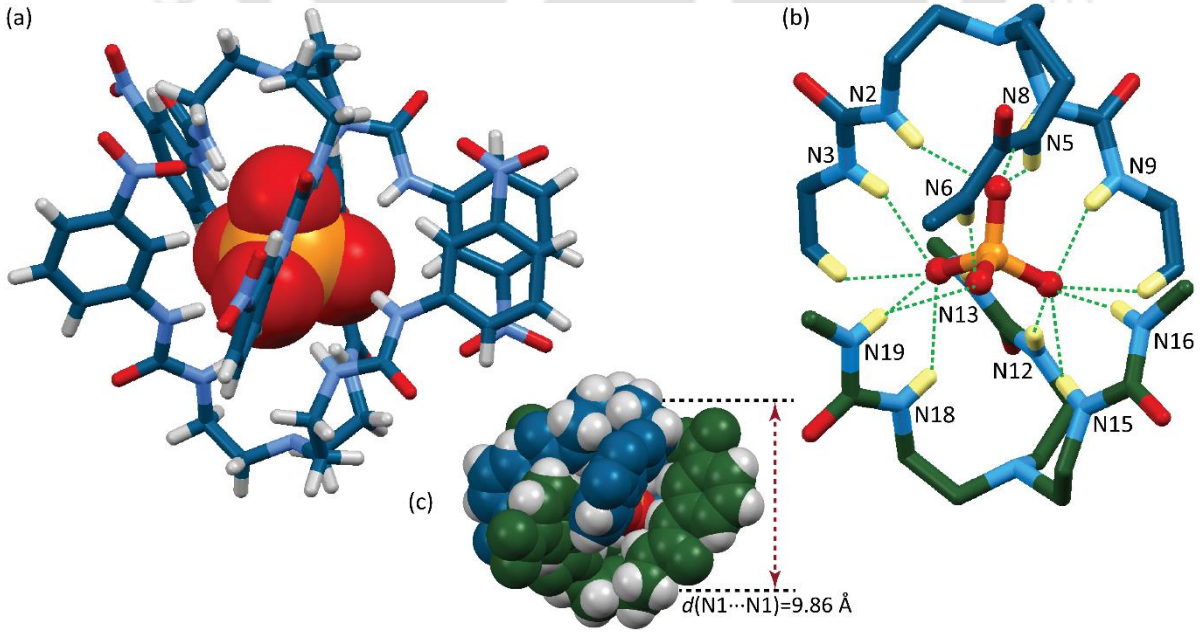

Figure 4.4 (a) X-ray structure of **4a** depicting the encapsulation of a HPO_4^{2-} (spacefilled) anion within the dimeric capsular assembly of $\mathbf{L_4}$,(b) Ball-and-stick representation (magnified view) depicting the 15 hydrogen bonding contacts on HPO_4^{2-} and (c) spacefill representation depicting the full encapsulation of the guest (*n*-TBA counter cations are omitted for clarity).

13 N−H···O bonds are in the strong H- bonding interaction region of d(H···O) ≤ 2.5 Å and d(N···O) ≤ 3.2 Å (Annexure 4, Table A4.3). The **L_4** molecules are flipped inward toward each other in a face-to-face fashion with a distance of 9.859(5) Å between the apical nitrogen atoms and thereby, generate a rigid dimeric capsule assembled by π···π interactions of the phenyl rings.

4.3.4 Terephthalate complex of L_4 (4b)

Terephthalate complex 3(*n*-TBA)[**L_4**($C_8H_4O_4^{2-}$)$_{1.5}$] (**4b**) was obtained as suitable crystals for SC-XRD analysis exactly in the same way as complex **3b**. Complex, **4b** crystallizes in the triclinic *P*-1 space group with three lattice water molecules as the solvent of crystallization. Structural elucidation revealed the formation of a 1:1.5 host−guest complex, where each tripodal side arm of a receptor molecule is coordinated to a carboxylate function of three individual terephthalate dianions (Figure 4.5). Each carboxylate group is coordinated to a urea function via double hydrogen bonding interactions, and each terephthalate dianion is sandwiched between the side arms of two receptor molecules generating an extended 2D sheet-like structure (Figure 4.5). The carboxylate groups are bound with an active and equal participation from both the aliphatic −NH_a and aromatic −NH_b protons with an average donor-to-acceptor distance of 2.806 Å (Annexure 4, Table A4.3).

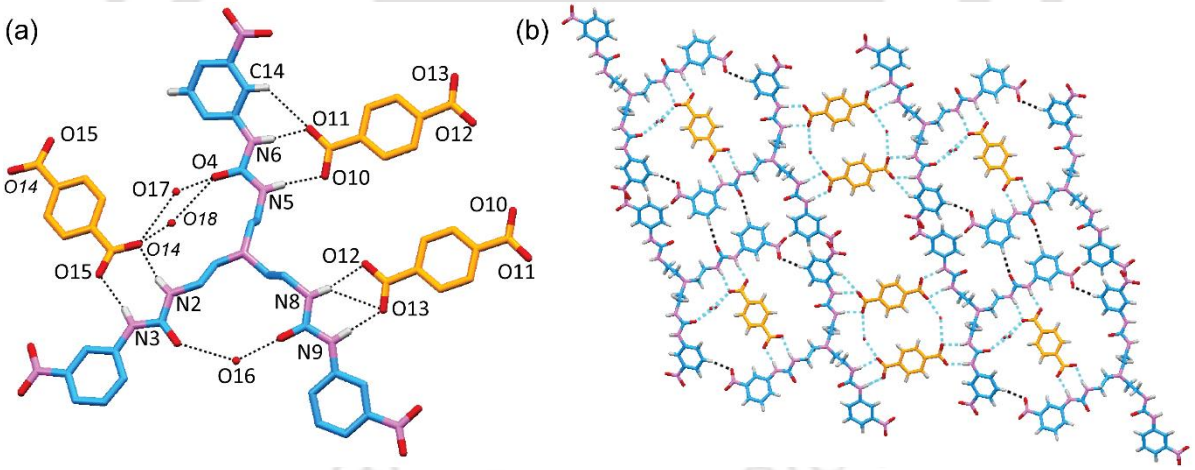

Figure 4.5 (a) X-ray structure of **4b** depicting the double H-bonding contacts on −COO^- functions of terephthalate dianion and (b) 2D sheet like assembly formed by the extension of H-bonding interactions in **4b** (*n*-TBA cations are omitted for clarity).

Unlike the terephthalate complex of **L_3** (**3b**), the receptor molecule in **4b** could not include the terephthalate guest within the tripodal cavity, presumably due to the steric hindrance provided by the meta-nitro substitution of the peripheral aryl functions, and thereby adopts an extended trigonal planar-like geometry by interacting with multiple anionic residues. The inclusion of three H_2O molecules in the crystal lattice provide added stabilization to the complex by forming hydrogen bonds with the urea oxygen atoms and with a carboxylate oxygen (O14) of a

terephthalate dianion. Furthermore, the H_2O molecules are weakly hydrogen bonded to the TBA cations and thereby strengthen the interactions between the cation-anion layers.

4.4 Effect of Positional Isomerism in Solution-State Anion Binding

^{1}H NMR analyses (DMSO-d_6) of the isolated anion complexes (**3a**, **3b**, **4a** and **4b**) and of receptors $\mathbf{L_3}$ and $\mathbf{L_5}$ in presence of equivalent amounts of different anions such as F^-, HCO_3^-, and $H_2PO_4^-$ further demonstrate the effect of positional isomerism in nitrophenyl functionalized urea receptors. 2D-NOESY NMR experiments (DMSO-d_6) performed with the isolated anion complexes and receptors $\mathbf{L_3}$ and $\mathbf{L_5}$ provide insight into the solution-state encapsulation of inorganic anions. ^{1}H NMR analysis of the CO_3^{2-}-encapsulated complex **3a** showed an average downfield shift of 1.55 ppm for the –NH protons, indicating a strong solution-state binding of CO_3^{2-} with the urea functions (Figure 4.6a). ^{1}H NMR titration data of $\mathbf{L_3}$ with aliquots of standard TEA(HCO_3) solution gave the best fit for 1:1 host−guest stoichiometry with an apparent binding constant (log *K*) value of 4.07 (Annexure 4, Fig A4.1 and A4.2). Thus, binding of HCO_3^- with the *para*-isomer $\mathbf{L_3}$ is comparable to that of the *meta*-isomer $\mathbf{L_4}$.[11] On the other hand, titration of the ortho-isomer $\mathbf{L_5}$ with TEA(HCO_3) showed an average downfield shift of 0.66 ppm for the −NH protons, and the association constant (log *K*) was calculated to be 1.38 with a 1:1 host-guest stoichiometry in agreement with the Job's plot analysis (Annexure 4, Fig A4.5 and A4.6).

^{1}H NMR analysis of the F^- complex **1c** showed an appreciable downfield shift of 0.80 and 1.80 ppm for the $-NH_a$ and $-NH_b$ protons, respectively, suggesting that F^- is bound more strongly to the $-NH_b$ protons of the receptor (Figure 4.6a). Titration data of $\mathbf{L_3}$ with standard (*n*-TBA)F solution gave the best fit for 1:1 host-guest stoichiometry with an association constant (log *K*) value of 3.72 (Annexure 4, Fig 4.3 and 4.4). However, in a qualitative experiment, addition of 1 equivalent of (*n*-TBA)F to a solution of $\mathbf{L_3}$ in DMSO-d_6 resulted in a downfield shift of 1.45 and 1.14 ppm for the $-NH_a$ and $-NH_b$ protons, respectively (Figure 4.6b), indicating that $-NH_a$ protons are more strongly hydrogen bonded to F^- than $-NH_b$ protons. Similar to $\mathbf{L_3}$ and $\mathbf{L_4}$, titration of $\mathbf{L_5}$ with (*n*-TBA)F gave the best fit for 1:1 host-guest stoichiometry with an apparent binding constant (log *K*) value of 3.45 (Annexure 4, Fig 4.7 and 4.8). Similarly, in the qualitative test for $H_2PO_4^-$ binding, addition of 1 equiv. of the anion to the individual solutions of $\mathbf{L_3}$ and $\mathbf{L_5}$, resulted in a downfield shift of 1.46 and 0.77 ppm for the $-NH_a$ resonance and a shift of 1.22 and 0.65 ppm for the $-NH_b$ resonance of the isomeric receptors (Figure 4.6). Titration of $\mathbf{L_3}$ and $\mathbf{L_5}$ with (*n*-TBA)H_2PO_4 gave the best fit for 1:1 host-guest stoichiometry with apparent binding constant (log *K*) values of 4.14 and 1.86, respectively. From the ^{1}H NMR analyses, it can be argued that *ortho*-nitro substitution at the peripheral aryl function

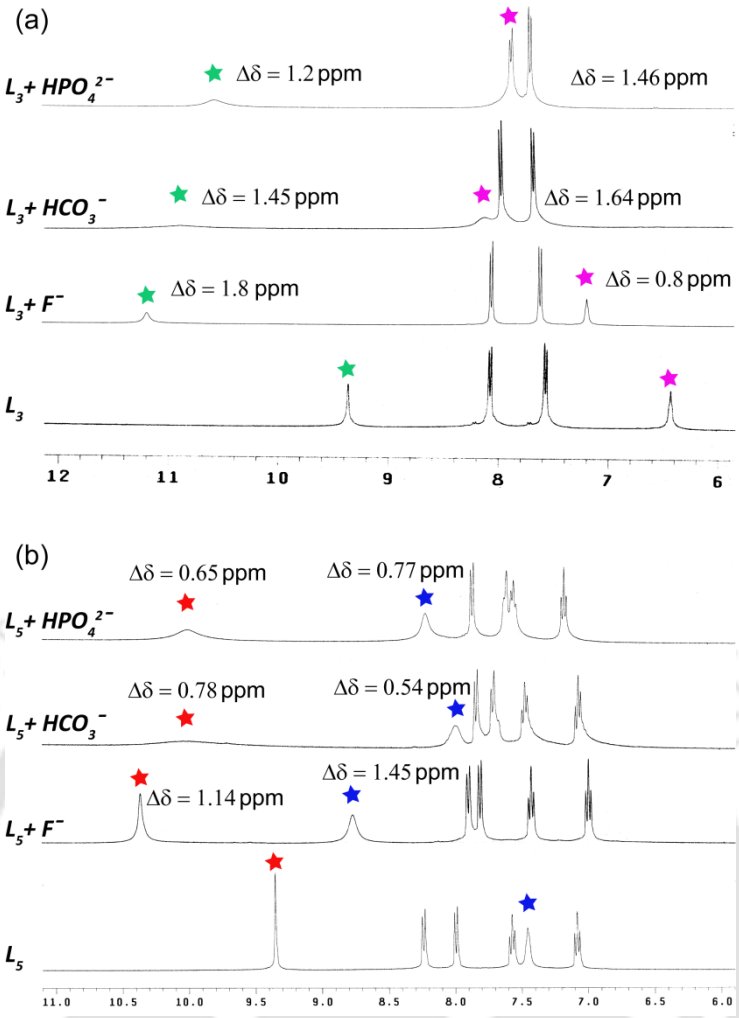

Figure 4.6 Comparison of the ^{1}H NMR spectra of (a) **L$_3$** and (b) **L$_5$** with one equivalent of F^-, CO_3^{2-} and $H_2PO_4^-$.

significantly reduces the ability of the tripodal urea scaffold toward binding and encapsulation of planar and tetrahedral oxoanions, as evident from the changes in −NH chemical shift values of the isomeric receptors in the presence of oxoanions such as HCO_3^- and $H_2PO_4^-$ and their log *K* values. However, fluoride is bound almost equally by the isomeric receptors. Furthermore, it is interesting to note that, in the ^{1}H NMR spectra of complexes **3a-c** and of an equimolar solution of **L$_3$** and $H_2PO_4^-$, there are no observable changes in the positions of the aryl protons relative to the free receptor (**L$_3$**), indicating the preorganization of the *para*-isomer that does not undergo any significant solution-state conformational changes upon binding and encapsulation of anions. However, ^{1}H NMR spectra of the ortho-isomer (**L$_5$**), in the presence of equivalent amounts of F^-, HCO_3^-, and $H_2PO_4^-$, showed a considerable upfield shift of the aryl protons, suggestive of a solution-state structural reorganization of the receptor side arms that could facilitate the formation of multiple N−H···A$^-$ hydrogen bonds to coordinate the anion within the receptor cavity via opening of the $-NO_2$ barricade. The most significant changes in chemical shift have been observed for the more acidic aryl protons $-H_c$ and $-H_f$, which get shifted upfield with an average Δδ value of 0.72 and 0.40 ppm, respectively (Figure 4.6b).

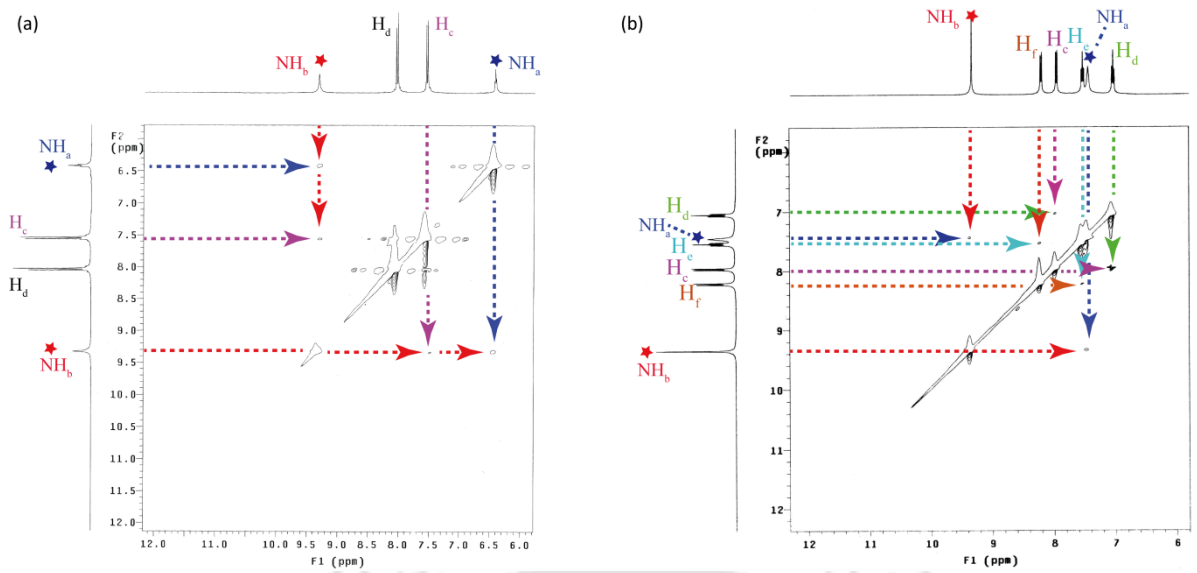

Figure 4.7 2D-NOESY NMR spectra of receptors (a) **L**$_3$ and (b) **L**$_5$ in DMSO-d_6.

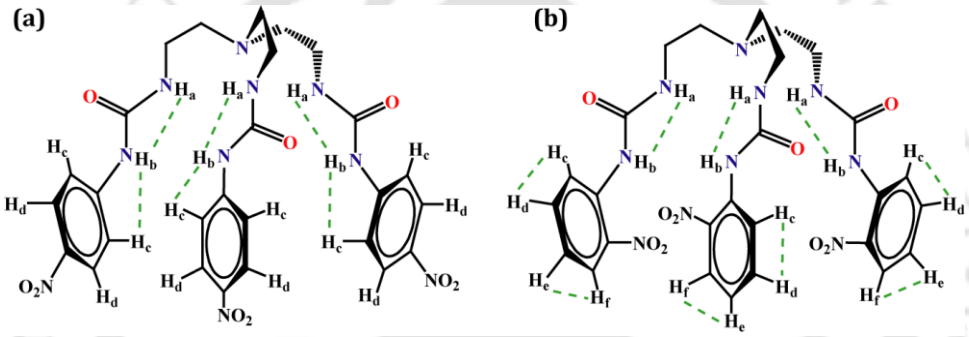

Scheme 4.2 Schematic representation of the through-space interactions between different sets of protons in (a) **L**$_3$ and (b) **L**$_5$, as established from the 2D NOESY NMR experiments of **L**$_3$ and **L**$_5$.

2D-NOESY NMR analyses of **L**$_3$ and **L**$_5$ in DMSO-d_6 (Figure 4.7) provide evidence of the conformational preorganization of the isomeric receptors. The *para*-isomer showed a strong NOE coupling between the urea protons ($H_a\cdots H_b$) and a comparatively weak coupling between the urea proton –H_b and ortho-aryl proton −H_c ($H_b\cdots H_c$) (Scheme 4.2a), whereas the *ortho*-isomer showed two NOE couplings between the different sets of aryl protons ($H_c\cdots H_d$ and $H_e\cdots H_f$) in addition to the urea $H_a\cdots H_b$ interaction (Scheme 4.2b).

The lack of through space $H_b\cdots H_c$ interaction in **L**$_5$ implies that the nitro-group is oriented toward the receptor cavity along with the urea −NH protons. Thus, ortho-nitro aromatic substitution to the N-bridged urea scaffold acts as a barricade for the receptor cavity that resists the binding and encapsulation of larger anions, in contrast to the *para*-isomer. Additionally, 2D-NOESY NMR analyses of the isolated anion complexes (Figure 4.8) further provide evidence of the subtle interplay of positional isomeric effect toward binding and/or encapsulation of anionic guests. NOESY NMR spectra of the carbonate and fluoride complexes **3a** and **3c** showed the disappearance of off-diagonal $H_a\cdots H_b$ coupling indicating the encapsulation of the respective

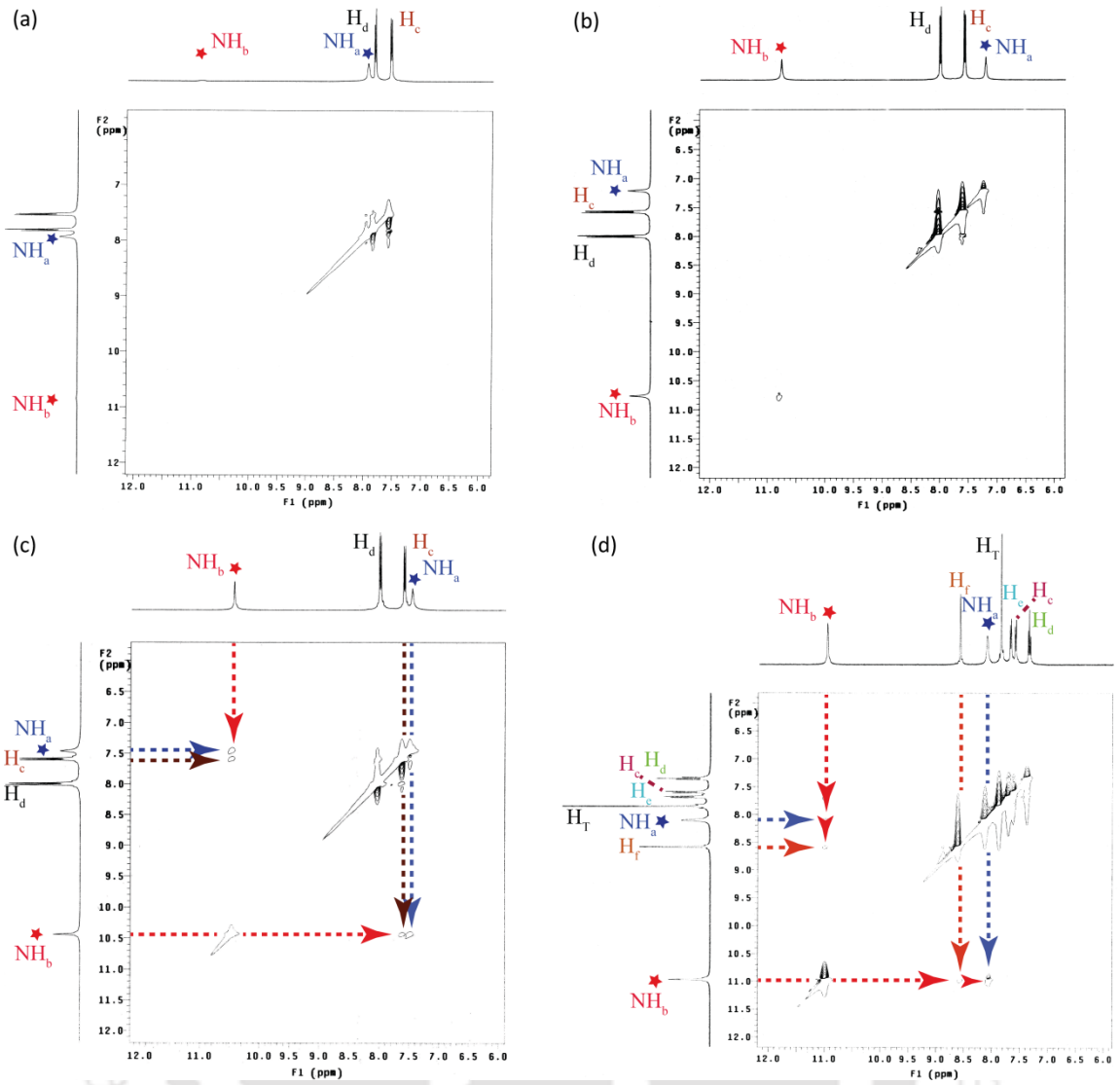

Figure 4.8 2D NOESY NMR spectra of isolated complexes (a) **3a**, (b) **3c**, (c) **3b** and (d) **4b**.

anions within the tripodal cavity of receptor **L_3**. However, the terephthalate complex of **L_3 (3b)**, showed the existence of off-diagonal $H_a\cdots H_b$ and $H_b\cdots H_c$ couplings as observed in the NOESY NMR spectrum of the free receptor, which suggests that the terephthalate dianion may not be engulfed within the receptor cavity in the solution state. Similar through space NOE couplings have also been observed in the 2D spectrum of the terephthalate complex of **L_4** (**4b**), which showed the presence of $H_a\cdots H_b$ and $H_b\cdots H_f$ interactions.

Part B

4.5 Dual-host–guest complex [$2L_3 2L_C(2K^+)(CO_3^{2-})$], (3d)

On the basis of the previous carbonate encapsulated complex **3a**, the stoichiometry for this three component complexation reaction had been maintained in a ratio of 2 : 2 : 1 = $\mathbf{L_3}$: $\mathbf{L_C}$: K_2CO_3 in DMSO. The resulting solution was stirred vigorously for about an hour at 60˚C. The solution was then allowed to cool at room temperature and filtered. Slow evaporation of the filtrate at room temperature yielded good quality colorless crystals suitable for single crystal X-ray crystallography analysis.

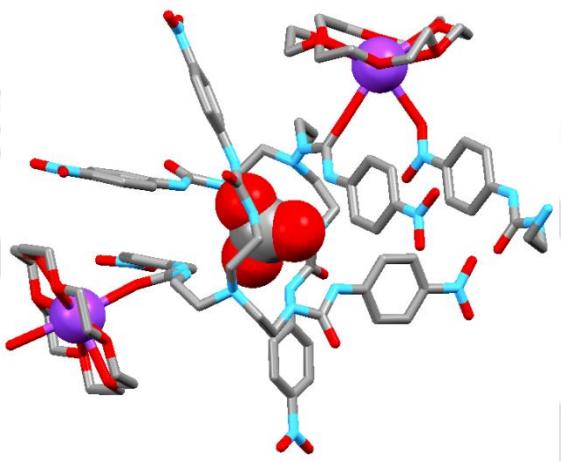

Figure. 4.9 Ball-and-stick representation of the dual-host–guest complex, **3d.**

Single crystal X-ray structure elucidation revealed the formation of a 1D coordination polymer composed of $\mathbf{L_3}$, $\mathbf{L_C}$ and K_2CO_3. The complex crystallizes in the triclinic system with the *P*-1 space group, where each potassium ion is bound within the cavity of the crown ethers ($\mathbf{L_C}$) and a CO_3^{2-} anion is encapsulated within a dimeric capsular assembly of $\mathbf{L_3}$ (Fig. 4.9). Each potassium ion, besides being coordinated with the crown etheric oxygen atoms, is also in coordination with a carbonyl group and a nitro group of each tripodal receptor unit of the CO_3^{2-}-encapsulated dimeric assembly. Two potassium ions experience different modes of binding within the network assembly. A tripodal unit of the dimeric assembly plays a key role in the formation a 1D coordination polymer by coordinating to the crown ether centered potassium ion by a carbonyl oxygen in one direction and a nitro oxygen in the other direction, donated from a different sidearm of the same receptor (Fig. 4.9). All six amide carbonyl oxygen atoms and nitro groups at the para-position of the phenyl ring of the dimeric assembly point outwards and this spatial orientation assists the formation of the polymeric assembly.

Carbonate encapsulation: Two symmetry independent molecules of $\mathbf{L_3}$ with opposite orientations form a capsular nano-cavity that encapsulates a CO_3^{2-} in its center via sixteen N–H···O hydrogen bonds to the six urea groups. The receptor molecules are flipped inwards to each

other in a face-to-face fashion with a distance of 8.451(5) Å between the apical nitrogen atoms. The planar CO_3^{2-} anion remains perpendicular to the C_3 axis, passing through the apical nitrogen atoms. This in turn opens the cavity of the ligand to make it more flat in comparison to the structure of the free ligand. Carbonate oxygen atoms O1 and O2 accept five N−H···O hydrogen bonds each whereas O3 accepts six N−H···O bonds from the dimeric assembly (Fig. 4.10a). The urea protons N3H, N5H, N6H, N9H, N13H, N15H, N16H and N19H donate one N−H···O hydrogen bond each to the carbonate oxygen atoms whereas N2H, N8H, N12H and N18H behave as bifurcated hydrogen bond donors, as detailed in Table 2. A correlation of the N–H···O angle versus the N−H···O distance shows that 10 out of the 16 hydrogen bonds are in the strong hydrogen bonding interaction regions of d(H···O) < 2.5 Å and d(D···O) < 3.2 Å (Annexure 4, Table A4.4). Participation of all the urea N–H bonds in the hydrogen bonding with the encapsulated CO_3^{2-} anion helps them to converge inside the cavity. Hence, all the amide carbonyl oxygen atoms are not directed outside the cavity and are available for metal coordination. This observation gives us a clue to explore the possibility of the CO_3^{2-} encapsulated dimeric capsular assembly to form a metal coordination network.

1D coordination polymer: In the dual-host complex (**3d**), each potassium ion is coordinated to a crown ether molecule by all six ethereal oxygen atoms. However, the potassium ion favours a coordination number of 8 or more. Hence, two additional oxygen atoms from each tripodal unit of the carbonate encapsulated dimeric assembly is coordinated to each crown ether centered potassium ion by a carbonyl group and a nitro group, satisfying eight coordinated bonds on each potassium ion. Due to the participation of the carbonyl and nitro oxygen atoms of $\mathbf{L_3}$ in K^+ coordination, two different types of coordination modes have been observed for the crown ether encapsulated potassium ions. A crown ether bound K^+ (labelled as $K1^+$ in the complex) is coordinated to a carbonyl oxygen and a nitro oxygen in an anti-fashion, donated from two adjacent symmetry identical receptor units of the extended dimeric assembly to form a 1D coordination polymer (Fig. 4.10b). However, the second crown ether bound K^+ (labelled as $K2^+$ in the complex) is also coordinated to a carbonyl oxygen and a nitro oxygen in a syn-fashion, donated from two neighboring symmetry identical receptor units of the carbonate encapsulated dimeric assembly to form a binuclear dimer (Fig. 4.10c). Due to the coordination of $K2^+$ in the complex in a syn-fashion, propagation of the coordination network in this direction is not possible. Therefore, we observed the formation of a 1D coordination polymer, despite the fact that two potassium ions are present in the dual-host complex. Because of the syn-binding fashion of the carbonyl oxygen and nitro oxygen, $K2^+$ is pushed out of the crown ether plane by a distance of 0.994 Å (Fig. 4.11), while $K1^+$ is placed almost in the plane of the crown ether

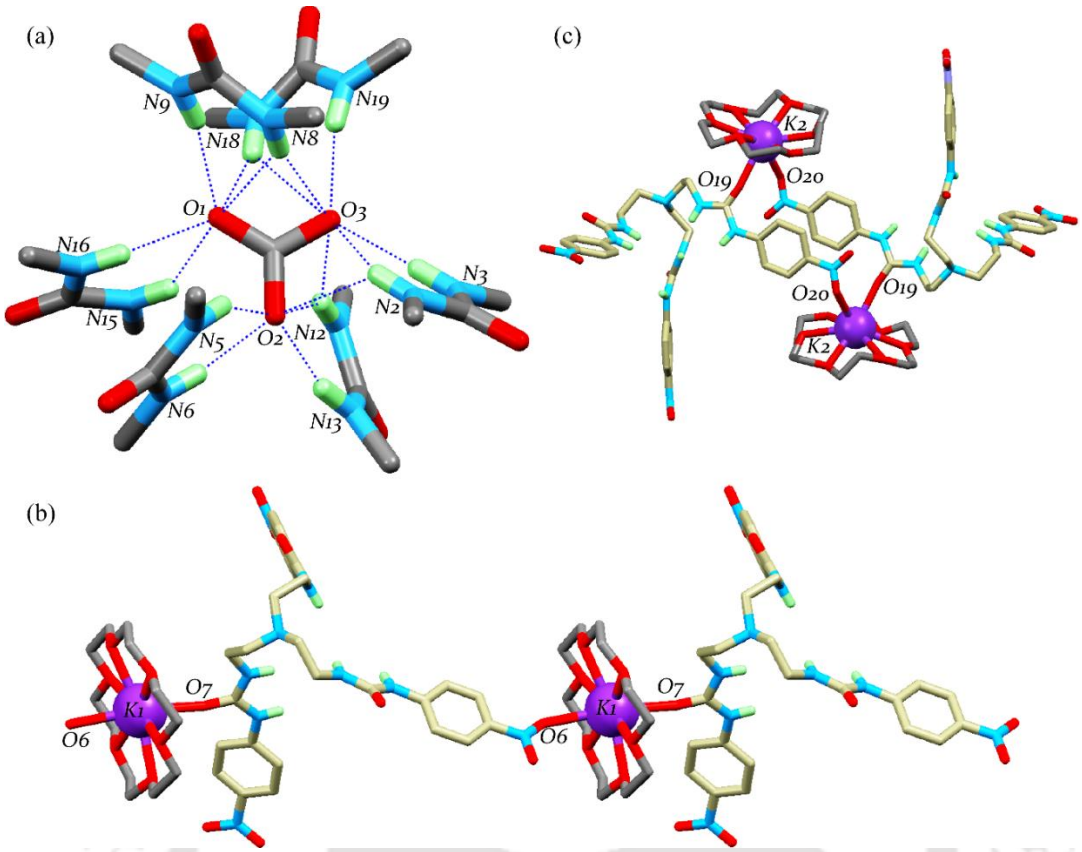

Figure 4.10 (a) A magnified ball-and-stick representation depicting the coordination environment of the CO_3^{2-} anion within the dimeric assembly, (b) coordination of $K1^+$ in an anti-fashion with a receptor of the dimeric assembly to form a 1D coordination polymer, and (c) coordination of $K2^+$ in a syn-fashion with a receptor of the dimeric assembly of complex **3d**.

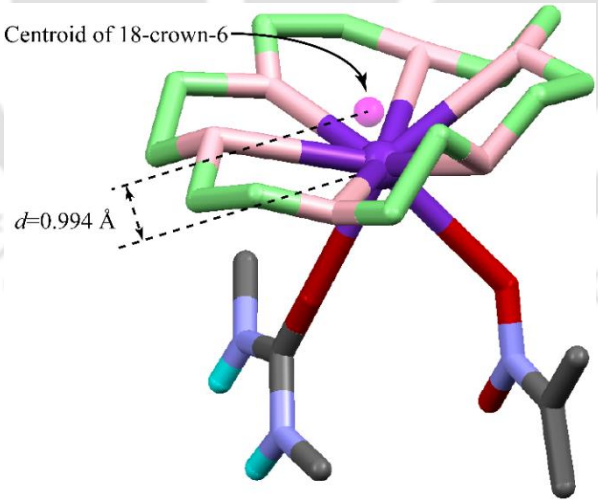

Figure 4.11 Ball and stick representation depicting the doming out of $K2^+$ from the crown-ether plane.

owing to the anti-binding fashion. In both cases, the K^+ ion is coordinated to the etheric oxygen atoms of $\mathbf{L_C}$ with distances of ~2.8 Å whereas, $K1^+$ is coordinated to the carbonyl oxygen (C=O7) and nitro oxygen (O=N−O6) with distances of 2.72 Å and 2.88 Å, respectively and $K2^+$ is coordinated to the carbonyl oxygen (C=O19) and nitro oxygen (O=N−O20) with distances of 2.62 Å and 2.97 Å, respectively.

4.6 Solution-state study by NMR analysis

The presence of potassium carbonate in the complex has also been confirmed by ^{1}H and ^{13}C NMR (in DMSO-d_6) analyses of the isolated crystals. ^{1}H NMR showed a high downfield shift of the urea −NH resonances with an average Δδ shift of 1.50 ppm relative to the free receptor (Fig. 4.12a).

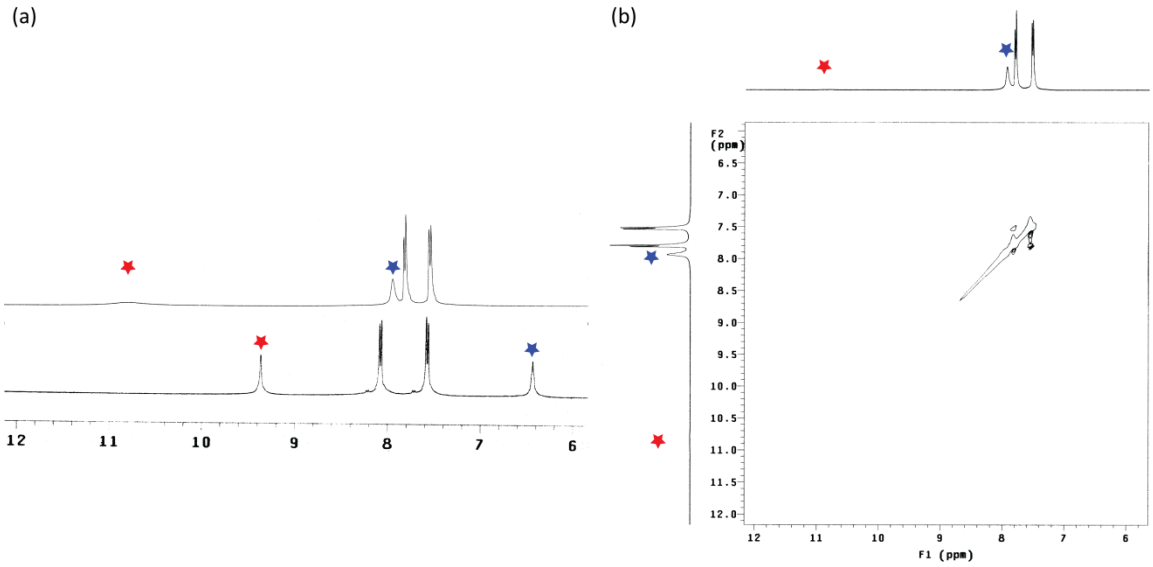

Figure 4.12 (a) Partial ^{1}H NMR spectrum of the dual-host–guest complex showing the spectral changes relative to receptor **L$_3$**, and (b) 2D NOESY NMR experiment of the dual-host–guest complex in DMSO-d_6.

In the ^{13}C NMR, the resonance for the encapsulated CO_3^{2-}anion occurs at 172.04 ppm (Annexure, Fig. A4.12) while $TEAHCO_3$ in DMSO-d_6 showed a sharp ^{13}C NMR resonance at 158.91 ppm, suggesting a strong solution-state binding of the anion. The solution-state encapsulation of carbonate has been confirmed by 2D NOESY NMR experiments of the isolated complex and free receptor (**L$_3$**) in DMSO-d_6 (Fig. 4.12b). In comparison to the molecule showed a strong NOESY signal between the urea protons $-NH_a$ and $-NH_b$ in the free receptor, the complex was showing no such interactions, indicating a different environment for the complex than the free receptor.

4.6 Conclusion

In conclusion, demonstrating the effect of positional isomerism in a set of nitrophenyl functionalized tripodal urea receptors toward solid and solution-state binding of anions of different dimensions we have shown that the *para*-nitrophenyl functionalized receptor **L$_3$** has the ability to encapsulate oxoanions of different sizes within the dimeric/ pseudodimeric capsular assembly of the receptor. Similarly, the *meta*-nitrophenyl functionalized receptor **L$_4$** has the capability to encapsulate divalent inorganic oxoanions such as HPO_4^{2-} within a dimeric capsular assembly of the receptor. However, in the presence of aromatic carboxylates such as

terephthalate dianion, the receptor molecule adopts an extended and flat conformation. Structural evidence of anion binding with receptor $\mathbf{L_5}$ could not be established, presumably because the nitro group substitution at the *ortho*-position acts as a barricade that resists the facile inclusion of oxoanions within the tripodal scaffold, as confirmed by 2D NOESY NMR analysis of the free receptor. Thus, the set of nitrophenyl functionalized tripodal urea scaffold can provide insight into the deliberate choice and incorporation of substituted aryl functions as peripheral groups for the design and synthesis of anion induced capsular self-assemblies of acyclic podand receptors having pendant arms.

Furthermore, we have structurally validated a supramolecular dual-host collaboration by employing the tris-urea receptor $\mathbf{L_3}$, as the anion recognition unit and 18-crown-6-ether ($\mathbf{L_c}$) as the potassium binding unit, for an ion-pair induced formation of an integrated 1D coordination polymer. Formation of a carbonate encapsulated dimeric capsular assembly by the participation of convergent hydrogen bonds employed by the six urea groups lead to a suitable orientation of the oxygen atoms of the carbonyl and nitro group for a coordination bond with the crown ether bound potassium ions.

References

1. (*a*) S. Valiyaveettil, J. F. J. Engbersen, W. Verboom and D. N. Reinhoudt, *Angew. Chem.*, **1993**, *105*, 942. (*b*) P. D. Beer, Z. Chen, A. J. Goulden, A. Graydon, S. E. Stokes and T. Wear, *J. Chem. Soc., Chem. Commun.*, **1993**, 1834.
2. (*a*) V. S. Bryantsev and B. P. Hay, *Org. Lett.*, **2005**, *7*, 5031. (*b*) O. B. Berryman, V. S. Bryantsev, D. P. Stay, D. W. Johnson and B. P. Hay, *J. Am. Chem. Soc.*, **2007**, *129*, 48.
3. (*a*) B. A. Moyer and P. V. Bonnesen, In Physical factors in anion separation, *Supramolecular chemistry of anions*; A. Bianchi, K. Bowman-James and E. Garcia-Espana, Eds.; Wiley-VCH: New York, **1997**. (*b*) X. B. Wang, X. Yang, J. B. Nicholas and L. S. Wang, *Science*, **2001**, *294*, 1322.
4. (*a*) S. E. Schneider, S. N. O'Neil and E. V. Anslyn, *J. Am. Chem. Soc.*, **2000**, *122*, 542. (*b*) C. Schmuck and M. Schwegmann, *J. Am. Chem. Soc.*, **2005**, *127*, 3373.
5. P. Ghosh, *Chem. Commun.*, **2011**, *47*, 8477.
6. (*a*) I. Ravikumar and P. Ghosh, *Chem. Commun.*, **2010**, *46*, 1082. (*b*) S. K. Dey, R. Chutia and G. Das, *Inorg. Chem.*, **2012**, *51*, 1727.
7. (*a*) J. L. Atwood and A. Szumna, *Chem. Commun.*, **2003**, 940. (*b*) B. Akhuli, I. Ravikumar and P. Ghosh, *Chem. Sci.*, **2012**, *3*, 1522.
8. (*a*) N. Busschaert, M. Wenzel, M. E. Light, P. Iglesias- Hernandez, R. Perez-Tomas and P. A. Gale, *J. Am. Chem. Soc.*, **2011**, *133*, 14136.
9. R. Chutia, S. K. Dey and G. Das, *Cryst. Growth Des.*, **2013**, *13*, 883.
10. S. K. Dey, R. Chutia and G. Das, *Inorg. Chem.*, **2012**, *51*, 1727.
11. R. Chutia, S. K. Dey and G. Das, *CrystEngComm*, **2013**, *15*, 9641.
12. S. K. Dey and G. Das, *Dalton Trans.*, **2011**, *40*, 12048.

Annexure 4

Table A4.1 Crystallographic parameters and refinement details of the complexes **3a**, **3b**, **4a, 4b**, $\mathbf{L_3}$ and **3d**.

Parameters	**3a**	**3b**	**4a**	**4b**	**L_3.DMSO**	**3d**
CCDC	894009	894010	894011	894012	937871	937872
Formula	$C_{71}H_{100}N_{22}O_{21}$	$C_{47}H_{68}N_{11}O_{11}$	$C_{86}H_{132}N_{22}O_{22}$	$C_{87}H_{144}N_{13}O_{19}$	$C_{29}H_{36}N_{10}O_{10}S$	$C_{158}H_{215.20}K_4N_{40}O_{66}$
Fw	1597.73	963.12	1857.11	1676.15	716.75	3887.30
Crystal system	Monoclinic	Triclinic	Triclinic	Triclinic	Monoclinic	Triclinic
Space group	C_2/c	P-1	P-1	P-1	P_21/c	P-1
a/Å	22.6830(7)	12.8426(11)	17.0817(9)	10.9000(3)	12.6341(8)	15.5320(5)
b/Å	21.3607(7)	14.3533(12)	17.6519(9)	20.4538(4)	35.035(2)	18.0531(6)
c/Å	17.8940(7)	14.6146(12)	19.7271(10)	24.2322(5)	8.0278(5)	18.7587(6)
α/°	90.00	90.561(4)	70.110(2)	110.0600(10)	90.00	96.715(2)
β/°	105.138(3)	103.049(4)	80.692(2)	94.7010(10)	104.375(3)	94.667(2)
γ/°	90.00	95.773(4)	65.396(2)	98.6720(10)	90.00	108.814(2)
V/Å^3	8369.2(5)	2609.6(4	5084.1(5)	4964.5(2)	3442.1(4)	4904.9(3)
Z	4	2	2	2	4	1
D_c/g cm^{-3}	1.268	1.226	1.213	1.121	1.383	1.316
μ Mo Kα/mm^{-1}	0.095	0.089	0.103	0.079	0.164	0.185
T/K	298(2)	298(2)	298(2)	298(2)	298(2)	298(2)
θ max.	28.65	28.38	28.05	20.27	20.79	28.35
Total no.of reflections	41828	34227	69838	33240	31049	61643
Independent reflections	10505	13012	24520	9551	8512	24430
Observed reflections	6075	5253	21245	6406	7756	21592
Parameters refined	519	626	1188	1079	453	1203
R_1, $I > 2\sigma(I)$	0.0624	0.0549	0.0735	0.0840	0.0950	0.0883
wR_2, $I > 2\sigma(I)$	0.2082	0.1546	0.2353	0.2143	0.2031	0.2884
R_1, (all data)	0.1107	0.1177	0.2423	0.1079	0.1497	0.1780
wR_2 (all data)	0.1779	0.1367	0.1678	0.1766	0.1733	0.2153
GOF (F^2)	1.194	0.990	0.955	1.012	1.273	1.028

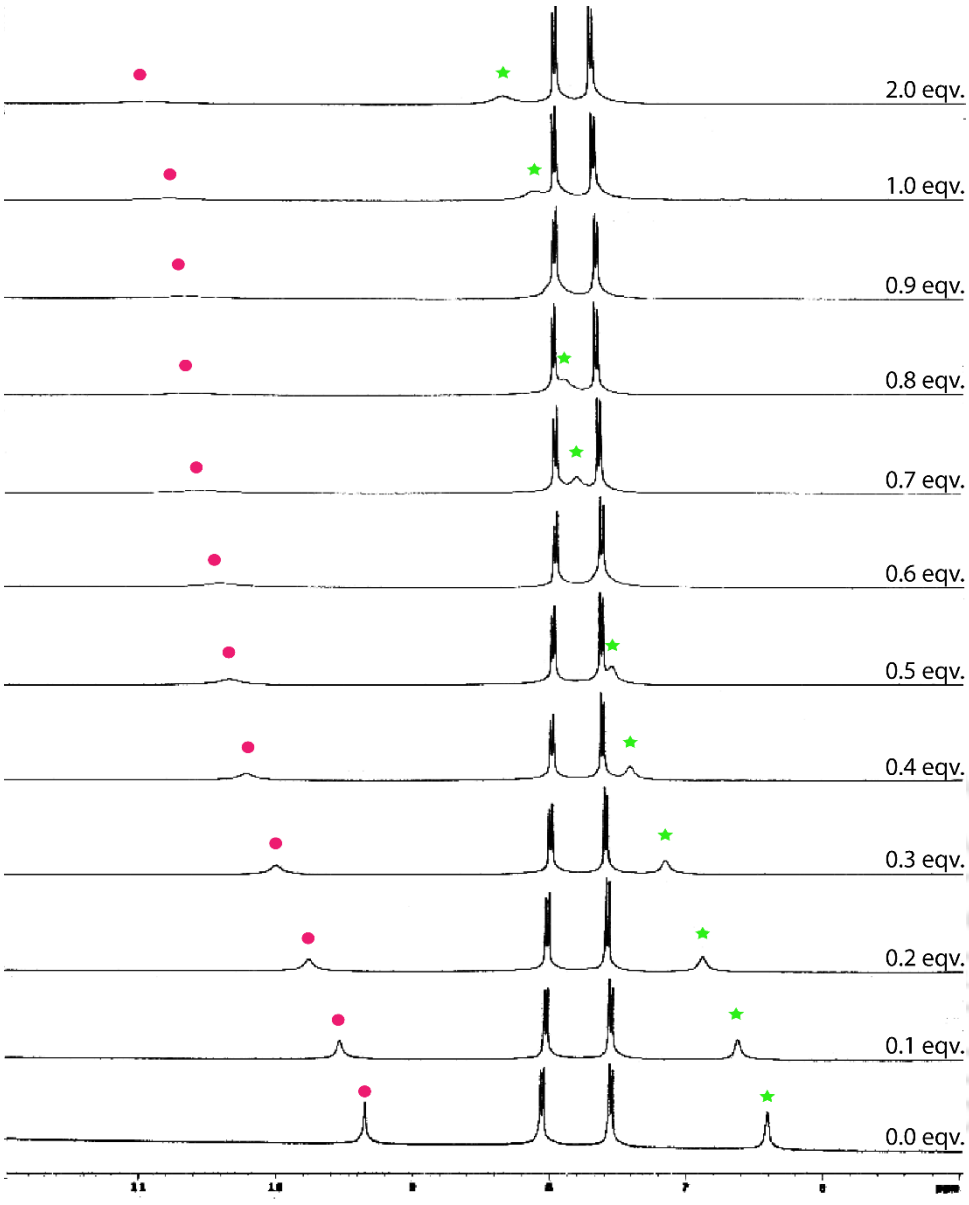

Figure A4.1 Expanded partial ^{1}H NMR spectra of **L$_3$** upon titration with TEAHCO3 in DMSO-d_6.

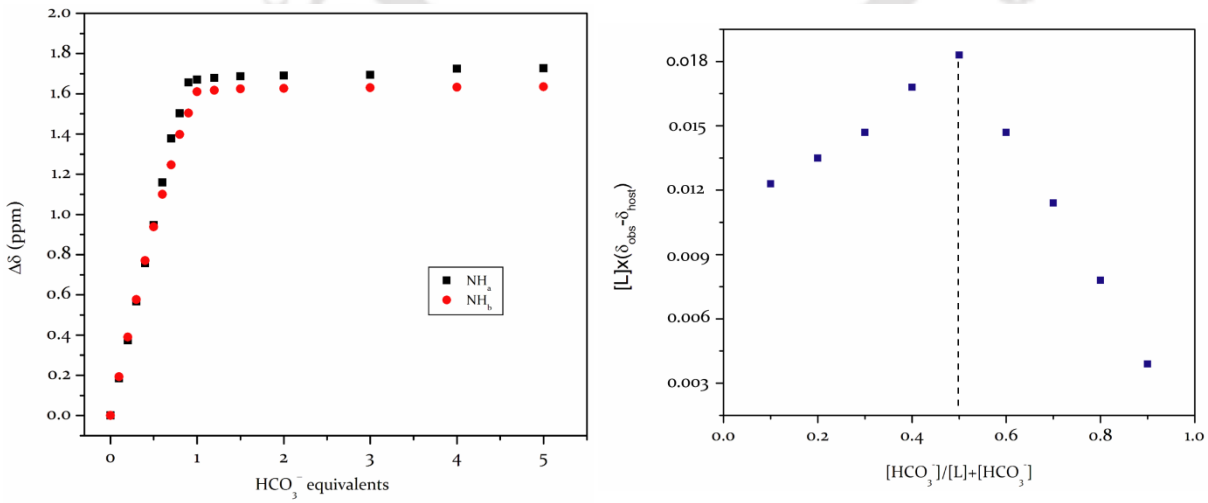

Figure A4.2 Change in chemical shift of –NH resonances of **L$_3$** (5 mM) with increasing conc. of standard HCO_3^- solution (50 mM) in DMSO-d_6 at 298 K and the corresponding Job's plot suggesting the formation of 1:1 host/guest complexes in solution.

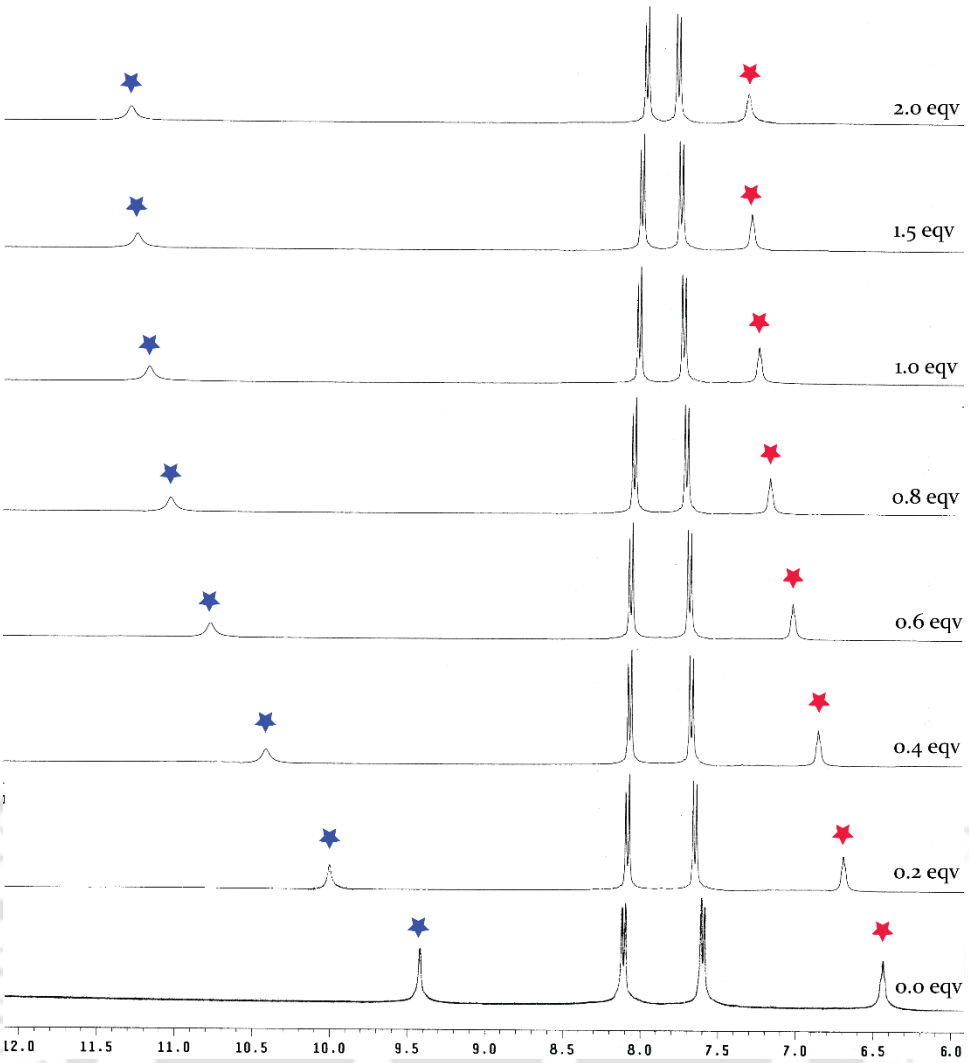

Figure A4.3 Expanded partial ^{1}H NMR spectra of $\mathbf{L_3}$ upon titration with (*n*-TBA)F in DMSO-d_6.

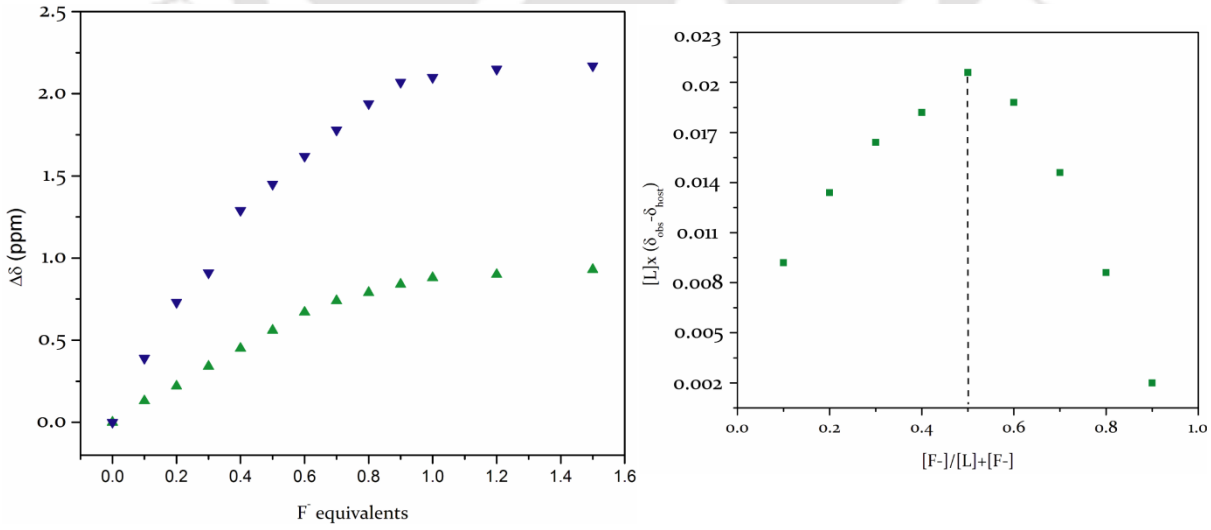

Figure A4.4 Change in chemical shift of –NH resonances of $\mathbf{L_3}$ (5 mM) with increasing conc. of standard F^- solution (50 mM) in DMSO-d_6 at 298 K and the corresponding Job's plot suggesting the formation of 1:1 host/guest complexes in solution.

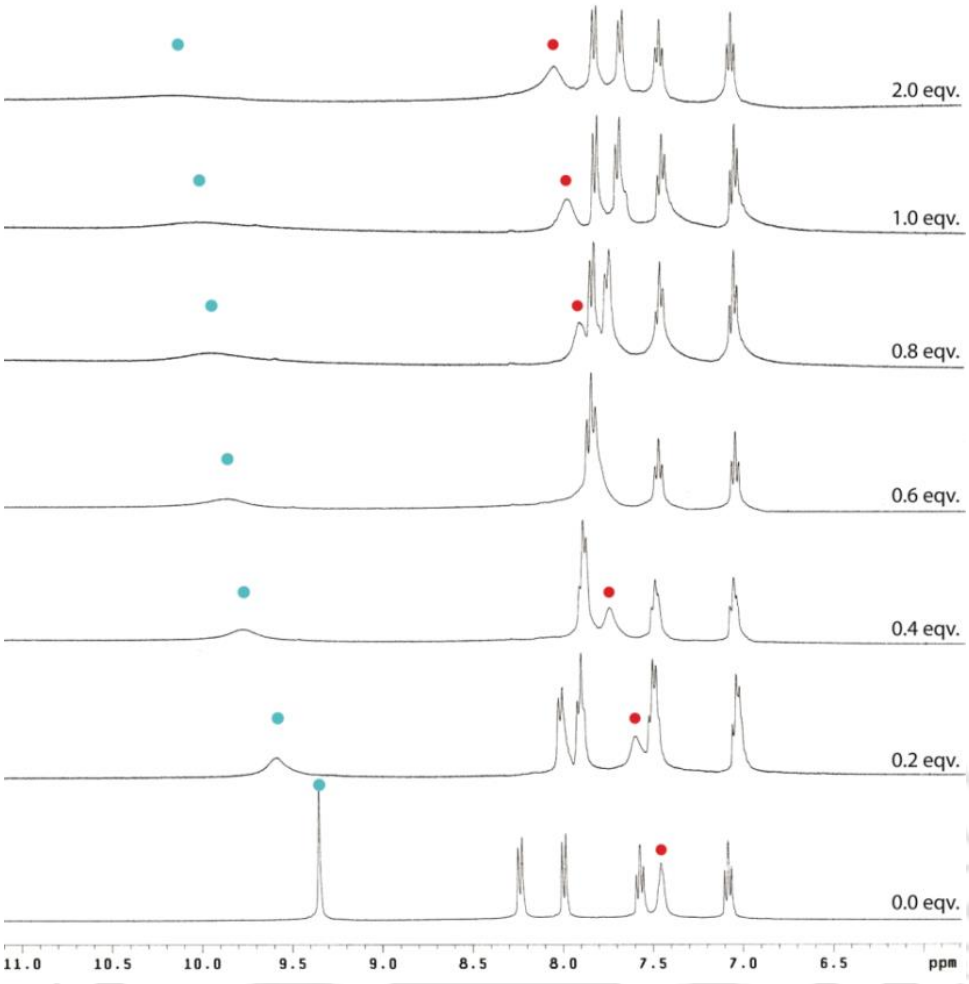

Figure A4.5 Expanded partial ^{1}H NMR spectra of $\mathbf{L_5}$ upon titration with (TEA)HCO_3 in DMSO-d_6

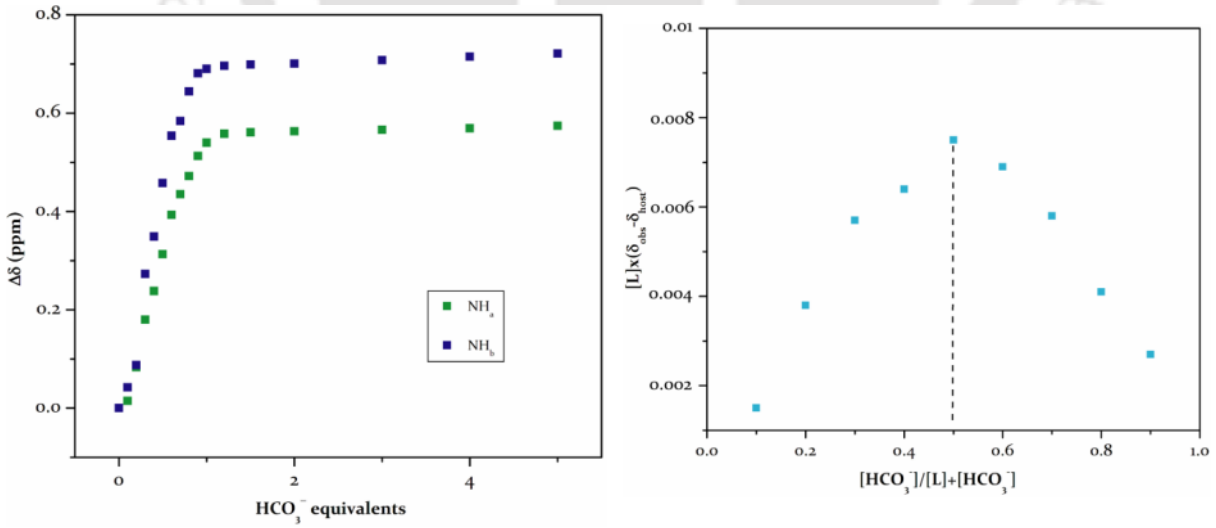

Figure A4.6 Change in chemical shift of –NH resonances of $\mathbf{L_5}$ (5 mM) with increasing conc. of standard HCO_3^- solution (50 mM) in DMSO-d_6 at 298 K and the corresponding Job's plot suggesting the formation of 1:1 host/guest complexes in solution.

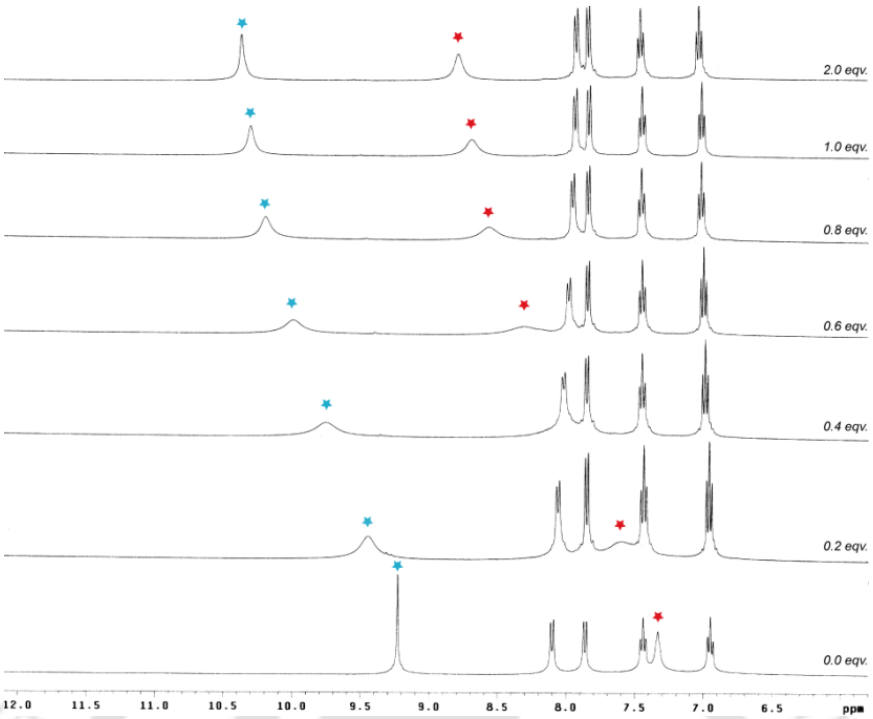

Figure A4.7 Expanded partial ^{1}H NMR spectra of $\mathbf{L_5}$ upon titration with (*n*-TBA)F in DMSO-d_6.

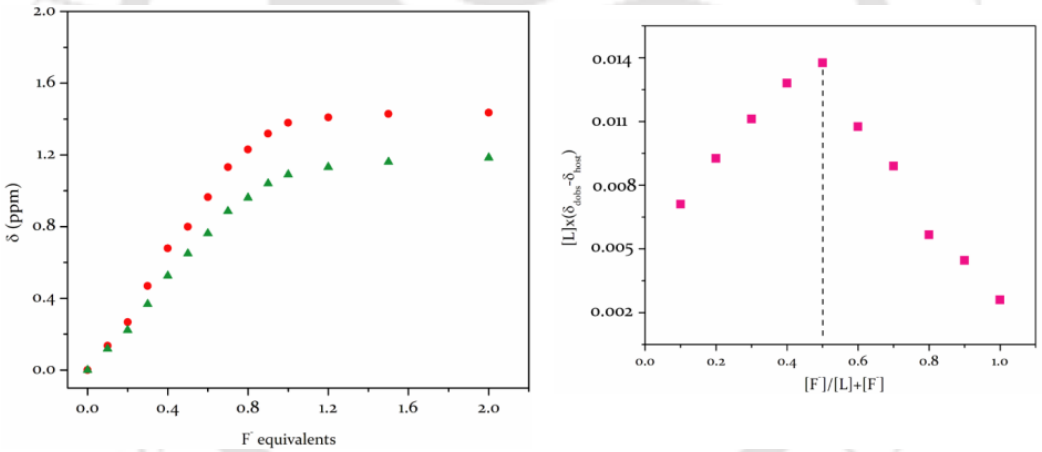

Figure A4.8 Change in chemical shift of –NH resonances of $\mathbf{L_5}$ (5 mM) with increasing conc. of standard F^- solution (50 mM) in DMSO-d_6 at 298 K and the corresponding Job's plot suggesting the formation of 1:1 host/guest complexes in solution.

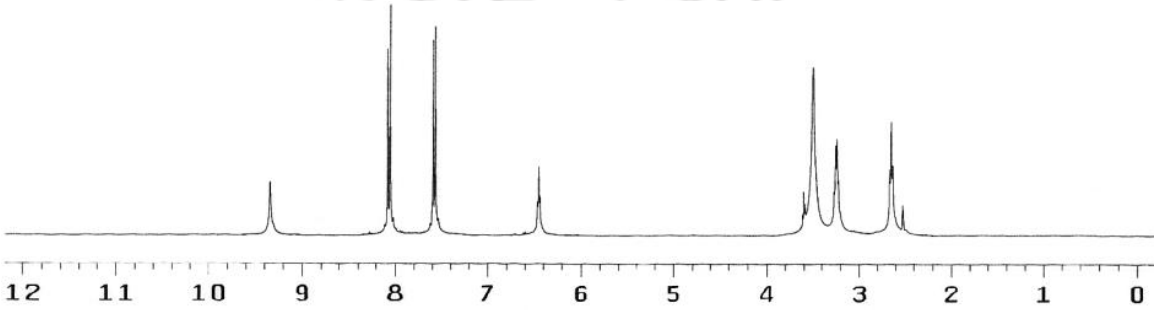

Figure A4.9 ^{1}H NMR spectrum of receptor $\mathbf{L_3}$ in DMSO-d_6 (Varian-400 MHz) at 298 K.

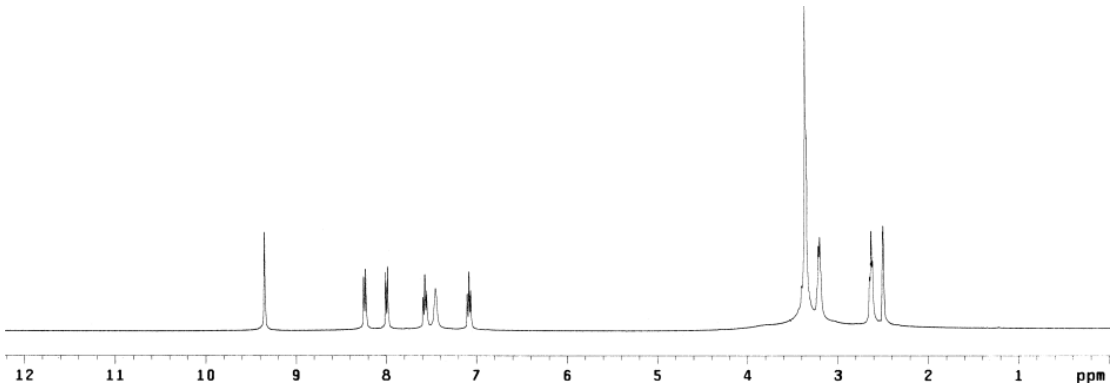

Figure A4.10 ^{1}H NMR spectrum of receptor $\mathbf{L_5}$ in DMSO-d_6 (Varian-400 MHz) at 298 K.

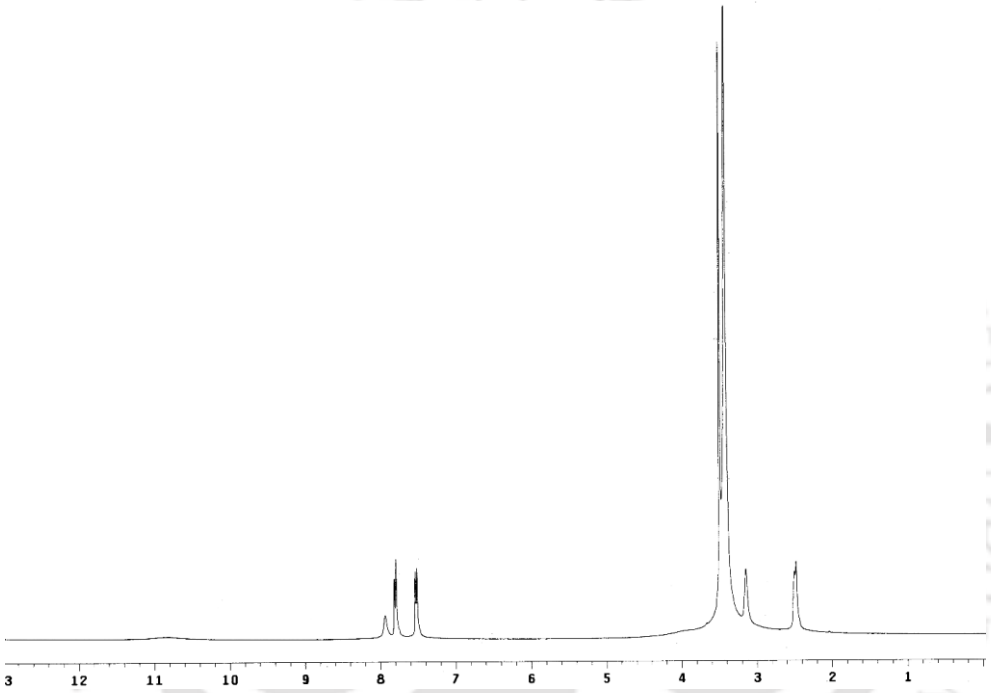

Figure A4.11 ^{1}H NMR spectrum of the dual-host complex **3d** in DMSO-d_6 (Varian-400 MHz) at 298 K.

Table A4.3 Details of Hydrogen Bonding contacts in the complexes **3a, 3b**, **4a** and **4b**.

Complex	D–H···O	*d*(H···O)/Å	*d*(D···O)/Å	<D–H···O/°
3a	N2–H···O10	2.22(4)	2.988(2)	147(1)
	N3–H···O10	1.99(1)	2.807(2)	158(1)
	N5–H···O11	2.23(2)	3.001(3)	148(1)
	N6–H···O11	2.00(2)	2.828(3)	161(1)
	N8–H···O11	2.63(2)	3.355(2)	143(1)
	N8–H···O11	2.50(2)	3.230(2)	142(1)
	N9–H···O11	1.89(2)	2.746(2)	169(1)
3b	N2H···O11	2.51(2)	3.255(2)	144(1)
	N2H···O10	2.39(2)	3.145(2)	146(1)
	N3H···O11	1.98(1)	2.838(2)	171(1)
	N5H···O10	2.14(1)	2.927(2)	151(1)
	N6H···O10	2.06(1)	2.855(2)	153(1)
	N8H···O11	2.56(1)	3.303(2)	145(1)
	N9H···O11	2.01(1)	2.851(2)	165(1)

4a	N2H···O21	2.15(3)	2.974(4)	158(2)
	N3H···O20	2.23(2)	3.054(4)	160(2)
	N5H···O21	2.04(3)	2.814(5)	148(2)
	N6H···O19	2.12(3)	2.964(5)	164(2)
	N8H···O21	1.98(2)	2.803(3)	159(3)
	N9H···O22	2.31(2)	3.150(4)	164(2)
	N12H···O22	2.04(3)	2.880(5)	164(2)
	N13H···O20	2.09(2)	2.913(4)	159(2)
	N15H···O22	2.31(2)	3.078(4)	148(2)
	N16H···O22	1.94(3)	2.782(4)	163(2)
	N18H···O20	2.37(3)	3.076(5)	139(3)
	N19H···O20	1.98(2)	2.816(4)	162(3)
	N19H···O19	2.68(3)	3.324(5)	132(3)
	C5H···O20	2.57(3)	3.352(6)	141(3)
	C27H···O22	2.59(2)	3.404(5)	146(3)
4b	N2H···O14	2.02(4)	2.864(6)	166(3)
	N3H···O15	1.97(5)	2.785(6)	158(3)
	N5H···O10	2.05(4)	2.866(6)	157(3)
	N6H···O11	1.92(4)	2.737(6)	158(3
	N8H···O12	2.03(4)	2.878(6)	167(3)
	N8H···O13	2.65(6)	3.346(7)	138(3)
	N9H···O13	1.85(4)	2.709(5)	177(3)
	C14H···O11	2.70(5)	3.393(8)	132(4)

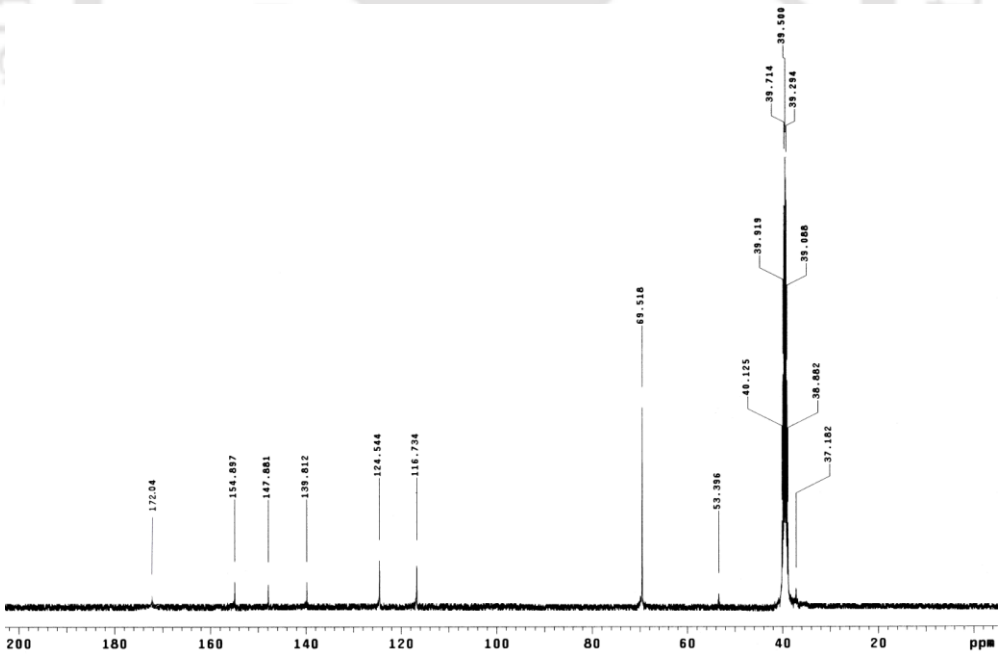

Figure A4.12 ^{13}C NMR spectrum of the dual-host complex **3d** in DMSO-d_6 (Varian-100 MHz) at 298 K.

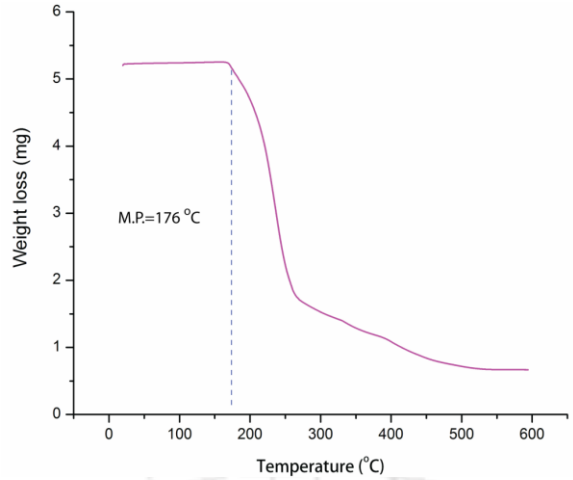

Figure A4.13 Thermo gravimetric (TGA) curve of complex **3d** obtained at a heating rate of 5°C/min in N_2 atmosphere.

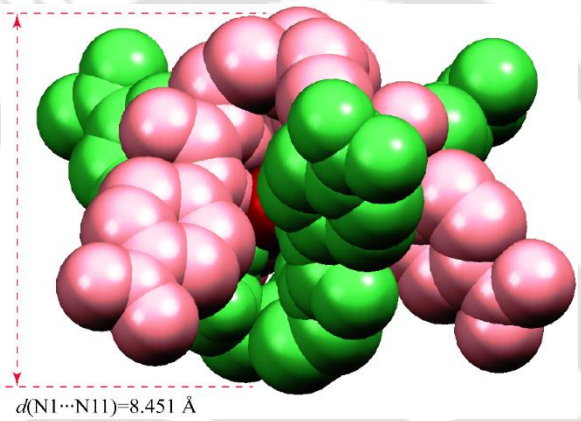

Figure A4.14 Spacefill representation depicting full encapsulation of the CO_3^{2-} anion and capsule size in complex **3d**.

Table A4.4 Details of hydrogen bonding contacts in the dual-host complexes **3d**.

D–H···O	*d*(H···O)/Å	*d*(D···O)/Å	∠D–H···O/°
N2–H···O1	2.59(4)	3.222(7)	130.8(3)
N2–H···O3	2.41(4)	3.145(7)	144.2(3)
N3–H···O3	1.91(3)	2.764(6)	169.0(3)
N5–H···O1	2.33(3)	3.089(5)	147.9(4)
N6–H···O1	1.96(4)	2.807(6)	167.8(3)
N8–H···O3	2.53(4)	3.378(6)	167.6(4)
N8–H···O2	2.51(4)	3.210(6)	139.7(4)
N9–H···O2	2.01(3)	2.815(5)	156.0(3)
N12–H···O1	2.63(3)	3.348(5)	141.3(3)
N12–H···O3	2.55(5)	3.343(6)	154.9(3)
N13–H···O2	1.99(3)	2.824(4)	163.8(2)
N15–H···O2	2.31(4)	3.058(7)	145.2(4)
N16–H···O2	2.01(4)	2.838(7)	161.3(4)
N18–H···O2	2.27(4)	3.093(7)	161.4(4)
N18–H···O3	2.58(4)	3.262(6)	137.4(4)
N19–H···O3	1.92(3)	2.740(5)	160.1(3)

Chapter 4

Tetrameric Mixed Phosphate Cluster Encapsulation/Recognition by a Tris(urea) Receptor

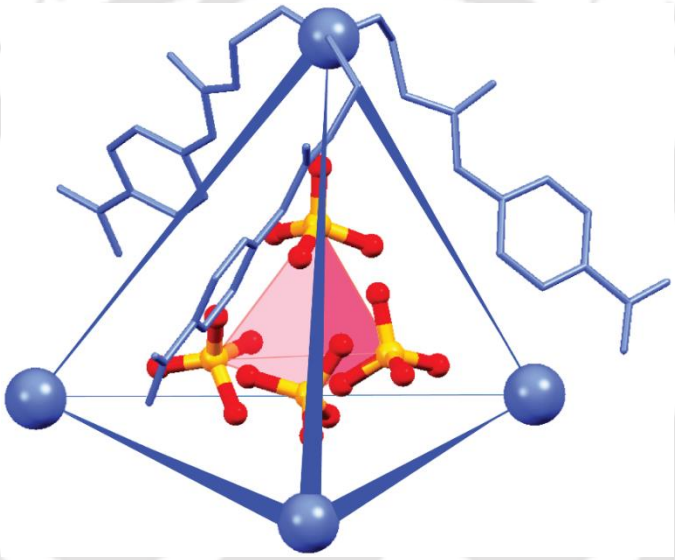

5.1 Background and Focus of the Chapter

Self-assembly process results from very simple to highly complex molecular and supramolecular systems. Out of multiple possibilities, this natural process elucidates us with specific and highly symmetric systems. Self-assembled supramolecular structures with an internal cavity to accommodate guest molecules have attracted much attention in recent times.[1] Nature has often utilized the principle of encapsulation for purposes such as the protection of fragile structures and compartmentalization of functions.[2] One of the most fascinating features of capsular assemblies is their ability to isolate a guest molecule from the competitive bulk media by encapsulation, and it is the topological complementarity of the capsular cavity, which dictates the encapsulation of specific guest(s). Along this line, anion-induced formation of capsular assemblies represents one of the main approaches in the area of supramolecular self-assembly, and also molecular recognition.[3] Tripodal receptors constitute a special class of acyclic ionophores with C_{3v} symmetry, whose side arms upon functionalization with appropriate anion binding elements (amide and urea/thiourea) can recognize anions/hydrated anionic guest via formation of stable host-guest capsular assemblies.[3b]

Recognition of tetrahedral oxyanions mainly sulfate(s) and phosphate(s) has been the focus of special research interest because of their roles in biological and physiological processes,[4] especially in sulfate and phosphate binding proteins.[5] Inorganic phosphate exists in three different forms $H_2PO_4^-$, HPO_4^{2-} and PO_4^{3-} depending on its immediate environment, and $H_2PO_4^-$ is the most abundant among all. Interestingly, the $H_2PO_4^-$ anion shows donor-acceptor properties similar to the water molecule. In the solid state, self-complementary hydrogen bonding among $H_2PO_4^-$ anions under certain conditions generate self-aggregated anion assemblies, known as "anion clusters" that are relatively new in "cluster chemistry". Well-defined oligomeric structures of $H_2PO_4^-$ anions containing cyclic dimers,[6] trimers,[7] tetramers,[8] hexamers,[7] and octamers,[9] are known in the literature and have overwhelming structural similarities to different cyclic "water clusters".[10] While, structural evidences of monotopic recognition of phosphate ($H_2PO_4^-$, HPO_4^{2-} and PO_4^{3-}) inside acyclic and macrocyclic systems are numerous,[11] instances of discrete phosphate cluster encapsulation inside the self-assembled caged supramolecular structure of synthetic organic receptor are very few.[12]

Tris(2-aminoethyl)amine-based pentafluorophenyl-functionalized urea/thiourea receptor showed evidences of $(H_2PO_4^-)_2$ encapsulation within a dimeric capsular assembly of the receptor,[12a,b] and adamantane-based bis-urea receptors showed evidences of tetrameric phosphate $(H_2PO_4^-)_4$ encapsulation within the self-assembled molecular cage of four receptor molecules.[8a]

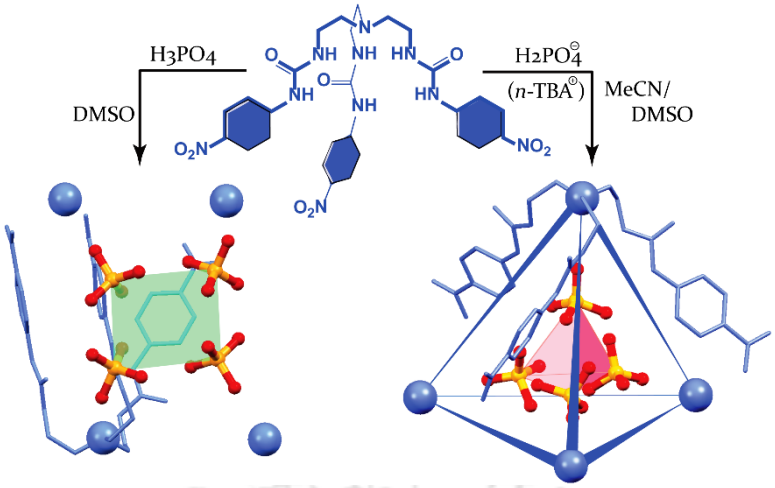

Scheme 5.1 Structure of receptor $\mathbf{L_3}$ and schematic representation depicting the formation of tetrahedral phosphate $(H_2PO_4^-{\cdot}HPO_4^{2-})_2$ encapsulated tetrahedral cage complex **3e**, and cyclic anion-acid $(H_2PO_4^-{\cdot}H_3PO_4)_2$ sandwich complex **3f**.

However, solid-state evidences of mixed phosphate cluster ($H_2PO_4^-$ + HPO_4^{2-}) and its entrapment within a self-assembled cage of synthetic anion receptor has been unknown.

This chapter describes encapsulation of tetrameric tetrahedral cluster of phosphate anion and within a tetrahedral cage assembly of the tris-urea receptor $\mathbf{L_3}$ in its electronically neutral state as well as side cleft binding of tetrameric cyclic cluster in its positively charged state.[13] The tris-urea receptor $\mathbf{L_3}$ has furnished an unusual example by self-assembling as tetrahedral cage for the engulfment of a tetrameric mixed phosphate $(H_2PO_4^-{\cdot}HPO_4^{2-})_2$ cluster in presence of excess (*n*-TBA)H_2PO_4 as complex (*n*-TBA)$_6$[4$\mathbf{L_3}$$(H_2PO_4^-{\cdot}HPO_4^{2-})_2$] (**3e**) (Scheme 5.1). Exceptionally, the existence of a tetrameric anion-acid cluster $(H_2PO_4^-{\cdot}H_3PO_4)_2$ has also been observed in the solid-state in complex [$(\mathbf{L_3}H)^+(H_2PO_4^-{\cdot}H_3PO_4)$DMSO·$H_2O$] (**3f**). In a proof of concept experiment, transformation of complex **3f** with cationic host into a phosphate encapsulated complex with neutral host has been demonstrated in solution-state by quantitative ^{1}H NMR titration with (*n*-TBA)OH in DMSO-d_6 (298K). Further study of receptor $\mathbf{L_3}$ with the spherical shaped halides to get solid-state result have revealed the formation of a pseudodimeric (2+2) capsular self-assembly with 1:1 host: guest ratio in fluoride encapsulated complex, (TEA)[$\mathbf{L_3}$(F)] (**3g**).

5.2 Structural aspects of phosphate anion binding with $\mathbf{L_3}$ in its neutral and charged state

The encapsulation of divalent terephthalate anion along with carbonate anion within the respective dimeric capsular assemblies of $\mathbf{L_3}$ in a 2:1 host-guest stoichiometry[14] depicts it's speciality in comparison to its other analogues. Hence, it may be predicted that the formation of capsular assemblies in presence of larger oxoanions in solid-state with tris-urea functionalized tripodal molecules is conceivable as larger oxoanions (*viz.* phosphates) requires more number of

H-bond bonding sites to form stable complexes. But any solid-state outcome of this tris(urea) receptor **L$_3$** with the key anion, phosphate has been unrevealed yet, which and specially the beautiful rugby ball shaped ($SO_4^{2-}\cdot 3H_2O\cdot SO_4^{2-}$) architecture with similar sulphate anion[15] encouraged us to study so in its neutral as well as charged state.

5.2.1 Phosphate tetrameric tetrahedral cluster caged complex (3e)

Caged cluster complex 6(*n*-TBA)[4**L$_3$**($H_2PO_4^-$)(HPO_4^{2-})$_2$], **3e** was obtained as suitable crystals for X-ray diffraction analysis upon slow evaporation of a 15 mL MeCN solution of **L$_3$** in presence of excess (*n*-TBA)H_2PO_4. Structural elucidation revealed that the phosphate cluster caged complex, **3e** crystallizes in the monoclinic system with centrosymmetric space group C_2/c. The asymmetric unit of the crystal contains two receptor molecules, two phosphate anions and three *n*-TBA cations. It was not possible to locate the hydrogen atoms on the phosphate anions, in order to unambiguously determine the degree of protonation and charge upon the oxyanion. However, the presence of three *n*-TBA cations indicated the only possible combination of a monovalent and a divalent phosphate, each encapsulated within a tripodal receptor cavity by −NH hydrogen bonds. Interestingly, a pair of monovalent and divalent phosphate ($H_2PO_4^-\cdot HPO_4^{2-}$) interacts with another pair of ($H_2PO_4^-\cdot HPO_4^{2-}$) to form a tetrameric mixed phosphate cluster ($H_2PO_4^-\cdot HPO_4^{2-}$)$_2$ of tetrahedral arrangement (Fig. 5.1c). The distance between any two phosphorus atoms of ($H_2PO_4^-\cdot HPO_4^{2-}$)$_2$ cluster ranges between 4.31−4.72 Å with an average of 4.53 Å (Fig. 5.1b), suggesting strong O−H···O hydrogen bonding interactions [*d*(D···A) = 2.48−2.89 Å] between the $H_2PO_4^-$ and HPO_4^{2-} anions. Based on the P−O bond distances we have designated the two different phosphate anions as **P$_1$** and **P$_2$**, where **P$_1$** stands for HPO_4^{2-} and **P$_1$** stands for $H_2PO_4^-$. The difference in nomenclature is completely based on the difference in P−O distances and the H-bonding modes among the phosphate moieties in the cluster.

In order to provide a complementary cavity and adequate H-bond stabilization to the tetrameric ($H_2PO_4^-\cdot HPO_4^{2-}$)$_2$ cluster, four receptor molecules are self-assembled in a tetrahedral arrangement around the ($H_2PO_4^-\cdot HPO_4^{2-}$)$_2$ cluster (Fig. 5.1a). The distance between any two bridgehead *N*-atoms of tetrahedral (**L$_3$**)$_4$ cage ranges between 11.70−12.80 Å with an average of 12.45 Å. Thus, the phenomenon of anion-induced supramolecular self-assembly has resulted in a tetrahedral cage structure of tripodal tris(urea) receptor **L$_3$** for the full encapsulation (Fig. 5.2d) of an unique mixed phosphate tetrameric cluster of tetrahedral arrangement (Fig. 5.2a).

In the tetrahedral cage structure, each of the four receptor units coordinate to a phosphate anion ($H_2PO_4^-/HPO_4^{2-}$) axially by six −NH hydrogen bonds donated from the three urea functions

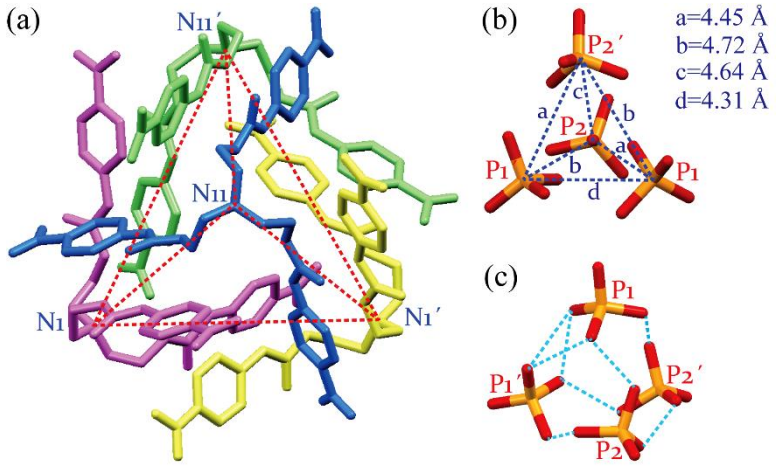

Figure 5.1 (a) Tetrahedral cage assembly of $\mathbf{L_3}$ in complex **3e** (encapsulated $(H_2PO_4^-{\cdot}HPO_4^{2-})_2$ cluster is not shown), (b) tetrahedral arrangement of tetrameric mixed phosphate $(H_2PO_4^-{\cdot}HPO_4^{2-})_2$ cluster, and (c) hydrogen bonds within the $(H_2PO_4^-{\cdot}HPO_4^{2-})_2$ cluster. Countercations are omitted for clarity.

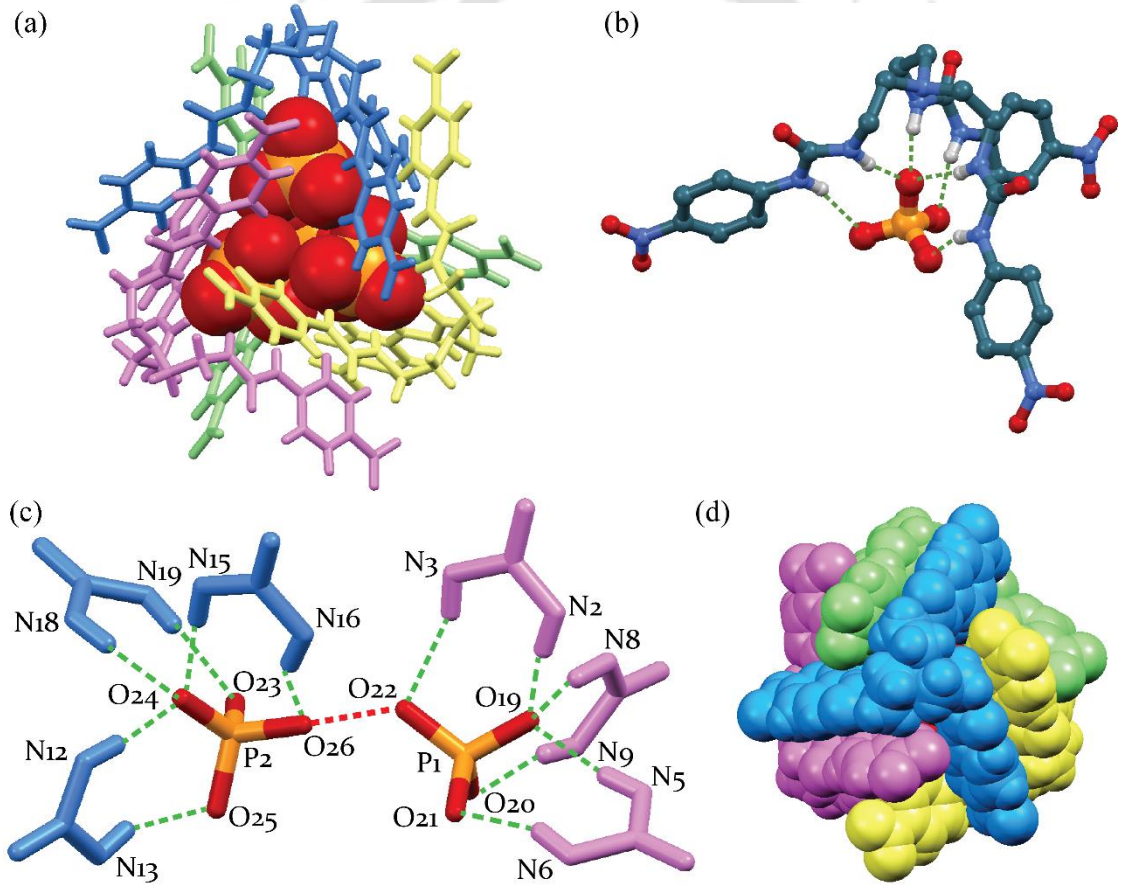

Figure 5.2 (a) X-ray structure of complex **3e** showing the encapsulation of tetrameric mixed phosphate $(H_2PO_4^-{\cdot}HPO_4^{2-})_2$ cluster within the tetrahedral cage $(\mathbf{L_3})_4$ (Anions are shown in spacefill and $\mathbf{L_3}$ in ball and stick), (b) Partial X-ray structure (ball and stick) showing phosphate anion encapsulation within a tripodal receptor cavity by 6 −NH hydrogen bonds. (c) Magnified view of the coordination environment on phosphate anions. (d) Spacefill representation of the cage complex showing full engulfment of the phosphate cluster. Countercations are omitted for clarity.

(Fig. 5.2b and 5.2c). The axial phosphate oxygen accepts three −NH hydrogen bonds from the aliphatic urea protons (upper −NH fragments), and each of the other three phosphate oxygen accepts one −NH hydrogen bond from an aromatic urea proton (lower −NH fragment). Thus, a

total of 24 −NH hydrogen bonds stabilizes the tetrameric $(H_2PO_4^-{\cdot}HPO_4^{2-})_2$ cluster within the tetrahedral $(\mathbf{L_3})_4$ cage (Annexure 5, table A5.2), with an average donor-acceptor distance of 2.94 Å. Moreover, several weaker interactions [d(D···A) > 3.20 Å] involving the urea −NH and aryl −CH protons could be added to the encapsulated $(H_2PO_4^-{\cdot}HPO_4^{2-})_2$ cluster, which provide additional stability to the (4+4) tetrahedral cage complex.

5.2.2 Phosphate anion-acid tetrameric cyclic cluster complex (3f)

Complex **3f,** $[(\mathbf{L_3}H)^+(H_2PO_4^-{\cdot}H_3PO_4)DMSO{\cdot}H_2O]$ was obtained at room temperature by slow evaporation of a DMSO solution containing orthophosphoric acid (H_3PO_4) and $\mathbf{L_3}$ The anion-acid cluster complex crystallizes in the monoclinic system with space group $P2_1/c$.

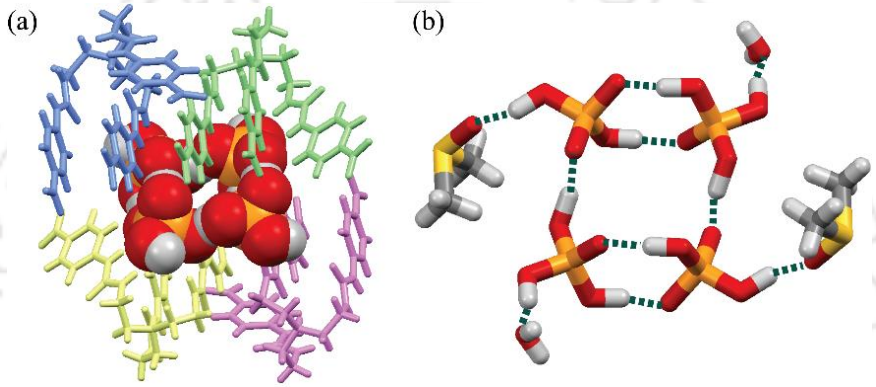

Figure 5.3 (a) X-ray structure of complex **3f** showing the sandwich-type binding of tetrameric anion-acid $(H_2PO_4^-{\cdot}H_3PO_4)_2$ cluster by four cationic receptor molecules (Anions are shown in spacefill and $(\mathbf{L_3}H)^+$ in ball and stick) (b) hydrogen bonding interactions within the tetrameric $(H_2PO_4^-{\cdot}H_3PO_4)_2$ cluster and with lattice solvents (DMSO and water) in complex **3f**.

The asymmetric unit contains a protonated receptor molecule, one dihydrogen phosphate anion ($H_2PO_4^-$), one phosphoric acid molecule (H_3PO_4) and two lattice solvents (DMSO and water). The bridgehead-*N* proton of the receptor cation is strongly hydrogen bonded to a carbonyl oxygen $(N{-}H)^+{\cdots}O$ [N1···O4 = 2.786(3) Å] and hence, restricts the opening of the tripodal cavity for $H_2PO_4^-$ encapsulation. Nonetheless, the $H_2PO_4^-$ anion is hydrogen bonded to two urea groups of the receptor cation, while the third urea group interacts with the H_3PO_4 oxygen (Fig. 5.4). Interestingly, a $H_2PO_4^-$ anion interacts concurrently with two H_3PO_4 molecules, which are in turn interacts with another $H_2PO_4^-$ anion generating a tetrameric anion-acid $(H_2PO_4^-{\cdot}H_3PO_4)_2$ cluster of rectangular planar arrangement (Fig. 5.3b). The O−H···O hydrogen bonding distances between H_3PO_4 and $H_2PO_4^-$ ions are in the range of 2.50−2.62 Å, and the distances between phosphorus atoms of the two pairs of H_3PO_4 and $H_2PO_4^-$ are 4.09 and 4.78 Å. The $(H_2PO_4^-{\cdot}H_3PO_4)_2$ cluster is further stabilized by lattice solvent molecules, where each $H_2PO_4^-$ anion is hydrogen bonded (O−H···O) to a DMSO molecule and each H_3PO_4 molecule is hydrogen bonded (O−H···O) to a water molecule (Fig. 5.3b). The $(H_2PO_4^-{\cdot}H_3PO_4)_2$ cluster is

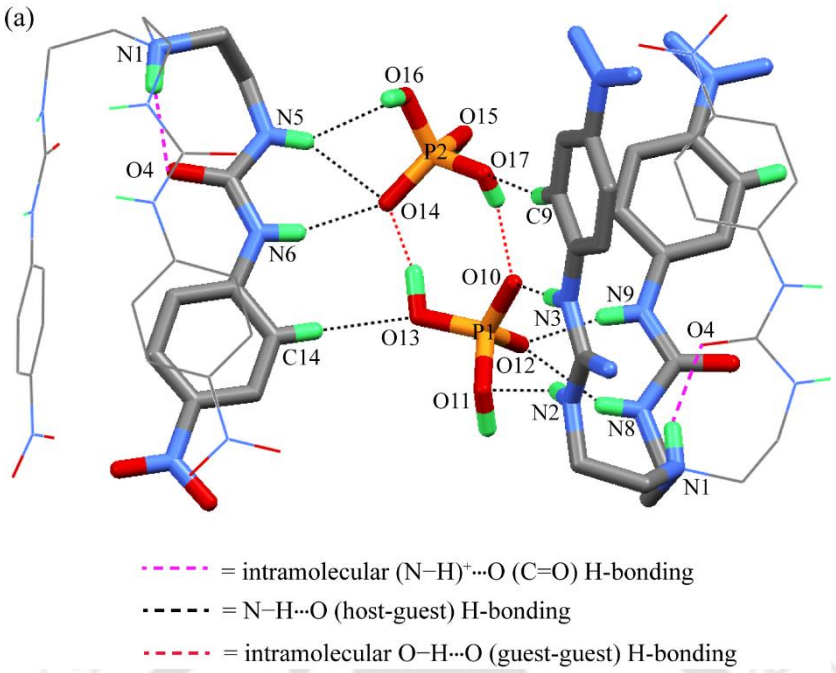

Figure 5.4 (a) Ball-and-stick representation depicting the H-bonding contacts on phosphate anion and phosphoric acid residues as well as intramolecular short contacts.

sandwiched between four receptor cations (2 up and 2 down) (Fig. 5.3a), by 24 −NH hydrogen bonds with an average distance of 2.96 Å (Annexure 5, Table A5.2).

Although oligomeric and polymeric structure formation by self-association of $H_2PO_4^-$ anions has frequently been observed in many crystal structures,[6-9] it is worthy to state that the receptor **L_3** encourages the formation of tetrameric phosphate cluster both in its neutral and cationic forms irrespective of the shape of assembled receptor. Primarily due to the charge differences and different source of $H_2PO_4^-$ anion [(*n*-TBA)$H_2PO_4^-$/H_3PO_4] used to obtain the phosphate complexes, variable composition and arrangement of tetrameric phosphate clusters have been observed in complexes **3e** and **3f**. It is noteworthy again that this receptor, **L_3** (*para*-isomer) had been authenticated to be self-assembled as dimeric or pseudodimeric capsule even encapsulating the comparatively larger terephthalate dianion (organic anion), while it's analogue, the *meta*-isomer was incapable of forming such capsular assemblies.[14] In presence of SO_4^{2-} anion, the host **L_3** encapsulated a rugby ball shaped (SO_4^{2-}·3H_2O·SO_4^{2-}) adduct as dimeric capsular assembly (2:2),[15] on the other hand the *meta*-isomer had been found to encapsulate a SO_4^{2-} anion as 2:1 host: guest dimeric capsule.[16] In the present study, we got a symmetrical tetrahedral cluster encapsulation (4:4) with $H_2PO_4^-$ as a guest. However the *meta*-isomer resulted in a 2:1 host: guest dimeric capsular assembly with a HPO_4^{2-} anion.[14] Thus the *para*-isomer has been continuing to exhibit highly symmetrical architectures in solid-state in presence of oxyanions. Furthermore in addition to its endeavour as exceptional anion host (**L_3**), one more crystallographic result has been authenticated to encapsulate F^- anion as 2:2 pseudodimeric

capsular assembly rather than being more usual 1:1 monomeric capsular assembly, which further displays its uniqueness.

5.2.3 Fluoride encapsulated complex (3g)

The Fluoride encapsulated complex TEA[$\mathbf{L_3}$F], (**3g**) was obtained as suitable crystals for X-ray diffraction analysis upon slow evaporation of a 15 mL MeCN solution of $\mathbf{L_3}$ in presence of excess TEAF. Complex **3g** crystallizes in the monoclinic system with space group P_21/c. Structural elucidation revealed the formation of a self-assembled (2+2) pseudodimeric cage in fluoride encapsulated complex. Two fluoride encapsulated receptor units [$\mathbf{L_3}(F^-)$] with opposite orientation are held together by aromatic C−H···O-nitro and nitro-O^-···π interactions between the peripheral nitro-aromatics to generate a dimeric cage of 16.77 Å (Fig. 5.5). A fluoride ion is bound within a receptor cavity by six −NH hydrogen bonds with an average donor-acceptor (N···F^-) distance of 2.82 Å (Annexure 5, Table A5.2), and the distance between two fluoride ions within the dimeric cage structure was measured to be 9.56 Å.

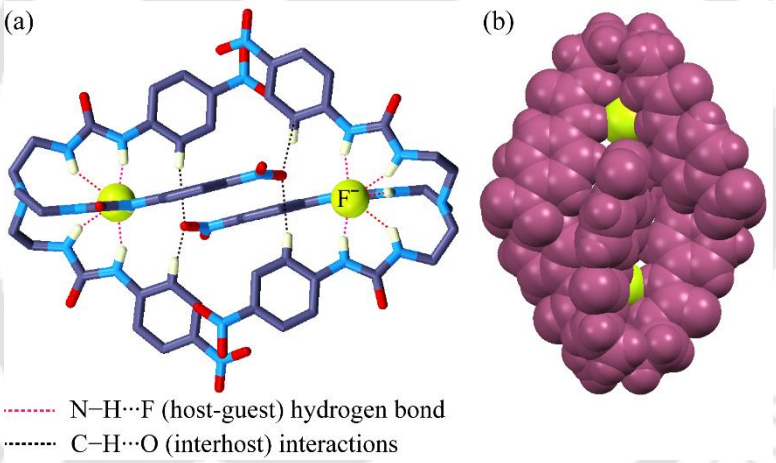

Figure 5.5 (a) Ball and stick model of the X-ray structure of complex **3g** depicting the formation of coordination environment of F^- in the (2+2) pseudodimeric cage structure, (b) Spacefill model of the (2+2) pseudodimeric cage. Countercations are omitted for clarity.

5.3 Solution-state study by NMR spectroscopy

Solution-state ^{1}H NMR and ^{31}P NMR analyses of complexes **3e** and **3f** revealed evidences of binding discrepancy of inorganic phosphates with the neutral and protonated form of receptor $\mathbf{L_3}$. ^{1}H NMR spectrum of complex **3e** (DMSO-d_6) showed significant downfield shift of the urea −NH resonances compared to $\mathbf{L_3}$, with Δδ values of 1.61 and 1.13 ppm for the urea −NH(a) and −NH(b) protons, respectively (Annexure 5, Fig. A5.1). In contrast, ^{1}H NMR of complex **3f** (DMSO-d_6) showed a minor downfield shift (Δδ) of 0.40 ppm of both the urea −NH protons and a notable shift of 0.24 ppm of aliphatic −NCH_2 protons, due to protonation at the bridgehead nitrogen (Annexure 5, Fig. A5.4). An association constant $K > 10^4$ M^{-1} has been calculated for

$H_2PO_4^-$ complexation by **L_3** using UV-Vis and ^{1}H NMR titrations, which also revealed a 1:1 host-guest stoichiometry.[14, 15] The ^{31}P resonance of complex **3e** was observed at 7.96 ppm, showing a downfield shift of 5.56 ppm relative to the free resonance of (*n*-TBA)H_2PO_4 at 2.40 ppm (Fig. 5.6). In contrast, the ^{31}P resonance of complex **3f** originated at −0.54 ppm showing an upfield shift of 2.94 ppm relative to the free resonance of (TBA)H_2PO_4 (Fig. 5.6).

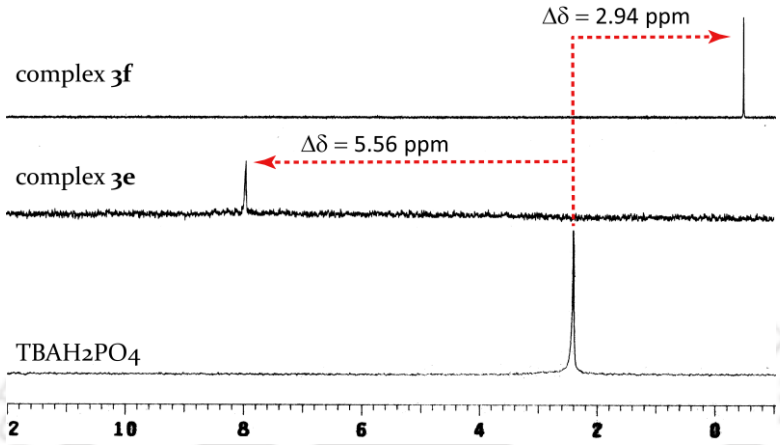

Figure 5.6 Shifting of ^{31}P resonance in different complexes **3e** and **3f** relative to the free (*n*-TBA)H_2PO_4 salt.

The tetrameric mixed phosphate $(H_2PO_4^-{\cdot}HPO_4^{2-})_2$ cluster observed in the solid-state is hard to trace in the solution-state. However, as protonation or deprotonation of phosphate ion to different states (H_3PO_4, $H_2PO_4^-$, HPO_4^{2-} and PO_4^{3-}) depends upon the solution environment, the binding affinity and the structure of the anion complex can be regulated by acid/base modulation, and traced by ^{1}H NMR spectroscopy. We tried to assess the transformation of the charged host complex **3f** to neutral host complex by controlled addition of (*n*-TBA)OH to a solution of **3f** in DMSO-d_6 (Fig. 5.7). Addition of base may result multiple deprotonation events in complex **3f** including deprotonation of the receptor cation (protonated at the bridgehead-N) and H_3PO_4 molecule. Regular addition of (*n*-TBA)OH (0.5 equiv. each time) to **3f (**DMSO-d_6) resulted in the gradual downfield shift of the urea −NH protons, indicating some conformational change of the host molecule which eventually favours a stronger anion binding mode in solution (Fig. 5.7). After the addition of 3 equivalents of base, the urea −NH resonances experienced an overall downfield shift of ~1.20 and ~1.0 ppm for −NH(a) and −NH(b) protons, respectively (compared to **3f**) and the ^{1}H NMR spectrum resembles with that of complex **3e**. Although, it will not be appropriate to claim the transformed complex to be the complex **3e**, but the appreciable spectroscopic changes has established it to be a 1:1 host-guest complex where the host is in electronically neutral state.

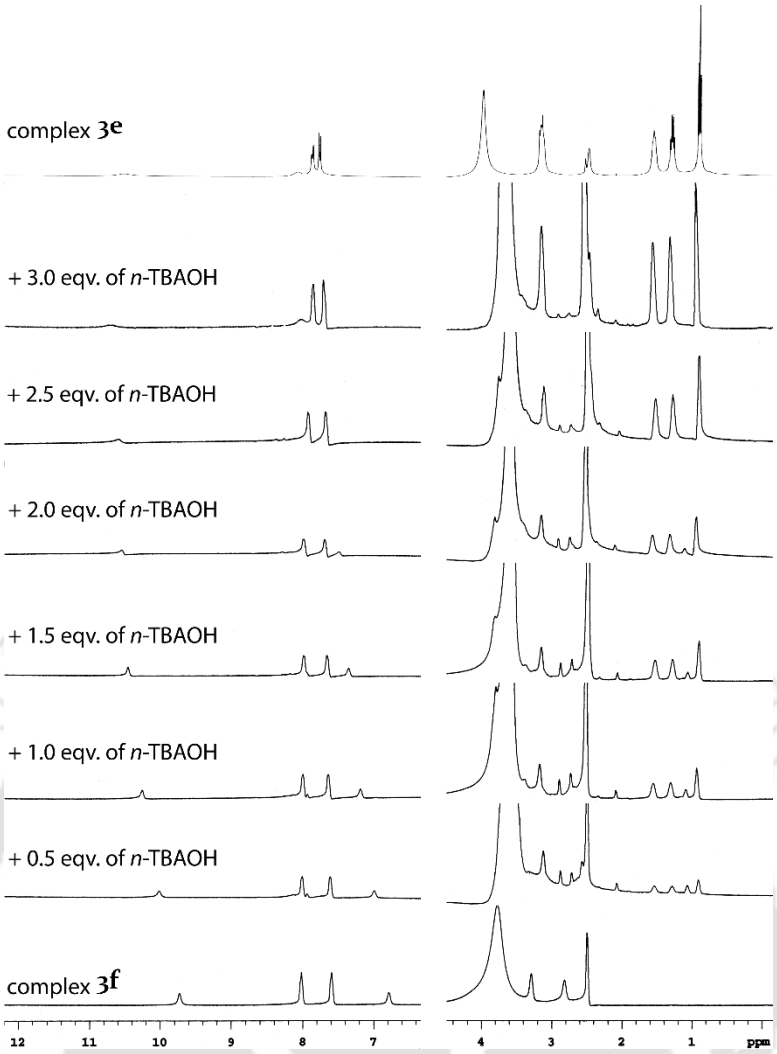

Figure 5.7 ^{1}H NMR experiment showing the transformation of charged host complex **3f** to neutral complex upon gradual addition of (*n*-TBA)OH in DMSO-d_6 (400 MHz, 298 K).

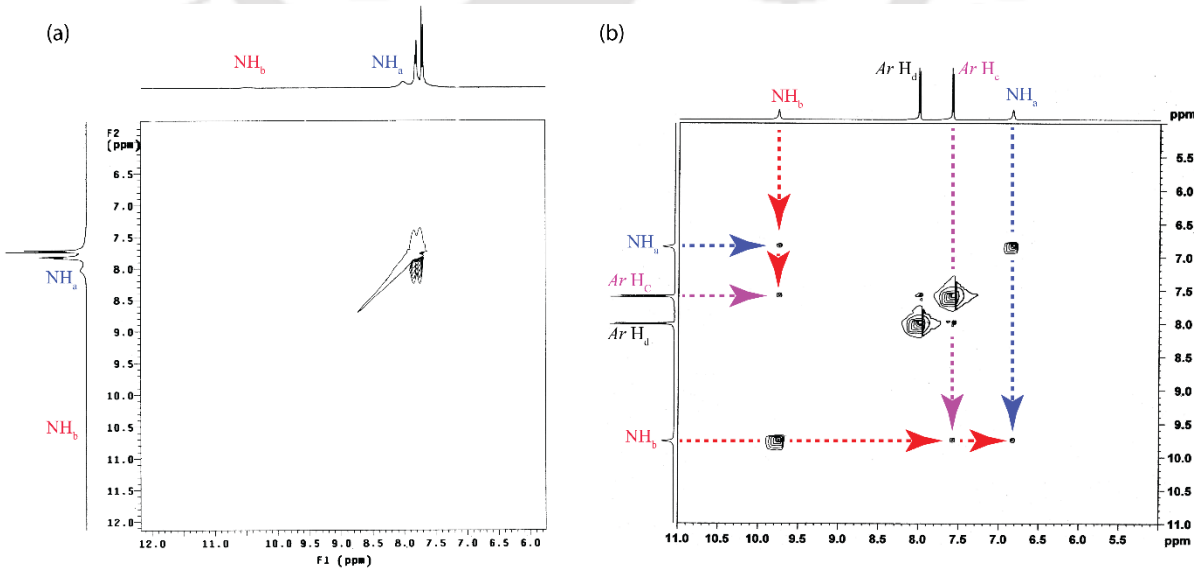

Figure 5.8 Partial (aromatic region) 2D-NOESY NMR spectrum of complex **3e** (a) and complex **3f** (b) in DMSO-d_6 at 298 K.

Finally, 2D-NOESY NMR analyses of the phosphate complexes **3e** and **3f** (DMSO-d_6) further validated the binding discrepancy of phosphate in solution by the host in neutral state (**L_3**) and in cationic state {(**L_3**H)$^+$}. The free receptor **L_3** showed strong NOE (Nuclear Overhauser Effect) coupling between the urea −NH protons (H_a···H_b) and weak coupling between the urea proton −NH(b) and an *ortho*-aryl proton −CH(c).[14] In the tetrahedral cage complex **3e**, disappearance of the signal corresponding to the urea −NH protons coupling (H_a···H_b) indicates the encapsulation of phosphate within the complementary receptor cavity (Fig. 5.8). Unlike **3e**, complex **3f** showed three distinct signals corresponding to NOE couplings between the urea −NH protons (H_a···H_b), between the aryl −CH protons (H_c···H_d) and between the urea −NH(b) proton and an *ortho*-aryl proton (H_b···H_c) (Fig. 5.8).

5.4 PO_4^{3-} binding by L_3: Efforts were made to examine the solid state binding of PO_4^{3-} by **L_3** as well as in solution by employing (*n*-TBA$^+$)$_3$$PO_4^{3-}$ [in-situ prepared from (*n*-TBA$^+$)$H_2PO_4^-$+{2(*n*-TBA$^+$)}OH^-]. But unfortunately we couldn't achieve any single crystal outcome except very less amount of solid precipitate even with repetitive attempt. However, we had characterised the solid by ^{1}H, ^{13}C, ^{31}P and NOESY NMR spectroscopy and FT-IR spectroscopy. Detail analysis of the ^{1}H NMR spectrum confirms the presence of three *n*-TBA$^+$ unit with respect to the two receptor unit. These observations leads to the confirmation of a dimeric capsular assembly encapsulating fully deprotonated PO_4^{3-} in solution as complex 3(*n*-TBA)[2**L_3**$(PO_4)_3$], (**3h**). The ^{1}H NMR spectrum showed huge spectral changes in the urea −NH resonances with a Δδ (w.r.t free **L_3**) value of 3.74 and 3.58 ppm for −NH_a and −NH_b protons respectively (Annexure 5, Fig. A5.5,), indicating a strong binding mode for PO_4^{3-}. The ^{31}P peak of **3h** shifted downfield to 8.14 ppm relative to the free resonance of *n*-TBA($H_2PO_4^-$) at 2.40 ppm. Since the PO_4^{3-} had been generated by employing two equivalent of (*n*-TBA$^+$)}OH^- with respect to (*n*-TBA$^+$)$H_2PO_4^-$ from external source, this possibly could lead to the conclusion that the phosphate moiety to recognize by the host is fully deprotonated PO_4^{3-}.

5.5 Conclusion

In conclusion, we have shown the dihydrogen phosphate induced self-assembly of **L_3** into a tetrahedral molecular cage (**L_3**)$_4$ that encapsulates a discrete tetrameric mixed phosphate ($H_2PO_4^-$·HPO_4^{2-})$_2$ cluster by 24 −NH hydrogen bonds, revealing the formation of a (4+4) cage complex **3e**. Whereas, a discrete tetrameric anion-acid ($H_2PO_4^-$·H_3PO_4)$_2$ cluster has been observed in complex **3f** obtained upon protonation of **L_3** with excess phosphoric acid. To the best of our knowledge, these are the first examples of tetrameric mixed phosphate ($H_2PO_4^-$·HPO_4^{2-})$_2$ cluster encapsulation and anion-acid ($H_2PO_4^-$·H_3PO_4)$_2$ cluster binding by the

same host in neutral and acidic condition respectively. Transformation of charged host complex **3f** to a neutral host complex under mild acid-base modulation process has been demonstrated by ^{1}H NMR spectroscopy. Because of its uniqueness, $\mathbf{L_3}$, can also form (2+2) pseudodimeric assembly in presence of fluoride (complex **3g**). $\mathbf{L_3}$ has also established to be capable to encapsulate fully deprotonated PO_4^{3-} anion and over all in this way, this tris-urea receptor has been authenticated as a potential receptor for phosphate anions ($H_2PO_4^-$, HPO_4^{2-} and PO_4^{3-}).

References

1. (*a*) M. M. Conn and J. Rebek Jr., *Chem. Rev.*, **1997,** *97*, 1647. (*b*) J. Rebek Jr., *Acc. Chem. Res.*, **2009**, *42*, 1660.
2. (*a*) C. J. Avers, *Molecular Cell Biology* Addison–Wesley: Reading, **1986**. (*b*) J. L. Atwood and A. Szumna, *J. Am. Chem. Soc.*, **2002**, *124*, 10646.
3. (*a*) P. Ballester, *Chem. Soc. Rev.*, **2010**, *39*, 3810. (*b*) M. Arunachalamand P. Ghosh, *Chem. Commun.*, **2011**, *47*, 8477.
4. (*a*) B. Alberts, D. Bray, J. Lewis, M. Raff, K. Roberts and J. D. Watson, *Molecular Biology of the Cell*. 2nd Ed, **1990**. (*b*) R. S. Kaplan, *J. Membr. Biol.*, **2001**, *179*, 165. (*c*) B. Moss, *Chem. Ind.*, **1996**, *407*. (*d*) C. Glidewell, *Chem. Br.*, **1990**, *26*, 137.
5. (*a*) Z. Wang, H. Luecke, N. Yao and F. A. Quiocho, *Nat. Struct. Biol*., **1997**, *4*, 519. (*b*) J. W. Pflugrath and A. Quiocho, *Nature*, **1985**, *314*, 257.
6. (*a*) I. R. Evans, J. A. K. Howard and J. S. O. Evans, *Cryst. Growth Des*., **2008**, *8*, 1635. (*b*) N. A. C. Baker, N. McGaughey, N. Fletcher, C. A. V. Chernikov, P. N. Horton and M. Hursthouse, *Dalton Trans*., **2009**, 965.
7. Y. Li, L. Jiang, X. –L. Feng and T. –B. Lu, *Cryst. Growth Des*., **2008**, *8*, 3689.
8. (*a*) V. Blazek, K. Molcanov, K. Majerski-Mlinaric, B. Kojic-Prodic and N. Basaric, *Tetrahedron* **2013**, *69*, 517. (*b*) A. Rajbanshi, S. Wan and R. Custelcean, *Cryst. Growth Des*., **2013**, *13*, 2233.
9. M. A. Hossain, M. Isiklan, A. Pramanik, M. A. Saeed and F. R. Fronczek, *Cryst. Growth Des*., **2012**, *12*, 567.
10. (*a*) K. Raghuraman, K. K. Katti, L. J. Barbour, N. Pillarsetty, C. L. Barnes and K. V. Katti, *J. Am. Chem. Soc*., **2003**, *125*, 6955. (*b*) S. Pal, N. B. Sankaran and A. Samanta, *Angew. Chem., Int. Ed.* **2003**, *42*, 1741. (*c*) R. Custelcean, C. Afloroaei, M. Vlassa and M. Polverejan, *Angew. Chem., Int. Ed.* **2000**, *39*, 3094. (*d*) C. Janiak and T. G. Scharman, *J. Am. Chem. Soc.*, **2002**, *124*, 14010. (*e*) P. S. Lakshminarayanan, E. Suresh, P. Ghosh, *J. Am. Chem. Soc*., **2005**, *127*, 13132.
11. (*a*) R. Dutta and P. Ghosh, *Chem. Commun.*, **2014**, *50*, 10538. (*b*) C. Bazzicalupi, A. Bencini and V. Lippolis, *Chem. Soc. Rev.*, **2010**, *39*, 3709.
12. (*a*) P. S. Lakshminarayanan, I. Ravikumar, E. Suresh and P. Ghosh, *Chem. Commun*., **2007**, 5214. (*b*) N. Busschaert, M. Wenzel, M. E. Light, P. Iglesias-Hernandez, R. Perez-Tomas and P. A. Gale, *J. Am. Chem. Soc*., **2011**, *133*, 14136.
13. R. Chutia, S. K. Dey and G. Das, *Cryst. Growth Des.*, **2015**, *DOI: 10.1021/acs.cgd.5b00926*
14. R. Chutia, S. K. Dey and G. Das, *Cryst. Growth Des.*, **2013**, *13*, 883.
15. D. A. Jose, D. K. Kumar, B. Ganguly, and A. Das, *Inorg. Chem*., **2007**, *46*, 5817.
16. S. K. Dey, R. Chutia, and G. Das, *Inorg. Chem.*, **2012**, *51*, 1727.

Annexure 5

Table A5.1 Crystallographic parameters and refinement details of the complexes **3e, 3f** and **3g**.

Parameters	**3e**	**3f**	**3g**
CCDC	1009053	1009052	1009054
Formula	$C_{204}H_{336}N_{46}O_{59}P_4$	$C_{29}H_{44}N_{10}O_{19}P_2S$	$C_{35}H_{50}N_{11}O_9F$
Fw	4501.07	930.75	787.86
Crystal system	Monoclinic	Monoclinic	Monoclinic
Space group	C2/c	$P2_1/c$	$P2_1/c$
a/Å	25.5951(7)	12.9811(14)	11.606(9)
b/Å	29.3619(9)	22.848(3)	26.10(2
c/Å	36.2011(15)	14.6435(15)	13.323(10)
α/°	90.00	90.00	90.00
β/°	109.597(2)	103.820(6)	95.56(2)
γ/°	90.00	90.00	90.00
V/Å^3	25630.0(15)	4217.4(8)	4017(5)
Z	4	4	4
D_c/g cm^{-3}	1.166	1.466	1.303
μ Mo Kα/mm^{-1}	0.109	0.240	0.099
T/K	298(2)	298(2)	298(2)
θ max.	27.59	21.86	18.99
Total no.of reflections	137383	64149	26833
Independent reflections	25684	10345	9755
Observed reflections	16393	6048	6118
Parameters refined	1410	584	513
R_1, I > 2σ(I)	0.1350	0.0678	0.0598
wR_2 (all data)	0.3814	0.2006	0.1455
GOF (F^2)	1.169	1.171	1.044

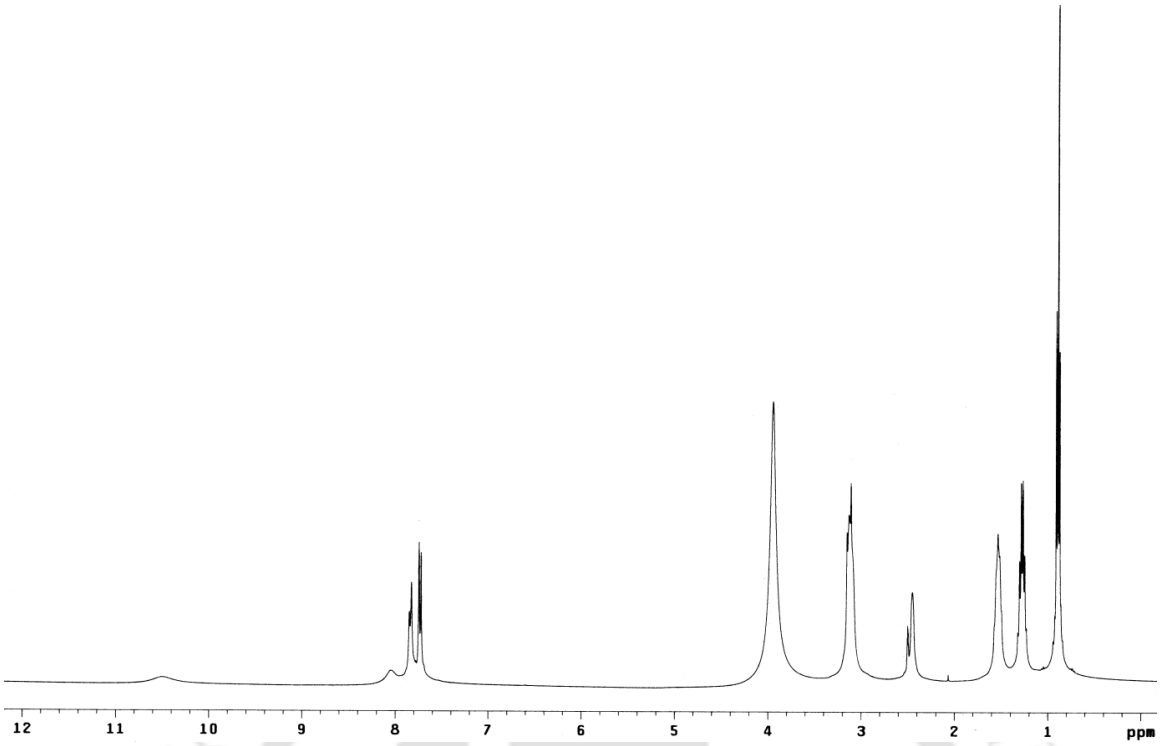

Figure A5.1 ^{1}H NMR spectrum of complex **3e** in DMSO-d_6 (Varian-400 MHz) at 298 K.

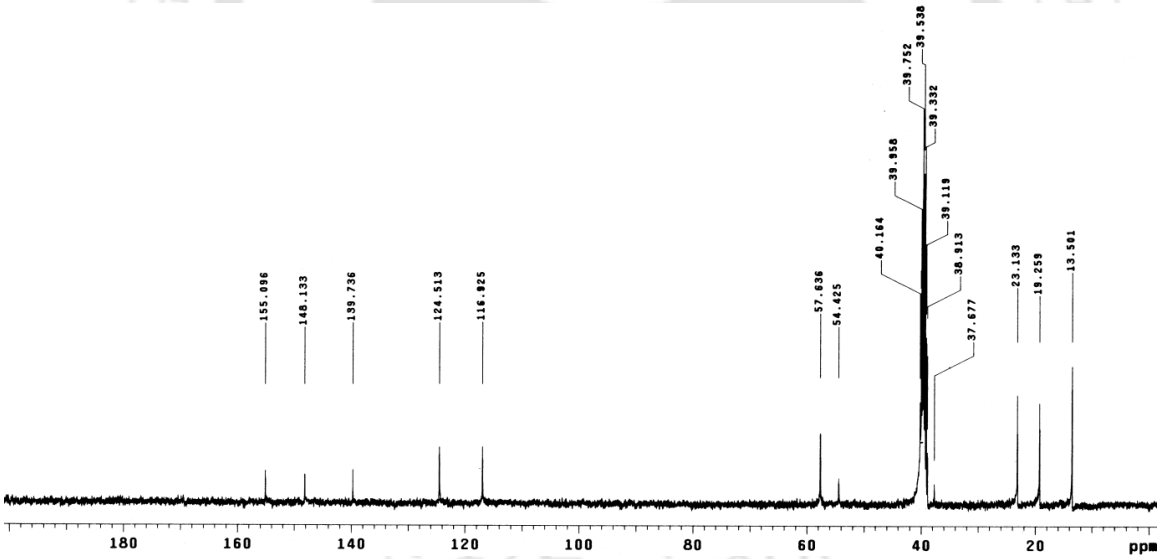

Figure A5.2 ^{13}C NMR spectrum of complex **3e** in DMSO-d_6 (Varian-400 MHz) at 298 K.

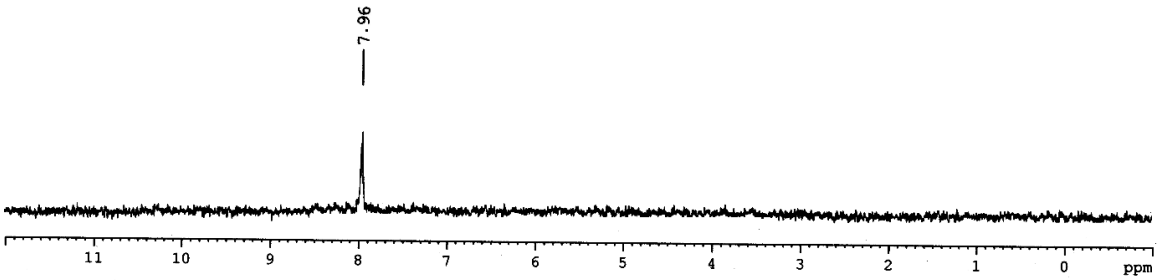

Figure A5.3 ^{31}P NMR spectrum of complex **3e** in DMSO-d_6 (Varian-242.94 MHz) at 298 K.

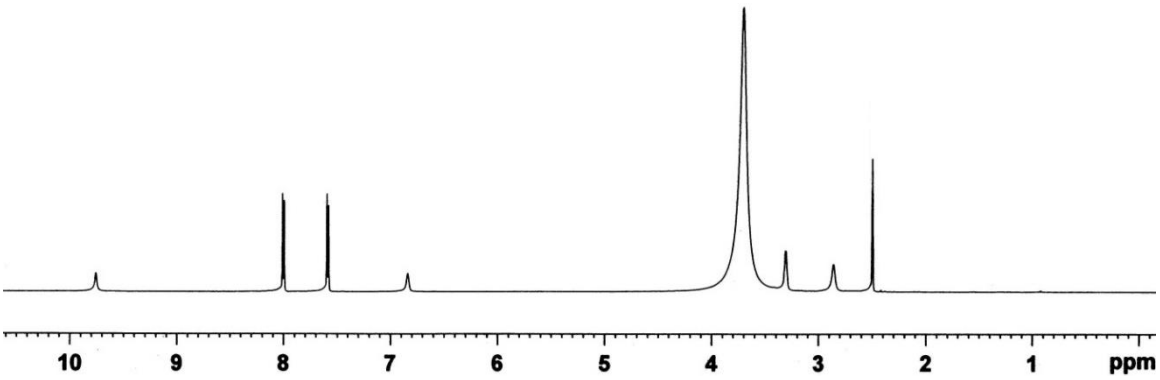

Figure A5.4 ^{1}H NMR spectrum of complex **3f** in DMSO-d_6 (Varian-600 MHz) at 298 K.

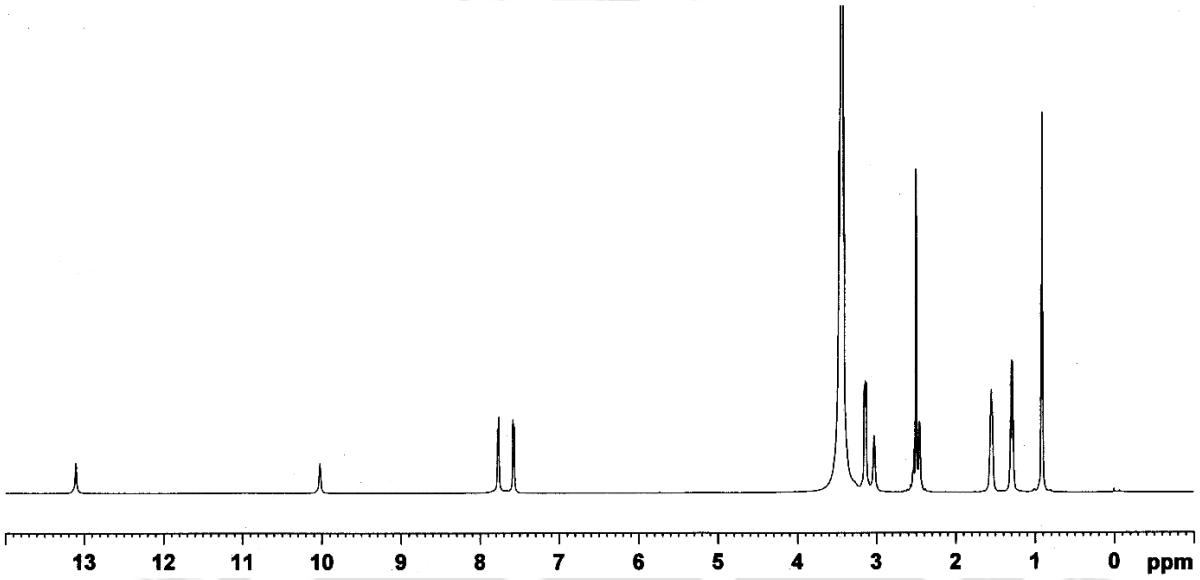

Figure A5.5 ^{1}H NMR spectrum of complex **3h** in DMSO-d_6 (Varian-600 MHz) at 298 K.

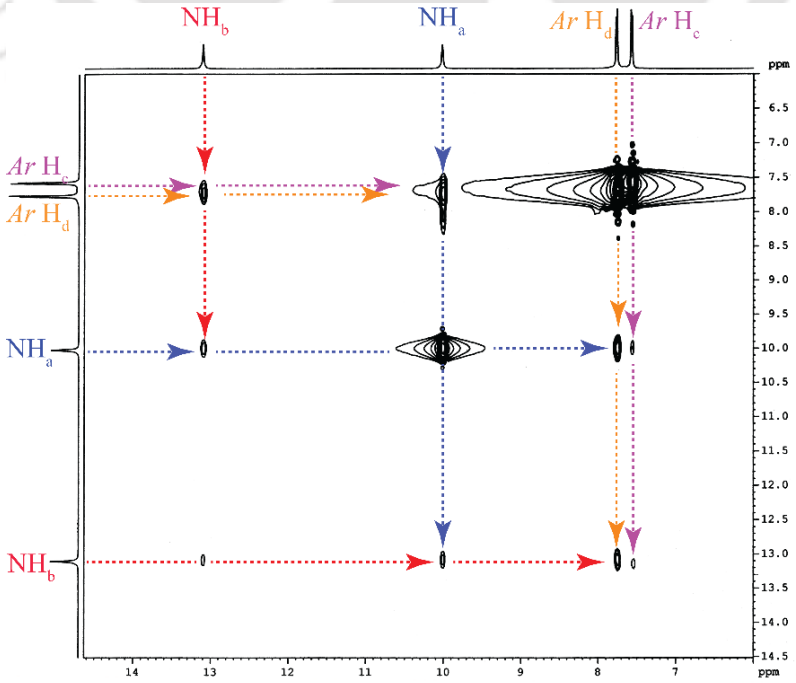

Figure A5.6 Partial (aromatic region) 2D-NOESY NMR spectrum of complex **3h** in DMSO-d_6 at 298 K.

Table A5.2 Detail of hydrogen Bonding Contacts in Complexes **3e, 3f** and **3g**.

complex	D–H···O	*d*(D···A), Å	*d*(H···A)/ Å	∠D–H···A,/deg
3e	N2–H···O19	2.88(1)	2.043	162.3
	N3–H···O22	3.22(1)	2.406	159.9
	N5–H···O19	2.903(7)	2.052	170.3
	N6–H···O21	2.935(6)	2.123	157.3
	N8–H···O19	2.894(7)	2.070	160.4
	N9–H···O20	2.963(8)	2.112	170.1
	C9···O22	3.393(9)	2.568	148.0
	C18···O21	3.33(1)	2.602	135.4
	C23···O20	3.42(1)	2.686	136.8
3e	N12H···O24	2.861(7)	2.005	1.748
	N13H···O25	2.895(8)	2.096	154.4
	N15H···O24	2.90(1)	2.043	175.5
	N16H···O26	2.967(8)	2.171	153.6
	N18H···O24	3.049(6)	2.220	168.9
	N19H···O23	2.891(7)	2.050	166.0
	C36···O25	3.22(1)	2.530	131.1
	C41···O26	3.162(9)	2.442	134.5
	C54···O23	3.331(9)	2.571	139.2
3f	N2–H··· O11	2.925(3)	2.164(2)	147.3(2)
$H_2PO_4^-$	N3–H··· O10	2.979(3)	2.120(2)	176.1(2)
	N8–H··· O12	3.112(3)	2.372(2)	144.3(2)
	N9–H···O12	2.822(3)	1.974(2)	168.6(2)
	C14–H···O13	3.429(4)	2.507(2)	170.9(2)
3f	N5–H··· O14	3.061(3)	2.279(2)	151.4(2)
H_3PO_4	N5–H··· O16	3.259(4))	2.517(3)	145.1(2)
	N6–H··· O14	3.028(3)	2.204(2)	160.1(2)
	C9–H···O17	3.373(4)	2.468(3)	164.2(2)
3g	N2–H··· F1	2.952(3)	2.228(2)	141.9(2)
	N3–H··· F1	2.708(3)	1.896(2)	157.0(2)
	N5–H··· F1	3.002(3)	2.244(2)	147.0(2)
	N6–H··· F1	2.681(3)	1.861(2)	159.0(2)
	N8–H··· F1	2.838(4)	2.03(3)	153(2)
	N9–H··· F1	2.800(3)	1.986(2)	157.4(2)

In conclusion, this thesis provides some significant results in the domain of Supramolecular Chemistry of anions and ion pairs, where the binding capabilities of some acyclic receptors have been explored in the solid and solution-state. In general, the present findings provide evidence of anion and ion pair induced formation of capsular, pseudo-capsular and polymeric assembly of the studied receptor molecules. Each receptor has shown some interesting properties in the presence of a specific anion or a set of ionic guests.

The receptor **L_1** (iodo-substituted) possesses a unique ability to form both hydrogen bonding (HB) and halogen bonding (XB) with selective guests like HCO_3^- and CH_3COO^- as evidenced by single crystal XRD analysis where the source of HCO_3^- is aerial CO_2. However, the bromo-analogue (**L_2**) displays only H-bonding governed coordination environment for the anions SiF_6^{2-} and CH_3COO^-. The isomeric set of multi armed tris-urea receptors (**L_3**, **L_4** and **L_5**) shows distinct behavior towards anions depending on size and shape of the latter which have been attributed to the isomeric position of the $-NO_2$ group in the phenyl ring. Besides, **L_3** in assistance with 18-crown-6-ether (**L_C**) has been structurally authenticated to be self-assembled into an integrated 1D coordination polymer in the presence K_2CO_3. Furthermore the *para*-nitrophenyl substituted tris-urea receptor (**L_3**) has furnished an unusual example of encapsulation of a tetrameric tetrahedral mixed phosphate cluster $(H_2PO_4^-{\cdot}HPO_4^{2-})_2$ with 24 −NH hydrogen bonds in its tetrahedral molecular cage.

The recognition of anions and ion pairs within molecular assembly or molecular cavity in solid state is profoundly a field which can expand considerably and bring immense advances in specialized applications such as drug delivery, membrane transport, catalysis *etc*. However, for these applications to reach their prospective, basic work in tuning anion, hydrated anion and ion pair binding inside the molecular capsules or molecular assembly is the need of the hour. Although the results included in this thesis are useful from a fundamental viewpoint, there are other challenging aspects in Supramolecular Chemistry that need to be developed, basically from an applicative approach. Research in these areas with a focus on technological and biomedical applications, based upon the remarkable anion and ion pair binding molecular assembly, appear to be forthcoming.

Romen Chutia

Date of Birth: 31-01-1987

Place of Birth: Namti Chariali, Sivasagar, Assam, India.

Nationality: Indian

Email: r.chutia@iitg.ernet.in, aorkromen@gmail.com, aorkromen@outlook.com

Academic Summary

2010-present: Ph.D. student at Indian Institute of Technology Guwahati, India.
(Thesis has been submitted)
Thesis title: "**Anion and Ion-Pair Directed Self-Assembly of Urea Functionalized Molecules**".

2008-2010: Masters in Chemistry (Specialization: Organic Chemistry)
Gauhati University, Assam, India.

2005-2008: Graduation (Chemistry), Sibsagar College, Joysagar, Assam, India.

2004: 12th (Science), AHSEC.

2002: 10th, SEBA.

Research Interests

- **Supramolecular chemistry of biologically and environmentally relevant anions:** Solid and solution-state studies of biologically and environmentally relevant anions in π–acidic systems (receptors), and anion templated synthesis of supramolecular architectures such as, catenanes, rotaxanes and molecular boxes.
- **Supramolecular capsules and pseudocapsules based on hydrogen bonds or metal-ligand coordination bonds:** The rational design and synthesis of supramolecular capsules with controllable encapsulation and release of a guest molecule remains an important subject, from the viewpoint of molecular recognition, stabilization of reactive intermediates, catalysis, and as microvesicles for drug delivery applications.
- **Ion-pair recognition:** Development of neutral and zwitterion receptors for the concurrent complexation of cations and anions in metal salts, for applications in various fields, such as salt extraction, trans-membrane ion transport and purification of industrial effluents.

Publications

1. Positional Isomeric Effect in Nitrophenyl Functionalized Tripodal Urea Receptors toward Binding and Encapsulation of Anions.
   Romen Chutia, Sandeep Kumar Dey, and Gopal Das; *Cryst. Growth and Des*. **2013**, *13*, 883.
2. A supramolecular Dual-Host Based Ion-Pair Induced Formation of 1D Coordination Polymer.
   Romen Chutia, Sandeep Kumar Dey, and Gopal Das; *CrystEngComm.* **2013**, *15*, 9641.
3. Hydrogen and Halogen Bonding in a Concert Act of Anion Recognition: F^- Induced Atmospheric CO_2 Uptake by an Iodophenyl Functionalized Simple Urea Receptor. **Romen Chutia** and Gopal Das, *Dalton Trans.* **2014***, 43,* 15628.
4. Self-assembly of a tris(urea) receptor as tetrahedral cage for the encapsulation of a discrete tetrameric mixed phosphate cluster $(H_2PO_4^-{\cdot}HPO_4^{2-})_2$.
   Romen Chutia, Sandeep Kumar Dey and Gopal Das, *Cryst. Growth and Des*. **DOI: 10.1021/acs.cgd.5b00926**
5. Oxyanion-Encapsulated Caged Supramolecular Frameworks of a Tris(urea) Receptor: Evidence of Hydroxide- and Fluoride-Ion- Induced Fixation of Atmospheric CO_2 as a Trapped CO_3^{2-} Anion.
   Sandeep Kumar Dey, **Romen Chutia** and Gopal Das; *Inorg. Chem*. **2012**, *51*, 1727.
6. Dual modes of binding on the hexafluorosilicate anion by a C3v symmetric flexible tripodal amide ligand in solid state.
   Arghya Basu, **Romen Chutia** and Gopal Das; *CrystEngComm.* **2014,** *16*, 4886

Conference attended

- Poster presented in ***Frontiers in Chemical Science*****,** Indian Institute of Technology Guwahati, Guwahati, 2012.
- Poster presented in ***International Conference on Structural Chemistry of Molecules and Materials*****,** Center for Research in Nanoscience and Nanotechnology (CRNN), University of Calcutta, 2014.
- Lecture presented in ***Frontiers in Chemical Science*****,** Indian Institute of Technology Guwahati, Guwahati, 2014.